

Wutec Geotechnical International

CASE STUDY OF LENIHAN DAM UNDER THE 1989 LOMA PRIETA EARTHQUAKE

Prepared by

G. Wu, Ph. D., P.Eng.

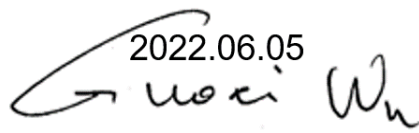
March 1, 2022



WGI-220301
2022-03-01

Report No. WGI-220301
March 1, 2022

Not to be reproduced without the permission of WGI

2022.06.05


by

Guoxi Wu, Ph.D., P.Eng.

Wutec Geotechnical International

Email: gwu@wutecgeo.com

Report No. WGI-220301
March 1, 2022

**CASE STUDY OF LENIHAN DAM UNDER
THE 1989 LOMA PRIETA EARTHQUAKE
TABLE OF CONTENTS**

Section	Subject	Page
1.0	INTRODUCTION.....	- 1 -
2.0	DAMAGES OF THE DAM IN LOMA PRIETA EARTHQUAKE	- 2 -
3.0	EMBANKMENT DAM FILLS AND THE UNDRAINED SHEAR STRENGTH	- 5 -
4.0	STATIC STRESS ANALYSIS OF THE DAM	- 9 -
	4.1 Analysis Model and Procedure	- 9 -
	4.2 Static Stresses of the Dam	- 11 -
5.0	NON-LINEAR DYNAMIC TIME-HISTORY ANALYSIS: A TOTAL STRESS APPROACH.....	- 13 -
	5.1 General Methodology	- 13 -
	5.2 Input Ground Motions	- 14 -
	5.3 VERSAT-2D Soil Constitutive Models.....	- 16 -
6.0	SEISMIC RESPONSE OF THE DAM: SECTION W-W	- 19 -
	6.1 Seismic Deformation and Strain: Case 2A(g).....	- 19 -
	6.2 Sensitivity Analyses: Effect of S_u and R_f	- 24 -
	6.3 Dam Crest Acceleration Response Spectra	- 27 -
	6.4 Effect of Dam Foundation Rock Stiffness.....	- 29 -
	6.5 Effect of Shear Wave Velocity of the Dam Fills	- 29 -
	6.6 Impact of Phreatic Surface in the Dam.....	- 30 -
7.0	SEISMIC RESPONSE OF SECTION B-B	- 32 -
	7.1 VERSAT Finite Element Model.....	- 32 -
	7.2 Seismic Deformation and Strain.....	- 33 -
8.0	DISCUSSION.....	- 34 -
9.0	CONCLUSIONS.....	- 35 -
	ACKNOWLEDGMENTS 致谢.....	- 35 -
	REFERENCE	- 36 -
APPENDIX A	BACKGROUND INFORMATION	
APPENDIX B	SECTION W-W AND S_u FOR ZONE 2L	
APPENDIX C	RSN3548_LOMAP_LEX(X, Y, Z) & CREST ACCELERATION	
APPENDIX D	VERSAT-2D INPUT AND OUTPUT FILES	
	Input File 1 Build the Dam in Dry	
	Input File 2 Add Reservoir Water.....	
	Output from Input File 2.....	
	Input Files 3 and 4 for Earthquake Loading	
	Output File from Input File 4 for Earthquake Loading	
APPENDIX E	FULL SIZE GRAPHS FOR MODEL & RESULT.....	

|

CASE STUDY OF LENIHAN DAM UNDER THE 1989 LOMA PRIETA EARTHQUAKE

1.0 INTRODUCTION

The Lenihan dam, 61-m high and constructed in 1953, is a compacted earthfill dam located in California (Fig. 1). The earthen embankment dam consisted primarily of low plasticity clayey sands and clayey gravels, whereas the lower core (Zone 2L) of the dam was comprised of highly plastic sandy clays to silty sands or sandy silts. Subjected to earthquake ground motions of the 1989 $M_w = 6.93$ Loma Prieta earthquake with estimated horizontal peak ground acceleration (PGA) of 0.44g at bedrock, the Lenihan dam developed longitudinal cracks on the dam faces and settled at its crest 0.25 m on average. This case history is of great value and can be used to validate current engineering procedures for nonlinear dynamic response history analysis and to evaluate currently available soil constitutive models for clayey soils.

In current study, the dynamic responses of the Lenihan dam in the 1989 Loma Prieta earthquake were analyzed using the finite element computer program VERSAT-2D (WGI 2019), and undrained response of the saturated dam fills was modelled using a total stress approach. The total stress method of analysis, using the Mohr Coulomb failure criterion and various forms of hysteretic stress-strain relations, is a common method for dynamic analysis of undrained response involving clayey or cohesive soils; it is widely used in geotechnical engineering (Wu et al. 2006; Wu 2010; Hadidi et al. 2014; Sweeney and Yan 2014; and others). The effective stress method of analysis, including calculation of earthquake-induced pore water pressure (PWP) during shaking and impact of the PWP on soil stiffness and strength, is becoming a standard approach for undrained response history analysis of sandy soils involving soil liquefaction and its induced large ground deformations (Wu 2001, 2015, 2018, 2021; Finn et al. 1986; Wu and Chen 2002; Sherstobitoff et al. 2004; Finn and Wu 2013; and many others), and it was adopted for clayey soils (Boulanger 2019) although it is less available than for sandy soils.

The difference between the VERSAT approach and other more complicated approaches (e.g., Boulanger 2019) is that the VERSAT analysis does not require calibration of soil parameters ahead of a dynamic analysis, but it uses more fundamental parameters of soils such as V_s for stiffness, undrained shear strength S_u , friction angle

(ϕ') for shear strength, normalized SPT blow count $(N_1)_{60}$ for liquefaction resistance, and residual strength if soil liquefies. The VERSAT approach is, in terms of soil parameters required, in kind of what an engineer would do when a limit equilibrium slope stability analysis is to be performed.

By presenting the analysis methodology and results of the analyses, this paper demonstrates the merits of using the VERSAT approach and its capability of capturing the key features of seismic performance for earthen dams in earthquakes, even in large earthquakes. The VERSAT approach would be more suitable for engineering analysis than for academic studies. Dynamic analyses of the dam were performed using the proposed S_u/σ'_m approach for calculating in-situ undrained strengths as well as sensitivity analyses on input ground motion, phreatic surface, undrained strength, and dam bedrock foundation stiffness on dynamic response of the dam. The computed responses are found to be in good agreement with the measured dam crest settlements and the observed lateral spreading deformation pattern. Limitations associated with the total stress analysis model, the input ground motions, the input soil parameters, and their potential implications on the analysis results are discussed.

2D plane-strain dynamic time-history analyses were carried out for two cross-sections of Lenihan Dam, i.e., the sections W-W' and B-B' as shown in Fig. 2. Section W-W' has a large 200 m wide area of dam fills (Zone 2L under the crest and Zone 4 in downstream) where bedrock surface is low at about elevation 147 m (482 ft); this section was developed by the current study to represent a more likely direction (than section B-B') of ground displacing under the 1989 Loma Prieta earthquake. In comparison, the bedrock surface in section B-B' is higher in elevation, where only about 110 m wide area has the low bedrock surface. A portion of section B-B' about 60 m upstream of the dam crest is on a rock knob where the rock surface is about 16 m higher than the low bedrock surface.

Results of dynamic analyses using both sections W-W' and B-B' are reported in this document.

2.0 DAMAGES OF THE DAM IN LOMA PRIETA EARTHQUAKE

Lenihan Dam, constructed in 1953 and named the Lexington dam at the time, is a 61-m-high compacted earthfill dam located on Los Gatos Creek in Santa Clara County of California. Lenihan Dam is located about 10 km downstream of the Austrian dam, as

seen in Fig. 1; dynamic analysis of the Austrian dam is carried out in another study (WGI, 220224).

A plan view of the Lenihan dam is shown in Fig. 2. The dam has a relatively flat 5.5:1 (horizontal to vertical) upstream slope along section B-B' (perpendicular to the dam axis); and a flatter slope of 6:1 along cross section W-W' (slightly skewed) as shown in Fig. 3. In the 1989 earthquake, the dam developed longitudinal cracks on the dam faces; the dam crest had horizontal movements of about 62 mm (2.5 in) towards the downstream and settled 0.25 m (10 in) on average. The reservoir elevation at the time of the earthquake was very low, approximately 30 m below the spillway elevation; the phreatic surface shown in Fig. 3 was estimated using data from piezometers installed after the 1989 earthquake but observed when the reservoir level was low and equivalent to that during the 1989 earthquake (Dawson and Mejia 2021).



Fig. 1. The 1989 Loma Prieta earthquake fault rupture zone by Harder et al. (1998.) in relation to ground motion recording stations (the Lexington station and the Corralitos station) and the Lenihan dam in California, US. (Map data © 2021 Google.)

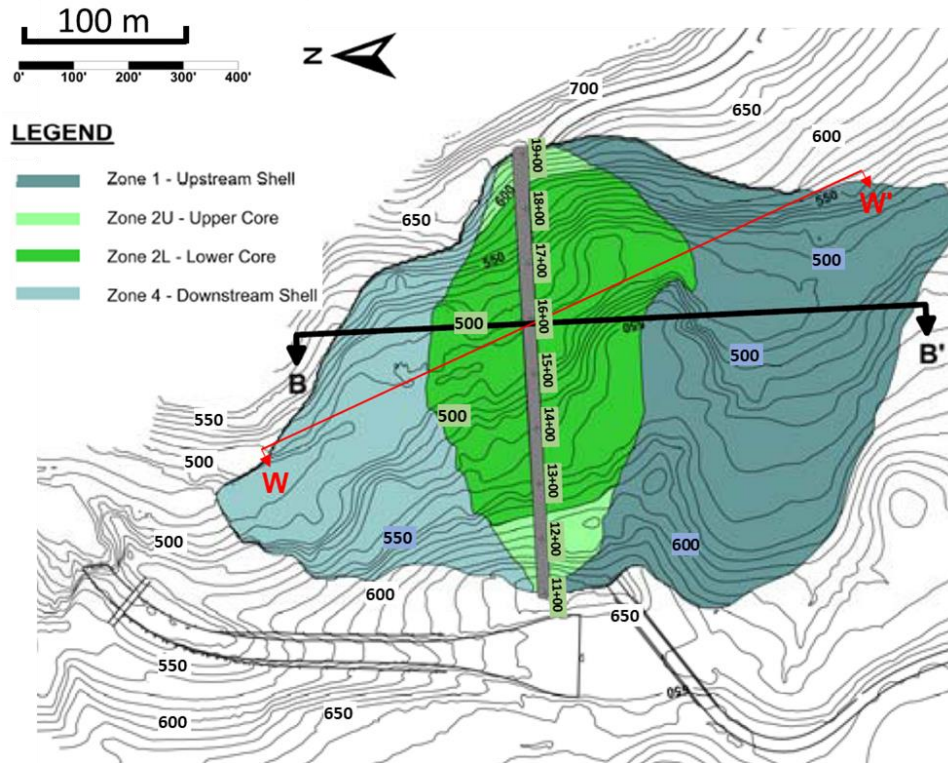


Fig. 2. Lenihan Dam: plan view showing the location of cross-sections W-W' and B-B'. (Modified from SCVWD 2012.)

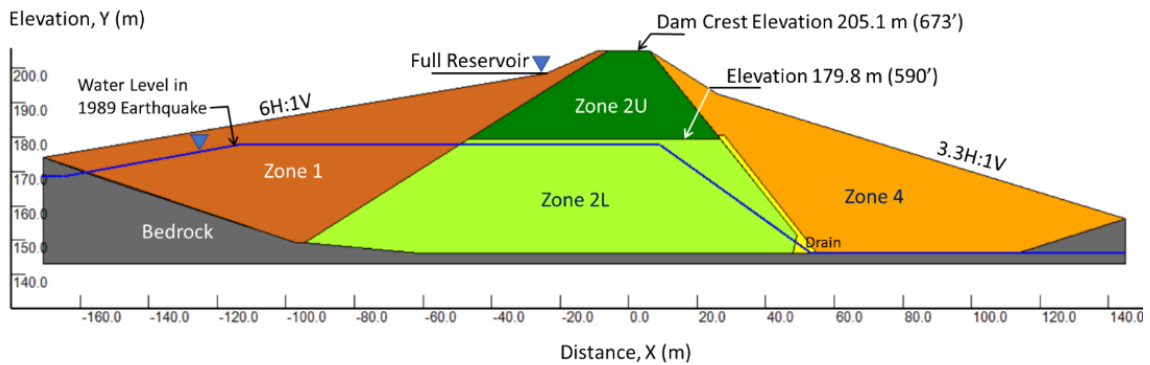


Fig. 3. Lenihan Dam: cross-section W-W' showing zones of dam fills and the inferred phreatic surface by Dawson and Mejia (2021). Note that side slopes (upstream 6H:1V and downstream 3.3H:1V) are flatter than these for cross-section B-B'

3.0 EMBANKMENT DAM FILLS AND THE UNDRAINED SHEAR STRENGTH

The majority dam fill of the Lenihan dam consisted primarily of low-plasticity clayey sands (SC) and clayey gravels (GC) with gravel content (coarser than 4.75 mm) ranging from 0 to 58% (mean of about 31%) and fines content (finer than 0.075 mm) ranging from 15 to 97% (mean of about 33%) for soils in Zones 1, 2U and 4, whereas the lower core (Zone 2L) of the dam was comprised of highly plastic sandy clays to silty sands or sandy silts. Soil classification, gradation, Atterberg limits, soil stiffness and strength data are summarized in Table 1. All soil data used in current study are compiled from Harder et al. (1998) and SCVWD (2012); the latter is the owner of the Lenihan dam.

Of particular interest to the current study are the data from the ICU triaxial tests conducted on undisturbed tube samples extracted from Lenihan Dam for soils in all four soil zones (Zones 1, 2L, 2U and 4). From the ICU triaxial test data, undrained shear strengths (S_u) for Zones¹ 1 and 2L were calculated and plotted in Fig. 4 against the consolidation stresses. The S_u is defined as the shear stress on the eventual failure plane at failure, and failure occurs when the principal stress ratio (σ'_1 / σ'_3) reaches its peak in shearing. In common language, this is the shear stress of the point on a Mohr circle that touches the failure envelope; it is less than the maximum shear stress in the Mohr circle. In current study, the undrained shear strengths of the saturated dam fills are related to the mean consolidation stress, σ'_m ; σ'_{3c} in Fig. 4 are the consolidated stresses used in ICU triaxial tests.

For the in-situ pre-earthquake stress conditions, except these with K_0 of 1.0, the soils are not isotropically consolidated. In the current study using the finite element method, the undrained shear strength of a saturated soil element is calculated using the following equation,

$$[1] \quad S_u = c + \sigma'_m \tan(\psi)$$

$$[2] \quad \sigma'_m = (\sigma'_x + \sigma'_y + \sigma'_z) / 3$$

where S_u is the undrained shear strength of a soil element; σ'_m is the mean consolidation pressure or stress at the soil element center prior to earthquake loading; σ'_x and σ'_y are the horizontal and vertical consolidation stresses, respectively, in two-

¹ S_u for Zones 2U and 4 are presented later in this document.

dimensional (2D) plane strain finite element analysis presented in this study; σ'_z is the horizontal consolidation stress in the direction perpendicular to the 2D plane. The cohesion (c) and the friction angle (Ψ) are undrained strength parameters that would either be obtained from in-situ shear tests or determined from undrained direct simple shear tests; for the current study, they are derived as shown in Figs. 4(a, b) from the ICU triaxial compression test data.

Using the proposed S_u/σ'_m method, the computed S_u that are based on or referenced to the mean consolidation pressure (σ'_m) are compared in Figs. 5(a, b) with the S_u calculated using the procedure adopted by Boulanger (2019). The Duncan and Wright (2005) procedure for evaluating slope stability with limit equilibrium method was extended and applied by Boulanger (2019) for his finite difference dynamic analysis of the Austrian dam. In general, S_u calculated using the proposed S_u/σ'_m method are lower (and thus more conservative) than S_u calculated using the procedure adopted in Boulanger (2019). The undrained shear strength S_u is about 5-8% lower at $K_0 = 0.5$; whereas the difference narrows to about 3% as K_0 increases to 0.8. For the high plasticity Zone 2L soils of Lenihan Dam, the S_u -ratios applied in this study using the S_u/σ'_m method and the calculated σ'_z for individual soil elements are about 8% lower than Boulanger (2019) as shown in Fig. 5(b); however, the range of S_u -ratios agrees well with that obtained from direct simple shear (DSS) tests on three samples of Zone 2L soils (SCVWD 2012). The proposed S_u/σ'_m approach might be more suitable for engineering practice as shown in the following dynamic analysis. The SHANSEP approach (Ladd and Foote 1974; Ladd and DeGroot 2004) or the S_u/p' approach (Duncan and Wright 2005) are often used for heavily over-consolidated fine-grained soils.

Table 1. Geotechnical properties of dam fills of the Lenihan dam

	Unit 1	Unit 2U	Unit 2L	Unit 4
USCS classification	SC, CL	SC, GC	CH, SM-MH	SC, GC
Percent coarser than 4.75 mm (%)	27 (0-43)	33 (3-58)	6 (0-29)	32 (13-56)
Percent finer than 0.075 mm (%)	39 (19-97)	31 (16-53)	79 (29-97)	30 (15-63)
Liquid limit	33 (30-39)	37 (30-48)	62 (43- 70)	33 (22-46)
Plasticity index (PI)	15 (6-24)	17 (14-29)	35 (15- 48)	15 (6-29)
Water content (%)	15 (10.3-26.5)	11.9 (6.0-17.7)	24.1 (17.8-37.1)	11.9 (6.2-19.9)
Dry unit weight (kN/m ³)	18.8 15.0-20.8	18.8 17.0-20.7	15.7 14.1-17.5	19.5 15.8-22.5
Saturated unit weight (kN/m ³)	21.7	20.8	19.5	22.0
K (m/s) ^a	398	363	207	473
Effective stress, c' (kPa)	0	0	0	0
Effective stress, ϕ' (°)	37.5	35.5	25.5	35

Sources: Data from Harder et al. (1998) and Engineering Report No. LN-3 (SCVWD 2012).

^a The shear wave velocity, V_s , is calculated using $V_s = K \cdot (\sigma'_y/P_a)^{0.25}$.

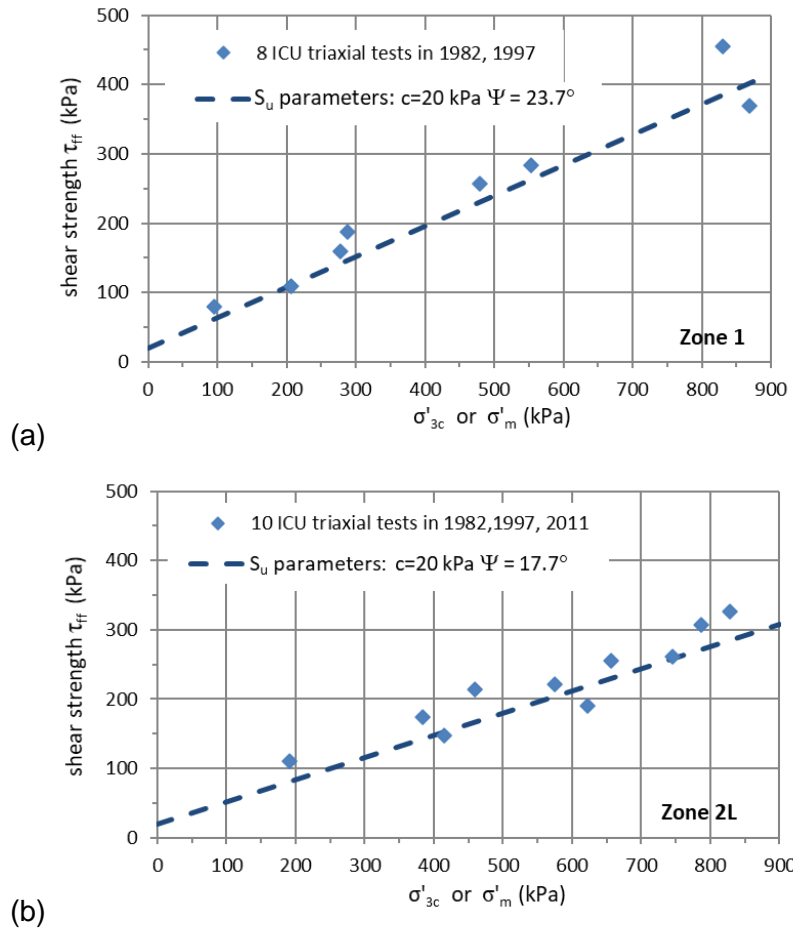
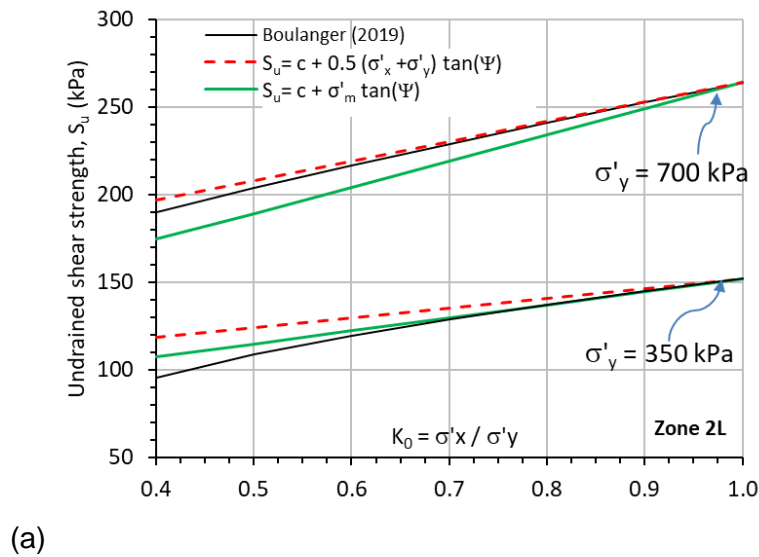
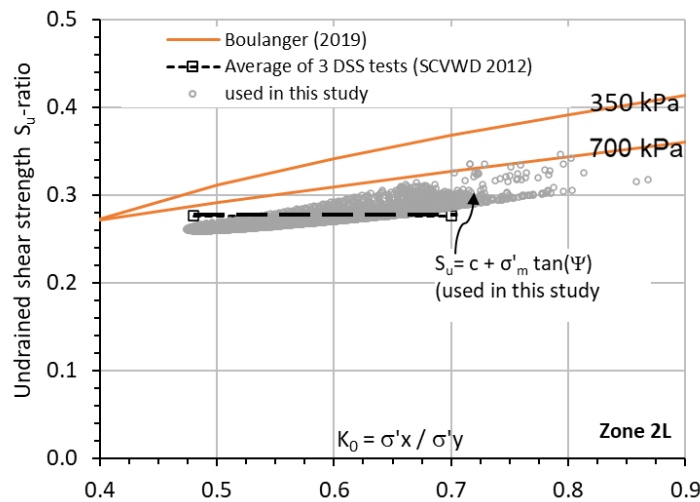


Fig. 4. Shear strengths and the mean consolidation pressure (σ'_m) derived from test data of the ICU triaxial test specimens from saturated soil samples of: (a) Zone 1; (b) Zone 2L.





(b)

Fig. 5 Undrained shear strength S_u of saturated high plasticity soils in Zone 2L of Lenihan Dam: (a) Comparison of S_u versus K_0 ($\sigma'_m = (2\sigma'_x + \sigma'_y)/3$, $\phi' = 25.5^\circ$, $K_f = 2.54$, $\tau_{xy} = 0$); (b) S_u -ratios ($=S_u/\sigma'_y$) applied in this study and from the DSS tests by SCVWD (2012)

4.0 STATIC STRESS ANALYSIS OF THE DAM

4.1 Analysis Model and Procedure

The total stress method of analysis is often adopted for evaluating seismic stability and deformation of embankment dams consisting in whole or in part of fine-grained soils (clays, silts), clayey sands or gravels (e.g., the Lenihan dam fills), or glacial till core of low permeability in other dams. The advantage of performing a total stress analysis, by using S_u , is that there is no need to evaluate or determine the amount of earthquake-induced dynamic pore water pressures (PWP) and their impact on shear strengths of these soil materials. However, to adequately determine the undrained shear strengths of saturated soils, the method requires a sound evaluation of the past maximum consolidation pressure, σ'_p ; this is more relevant to foundation soils (than to dam fills) as they are more likely to be over-consolidated due to their long geological history. In general, compacted dam fills are considered normally consolidated or lightly over-consolidated with an over-consolidation ratio (OCR) of less than 2 to 4; it is adequate to estimate the undrained shear strength of the saturated dam fills from the

ICU triaxial tests by relating the current in-situ effective stresses to the consolidation pressures applied in the ICU triaxial tests.

The static stresses of the dams were calculated using the static analysis module of VERSAT-2D, whereas an elastic perfectly plastic model with the Mohr-Coulomb failure criterion is adopted. Prior to failure, the shear modulus is modelled as linear and strain-level independent; however, the stress-level dependency of soil stiffness (shear and bulk moduli) is allowed by using equations [3] and [4] for calculating the two moduli as are used for the dynamic analysis. Note that soil stiffness parameters used for computing the in-situ effective stresses of the dam prior to earthquake shaking are normally determined using the static and drained loading tests, such as oedometer tests or triaxial tests. A general methodology for static stress analysis is described in another case study of Austrian Dam (WGI, 220224).

The finite element model for Lenihan Dam is shown in Fig. 6; it consists of 9122 soil elements (1.52 m wide and 0.91 m high each). The construction sequence of the dam was modelled by building the dam in 5-m thick layers. The stress-level dependent elasticity moduli (soil stiffness) are updated after each 5-m thick layer is added onto the model. After completion of the dam construction to its crest, reservoir water levels and the phreatic surface were raised gradually in small increments. The incremental loading process (or unloading due to water buoyancy) is an essential analysis element needed to achieve the required convergence in a nonlinear analysis involving plasticity and flow rule. Each of the load increment was considered complete if the total unbalanced force of the entire model is less than 0.5 kN.

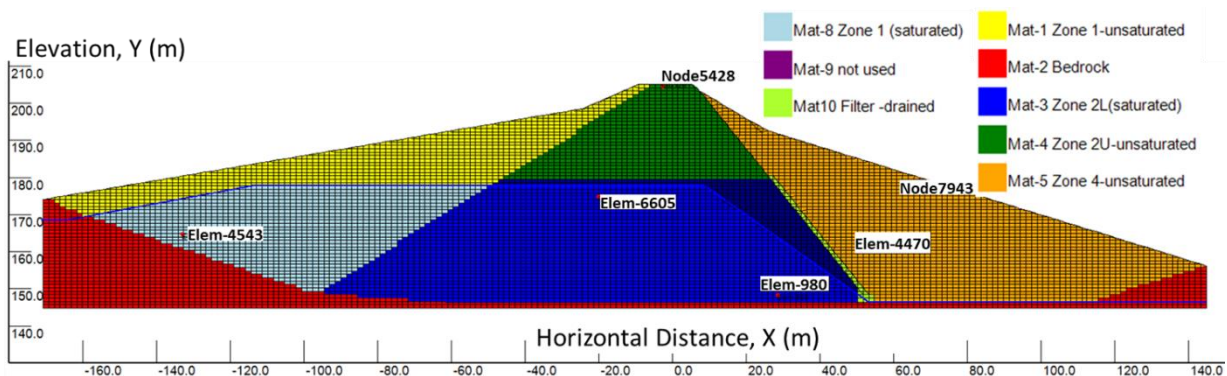


Fig. 6 VERSAT-2D finite element model of Lenihan Dam cross-section W-W' with finite element grids, soil and rock zones, reservoir water level and phreatic surface

The phreatic surface (water table) was applied as a piezometric surface; the pore-water pressure was computed as the vertical distance from the piezometric line to the point of interest, multiplied by the unit weight of water. When there is no vertical seepage gradient, this approach is a reasonable approximation (USBR 2019).

In the static stress analysis of the Lenihan dam, the drained shear strength parameters with zero cohesion ($c' = 0$ kPa) and effective stress friction angle (ϕ') were used for all dam fills (same ϕ' for saturated or unsaturated soils) associated with the Mohr Coulomb failure criterion. The soil unit weight and ϕ' used in the static stress analysis are the same as these used in the dynamic analyses, see Table 2. However, the stiffness parameters used in the static stress analyses are:

- $K_g = 619, 258, 613$ and 674 for soils in Zones 1, 2L, 2U and 4, respectively. They were estimated by taking $\frac{1}{4}$ to $\frac{1}{7}$ of the K_g used in the dynamic analyses.
- parameters $m = n = 0.5$ in equations [3] and [4] were used for all 8 materials except the bedrock.
- K_b was taken to be 5 times K_g for all soil materials. The adopted ratio of the bulk and shear moduli ($K_b / K_g = 5.0$) implies that a Poisson's ratio of 0.41 has been applied to the dam fills when constructing the dam in layers.

4.2 Static Stresses of the Dam

The calculated static stresses in the 2D plane are shown in Figs. 7(a, b, c) for vertical effective stresses σ'_y , coefficient of horizontal stress $K_0 (= \sigma'_x / \sigma'_y)$, and shear stresses (τ_{xy}), respectively. The vertical effective stresses are about 450-600 kPa for the upper half of the saturated Zone 2L under the dam crest below the water table, the lower half of the saturated Zone 2L are about 600-720 kPa. The K_0 values are about 0.4-0.5 for the same upper part and increase to 0.5-0.65 for the lower part; in general, the K_0 increase with depth and from the center (directly under the crest) to the areas under the upstream and downstream slopes. For soils in Zone 1 of the upstream slope and in Zone 4 of the downstream slope, the K_0 are generally higher at about 0.7-1.0 (in blue color).

It appears that the low stiffness of soils in Zone 2L have resulted in low lateral stresses (i.e., low K_0 values with $K_0 < 0.4$) in the upper core of the dam in Zone 2U. This low K_0 zone would have a relatively low static shear resistance and thus negatively impact the performance of the dam under earthquake loadings.

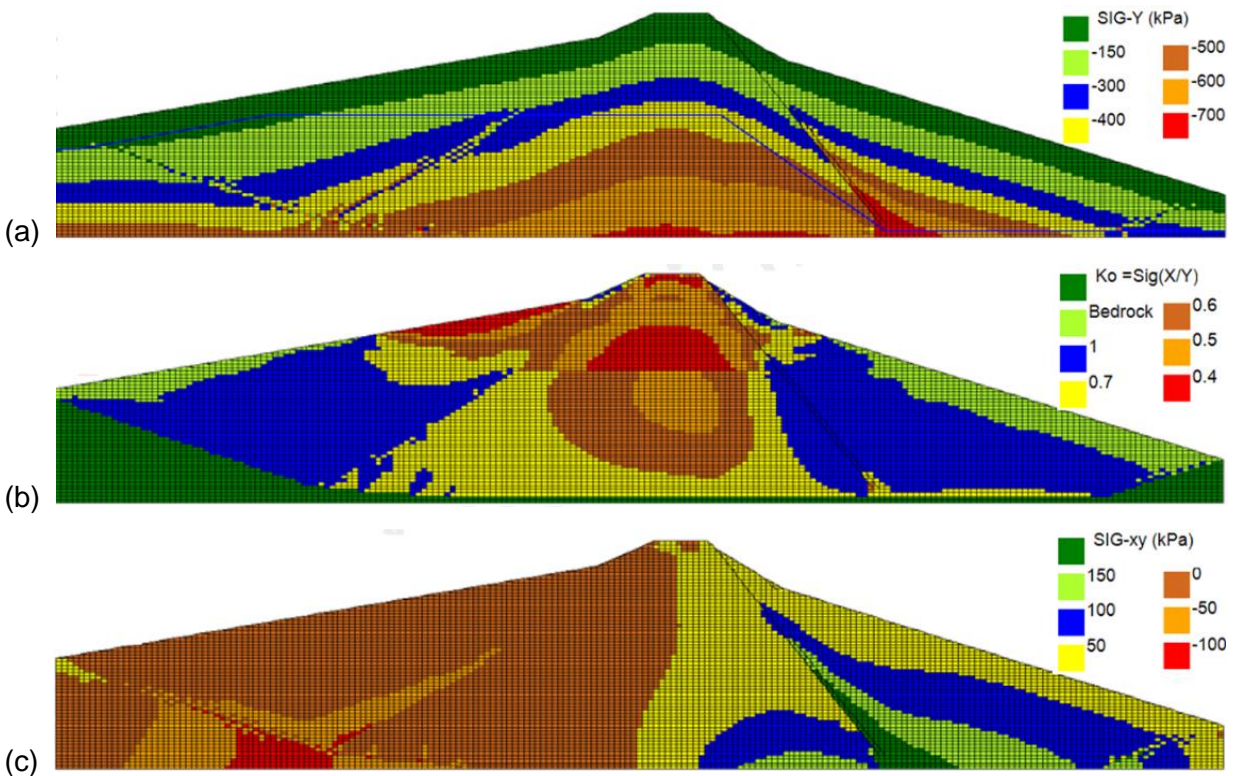


Fig. 7 Static stresses of the Lenihan Dam as calculated from VERSAT-2D: (a) vertical effective stresses σ'_y (negative sign represents compressive stresses); (b) horizontal stress coefficient $K_0 (= \sigma'_x / \sigma'_y)$ where σ'_x is horizontal effective stress; and (c) shear stresses τ_{xy} in the 2D plane XY

The undrained shear strengths of the saturated soils (the soils that are underneath the water table) were calculated using the proposed S_u/σ'_m approach in equation [1] where the σ'_m were calculated using the σ'_x , σ'_y , and σ'_z directly computed from the VERSAT-2D static analysis. Note that VERSAT-2D has the capability of computing the static stresses σ'_z . The computed S_u -ratios ($=S_u/\sigma'_y$) are plotted in Fig. 8. The S_u -ratios are about 0.26-0.28 for the entire centre-portion of the saturated soils in Zone 2L directly underneath the dam crest; they are slightly higher at about 0.28-0.32 for the remaining portion of Zone 2L soils. For the saturated soils in Zone 1 in the upstream slope, the S_u -ratios are about 0.4-0.5 in blue color (greater than 0.5 near the surface due to higher K_0). In general, high K_0 values would result in high S_u -ratios at a given vertical effective stress of σ'_y .

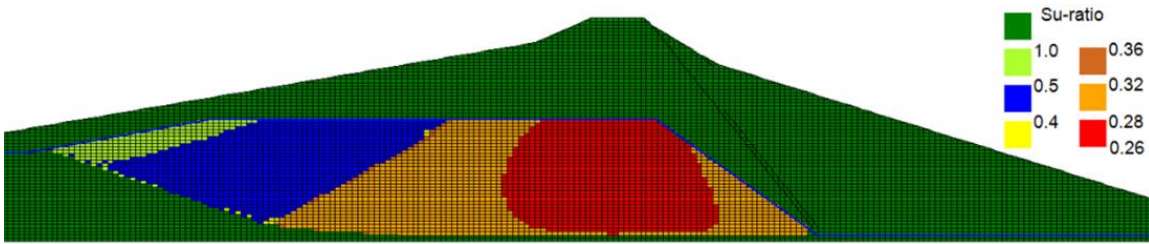


Fig. 8 Undrained shear strength ratio (S_u -ratio) using the proposed S_u/σ'_m approach: S_u -ratio is the ratio of S_u over the vertical effective stress, σ'_y .

5.0 NON-LINEAR DYNAMIC TIME-HISTORY ANALYSIS: A TOTAL STRESS APPROACH

The VERSAT-2D finite element model as used for the static stress analysis and shown in Fig. 6 are also used for the 2D nonlinear dynamic analyses of earthquake-induced deformations of the Lenihan dam using the total stress approach. The static stresses from VERSAT-2D static analysis were used as the starting point for the nonlinear dynamic analysis.

5.1 General Methodology

The VERSAT-2D (WGI 2019) dynamic analyses of seismic response are always carried out in an undrained condition, whereas a total stress analysis is performed for clayey soils using the VERSAT-CLAY model or an effective stress analysis is conducted for sandy soils using the VERSAT-SAND model; the latter can take into account the effect of PWP on shear strength of sandy soils (i.e., c' and ϕ') as the effective stresses decrease with the increase of PWP, and ultimately can model liquefaction of sandy soils. The VERSAT-SAND model had been adopted for modelling liquefaction of the hydraulic fills in the dynamic analysis of the Upper San Fernando dam (Wu 2001). When the VERSAT-CLAY model is used, the S_u are calculated using the pre-earthquake stresses (i.e., the static stresses), after which they are kept unchanged throughout the entire duration of earthquake loading.

This type of analysis approach was adopted and applied by Professor Finn (Finn et al., 1986) in early 1980's when seismic deformation analyses were still in the early stage and when numerical calculations or finite element dynamic analyses were not so easy or so convenient to perform. The simple and straight-forward analysis method was

further enhanced to become the VERSAT method and then applied in research and engineering design analysis, including simulation of soil liquefaction and its induced large ground deformation (Wu 2001; Finn and Wu 2013). The PWP models that were developed (Wu 2001) for effective stress analysis of sandy soils are not described in here as they are not relevant to the current total stress analysis of the Lenihan dam.

The fundamental difference between the VERSAT approach and other more complicated approaches (e.g., Boulanger 2019) is that the VERSAT method of analysis does not require calibration of soil parameters ahead of a dynamic analysis, but it uses the more fundamental parameters of soils such as V_s for stiffness, undrained shear strength S_u , friction angle (ϕ') for shear strength, normalized SPT blow count $(N_1)_{60}$ for liquefaction resistance, and residual strength if soil liquefies. The approach is in fact very similar to what an engineer would do when a limit equilibrium analysis is to be performed using a slope stability analysis program such as the program SLOPE/W developed by GEO-SLOPE International of Canada.

5.2 Input Ground Motions

Strong ground motions from the 1989 earthquake were measured on the left abutment, left crest and right crest of the Lenihan dam. The recorded accelerations at the left abutment on bedrock are directly used in this case study of Lenihan dam; this earthquake record has horizontal PGAs of 0.44g and 0.41g, and a vertical PGA of 0.14g. In addition, the ground motions calculated from analyses of the Lenihan dam are compared with these recorded at the dam crest in the 1989 earthquake.

Time histories of the recorded horizontal (00°) and vertical accelerations, and their associated displacements, are shown in Fig. 9. For finite element models having a rigid base, the base-case (or default) model in studies reported in here, acceleration time histories (horizontal and vertical) are applied directly at the rigid base, i.e., assuming the input motions were recorded at the rigid base.

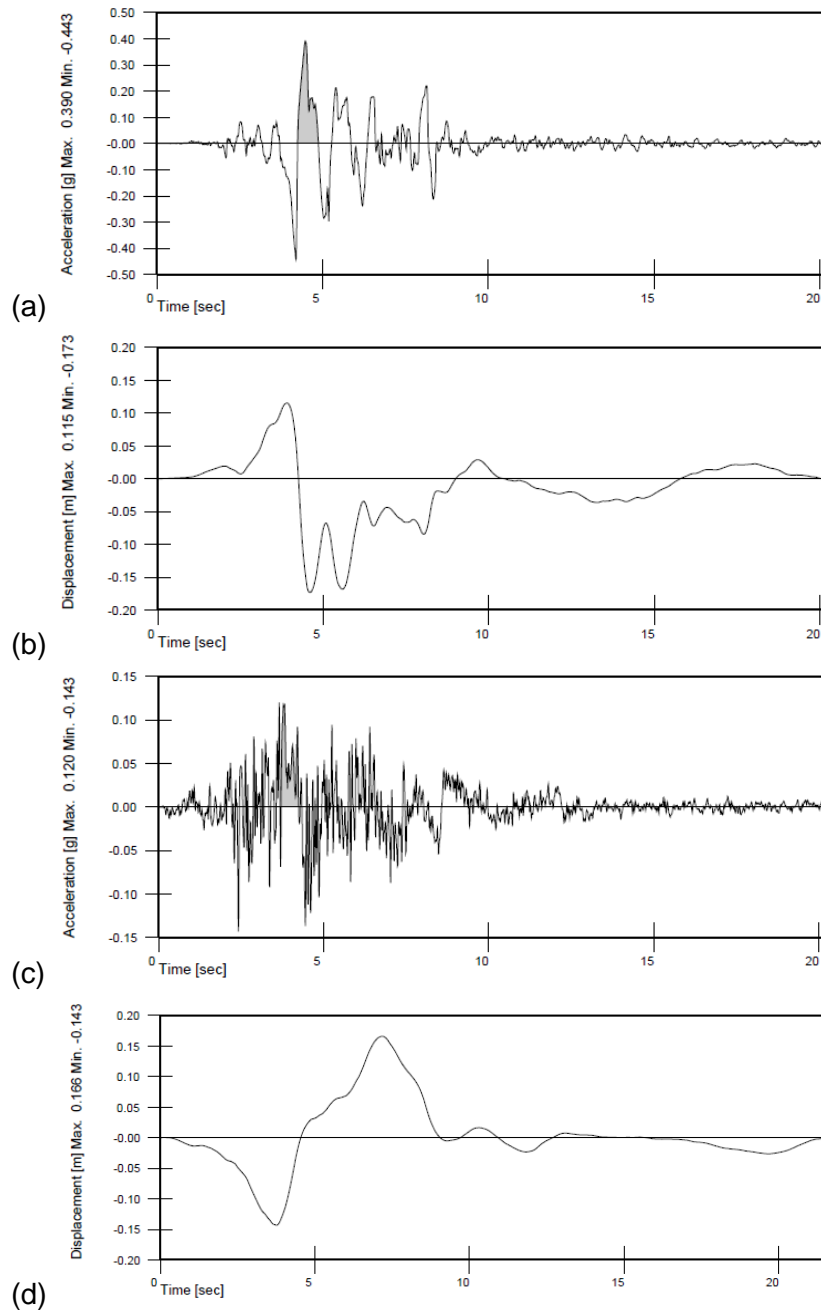


Fig. 9 Time histories recorded at the Lexington dam (showing only 20 s): (a) horizontal accelerations (00°); (b) horizontal displacements (00°); (c) vertical accelerations (UP); (d) vertical displacements (UP). See Appendix C for detailed data of X, Y & Z

5.3 VERSAT-2D Soil Constitutive Models

Soil constitutive models employed in VERSAT-2D dynamic analysis are comprised of the Mohr Coulomb failure criteria for simulation of soil shear strengths and the 2-parameter hysteretic shear stress-strain relationship for modelling of soil stiffness including shear modulus reduction and hysteretic damping increase with the increase of shear strains.

VERSAT-2D (WGI, 2019) uses the hyperbolic stress - strain model to simulate the nonlinear and hysteresis shear stress - strain relationship for soils. The low-strain shear modulus, G_{max} , and the bulk modulus, B , are stress level dependent as defined in the following:

$$[3] \quad G_{max} = K_g P_a \left(\frac{\sigma_m'}{P_a} \right)^m$$

$$[4] \quad B = K_b P_a \left(\frac{\sigma_m'}{P_a} \right)^n$$

where P_a is the atmospheric pressure, 101.3 kPa

K_b is bulk modulus constant

K_g is shear modulus constant; m and n are shear and bulk modulus exponentials, respectively; σ_m' is defined in equation [2].

The relationship between the shear stress, τ_{xy} , and the shear strain, γ , for the initial loading condition is modelled to be nonlinear and hyperbolic as follows:

$$[5] \quad \tau_{xy} = \frac{G_{max} \gamma}{1 + \frac{G_{max}}{\tau_{ult}} \bullet |\gamma|}$$

$$[6] \quad \tau_{xy} = \frac{G_{max} \gamma}{1 + R_f \bullet |\gamma|}$$

where τ_{ult} is the ultimate shear stress in the hyperbolic model; G_{max} is the low-strain shear modulus ($G_{max} = \rho V_s^2$ with ρ being the soil density and V_s being the shear wave velocity).

The τ_{ult} is conveniently determined by introducing a modulus reduction factor R_f , which is shown in equation [6] and detailed in Wu (2001). As shown in Fig. 10 and noted in Finn and Wu (2013), the use of R_f enhances the hyperbolic stress-strain model so that the model can provide a better match to the target dynamic modulus (G) and damping data. For an example, at a shear strain of 0.1%, the G/G_{max} ratio is 0.5 and the

hysteretic damping is 14.5% when R_f value is 1000; they become 0.33 and 22.4%, respectively, when R_f increases to 2000.

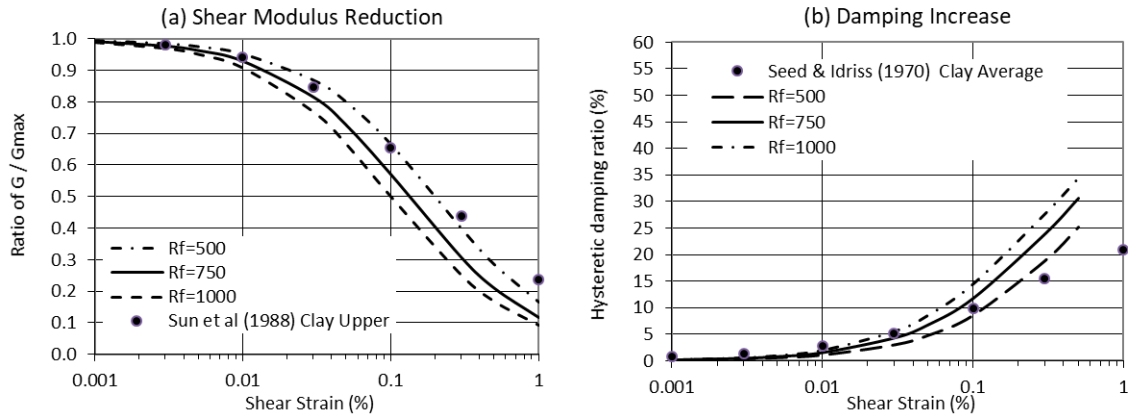


Fig. 10 Shear modulus and hysteretic damping relation with shear strain in VERSAT soil constitutive models: (a) shear modulus decreasing with strain; and (b) damping ratio increasing with strain

The shear stress-strain hysteresis response (simulated using the VERSAT-CLAY model) of soil elements subject to cyclic (sine wave) undrained loading are presented in Fig. 11. These graphs illustrate the difference between the numerical modelling response and the observed true laboratory test response (or the field response in an earthquake) of soils subject to constant stress amplitude cyclic loading.

In Fig. 11(a), when there is no static shear stress (e.g., a generic soil element within a level ground), sine-type input shear stresses do not cumulate strains (or displacements) on the soil element if the applied shear stress amplitude is less than the shear strength. In other words, prior to failure, cyclic shear strains of the element are independent of number of loading cycles. Repetitive loading cycles (either constant stress amplitude or constant strain amplitude) do neither change the size of the stress-strain loops; nor cause more strains (or displacements) on the soil element. When failure of the soil element occurs by applying cyclic stresses with an amplitude of 185 kPa, permanent shear strains cumulate. The portion of stress exceeding the strength (i.e., Δ -stress = 5 kPa) is redistributed to the adjacent soil elements. As shown in Fig. 11(a), the maximum shear stress of the soil element remains at 180 kPa after failure, the Δ -stress causes the element to deform to a new permanent configuration.

The response of soil elements situated on soil slopes with initial static shear stresses is illustrated in Figs. 11(b, c, d) using soil elements 980 and 4470 on the Lenihan dam; see Fig. 6 for their locations on the dam. In this simulation, the dam is subject to two levels of sine-wave accelerations (frequency of 1.0 Hz) at its base, a moderate level with a PGA of 0.2g and a high level with a PGA of 0.3g. In Fig. 11(b), soil element 980 fails in the direction of the static shear stress, causing the element to deform to a new permanent configuration. The portion of stress exceeding the S_u is redistributed to adjacent soil elements, and progressively carried on to other elements if the immediate soil element also fails in shear. The amount of irrecoverable shear strain Δ -strain in Fig. 11(b) that is caused by a loading cycle depends on both magnitude and duration of the loading cycle. The pattern of irrecoverable displacement on soil elements with non-zero static shear stress is somewhat similar to that of a sliding block on inclined plane.

Figs. 11(c, d) show 4-cycle response of soil elements 980 and 4470 subject to the high level of sine-wave accelerations with PGA of 0.3g, indicating much larger shear strains than for PGA of 0.2g. Under 0.3g, the amplitude of cyclic shear stresses in the opposite direction of the static shear stress significantly increases; for soil element 980, this opposite direction cyclic stresses reach an amplitude of about 178 kPa that indicates a near-failure stress condition. Each hysteresis loop for element 980 has a double strain amplitude of up to 0.25%, indicating a reasonable amount of hysteretic damping. The shear stress and strain loops in Fig. 11(d) for soil element 4470, located in the unsaturated Zone 4 soils, are typical response of frictional soils modelled using the VERSAT-SAND model.

It is seen that the shaking-induced pore water pressure (PWP) is irrelevant in the VERSAT total stress analysis. A more complicated constitutive model (often a plasticity model) would adopt the effective stress method of analysis for simulating the undrained response (Boulanger 2019); the response would be governed or greatly influenced by the amount of PWP predicted (or estimated) from the plasticity model. While having a more advanced soil model is beneficial and needed for understanding undrained response of the low or high plasticity clayey soils, use of total stress model in this study demonstrates the robustness and efficiency desired by practicing engineers in preliminary design or analyses.

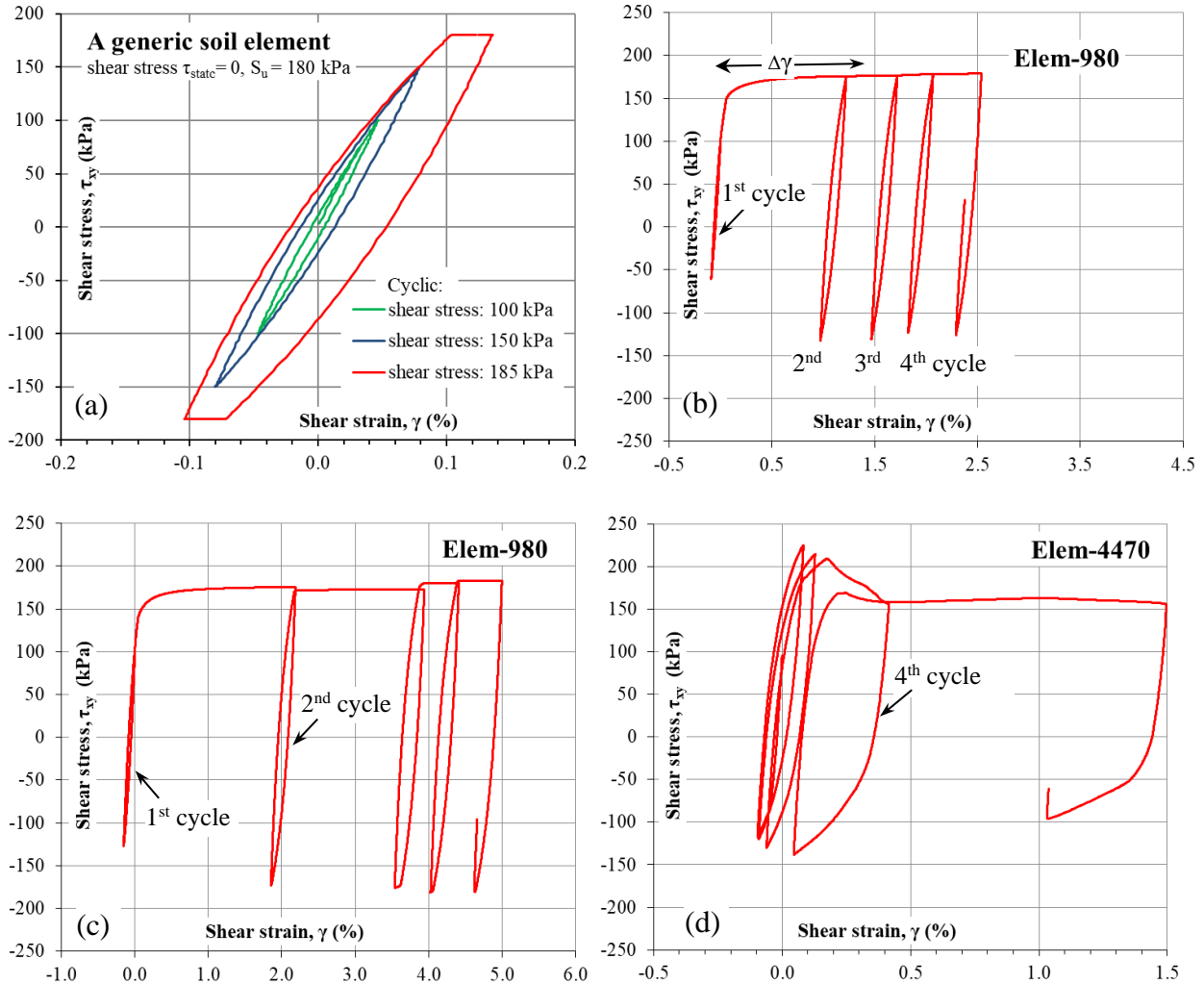


Fig. 11 Shear stress-strain response of the Lenihan dam fills in constant shear stress amplitude cyclic (sine wave) loading: (a) for a generic soil element ($\tau_{st} = 0$, $S_u=180$ kPa); (b) for soil element 980 ($\tau_{st} = 102$ kPa) under the 0.2g input accelerations; (c) for soil element 980 under the 0.3g input accelerations; and (d) for soil element 4470 in unsaturated Zone 4 under the 0.3g input accelerations.

6.0 SEISMIC RESPONSE OF THE DAM: SECTION W-W

6.1 Seismic Deformation and Strain: Case 2A(g)

The soil and model parameters for dynamic analyses of Section W-W' are shown in Table 2. During dynamic loading, the bulk modulus of a soil element is calculated from its static mean normal effective stress, after which it is kept unchanged in the dynamic

analysis. Other parameters used in the dynamic analyses include viscous damping of 2%, $DT = 0.001$ s and $R_f = 0.75 \cdot K_g$.

The end-of-earthquake deformations of the dam are presented in Figs. 12(a, b). The horizontal displacement contours in Fig. 12(a) indicate that the dam deforms in two opposite directions from the central part of the dam. The lateral spreading movements of the dam body caused the dam to settle in Fig. 12(b). The dynamic analysis calculated dam crest displacements of 0.06 m and -0.26 m (horizontal and vertical) using the LEX-00° horizontal and the vertical input accelerations; the calculated crest displacements are 0.13 m and -0.27 m (horizontal and vertical) using the LEX-90° horizontal and the vertical input accelerations. The computed dam crest settlements of 0.26-0.27 m are in good agreement with the actual dam crest settlement of 0.25 m observed immediately after the 1989 earthquake.

The deformation pattern of the dam is consistent with the computed shear strains of the dam, as shown in Fig. 13. Similar to observations of clay embankment in a limit equilibrium stability analysis, significant shear straining zone tends to develop first near the bottom of a slope due to high shear stresses. Shear strains between 1.5 and 3% were predicted to have occurred in the lower part of the upstream slope, i.e., in the saturated dam fills immediately above the bedrock. Soil elements in a large area near the bottom of the high plasticity soils (Zone 2L) under the downstream slope were predicted to have shear strains between 3 and 5%.

Shear stress-strain hysteresis response histories are of great interest and values in understanding a nonlinear dynamic analysis of soils. As shown in Fig. 14, the hysteretic stress-strain relation of soils provides an insight look of the model; it basically illustrates to a great extent how the soil material is modelled in a dynamic analysis. Shear stress-strain histories (or traces) obtained from the VERSAT-2D dynamic analysis of the Section W-W' are shown in Fig. 14(a) and in Fig. 14(b) for soil elements 4543 and 980, respectively. The locations of the two elements in the cross section are shown in Fig. 6. Although the cumulative shear strains are about -1.8% and +2.8% in elements 4543 and 980, respectively, the incremental strains in any hysteresis loops are less than or in order of 0.3%; the damping in the hysteresis loops is reasonable.

Table 2. Total stress dynamic response history analyses of Section W-W':
Case 2A(g) soil parameters

Unit	VERSAT model	K_b	n	K_g	m	Unit weight	Drained, ϕ' (°)	Undrained strength	model MAT#
Unit 1 ^c	CLAY	20500	0	3713	0.5	21.7		S_u ^b	Mat-8
Unit 1	SAND	11139	0.5	3713	0.5	18.8	37.5	-	Mat-1
Unit 2U	SAND	9195	0.5	3065	0.5	18.8	35.5	-	Mat-4
Unit 2L ^c	CLAY	20500	0	1033	0.5	19.5		S_u ^c	Mat-3
Unit 2L	SAND	3100	0.5	1033	0.5	17.6 ^d	25.5	-	Mat-6
Unit 4	SAND	14151	0.5	4717	0.5	19.5	35.0	-	Mat-5
Rock	ELAS	60000	0	30000	0	25.5			Mat-2

Note: Unit weight in kN/m^3 .

^a the portion of soil is below the inferred phreatic surface and saturated.

^b $S_u = c + \sigma_m' \tan(\Psi)$ where $c = 20 \text{ kPa}$, $\Psi = 23.7^\circ$.

^c $S_u = c + \sigma_m' \tan(\Psi)$ where $c = 20 \text{ kPa}$, $\Psi = 17.7^\circ$.

^d Moisture unit weight.

The shear stress-strain response of unsaturated dam fills in Zone 4, which was modelled using the VERSAT-SAND model and the drained shear strength parameters (i.e., $\phi' = 35^\circ$ and a cohesion of zero), is represented by the response of soil element 4470 (see Fig. 6 for its location on the dam) and shown in Fig. 14(c). The maximum shear strain of soil element 4470 is about 0.15%.

The computed time histories of horizontal (DIS-X) and vertical (DIS-Y) displacements at the dam crest are shown in Fig. 15(a). The graph also includes for comparison the computed horizontal displacements at the mid-height (node 7943) of the downstream slope of the dam. The analyses predicted, at the end of earthquake the dam crest moves 60 mm and node 7943 moves 200 mm, both horizontally and in the downstream direction. Majority (about 0.25 m) of the crest settlement (DIS-Y) was predicted to have occurred, as expected in an undrained total stress analysis, during the early 10 s of shaking; in reality, settling of the dam may have continued during shaking after 10 s. The time series of the computed horizontal accelerations at the dam crest is shown in Fig. 15(b); the input accelerations (LEX-00° with a horizontal PGA of 0.44g) at the bedrock foundation of the dam are also included in the figure

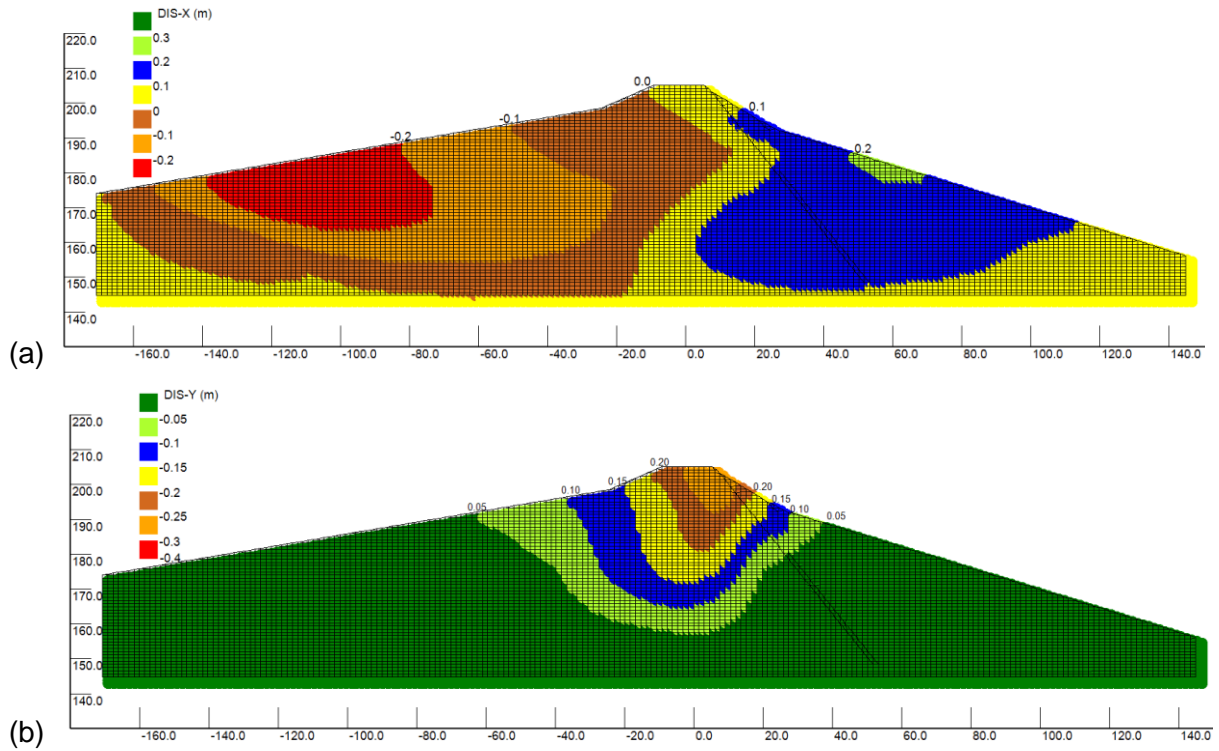


Fig. 12 Section W-W' at end-of-earthquake for LEX-00°: (a) contours of horizontal (DIS-X) displacements; (b) contours of vertical (DIS-Y) displacements (negative-Y sign represents settlement).

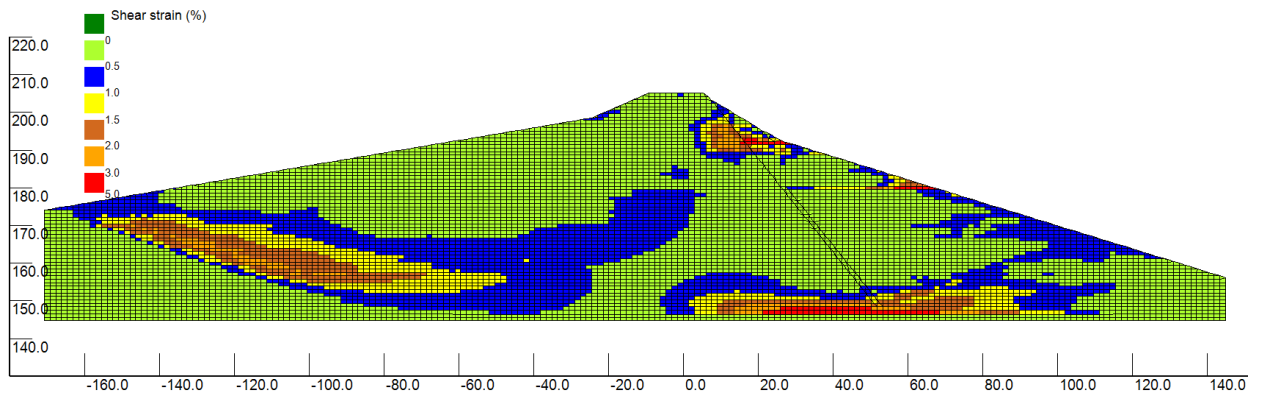


Fig. 13 Section W-W' at end-of-earthquake for LEX-00°: contours of absolute shear strains (%).

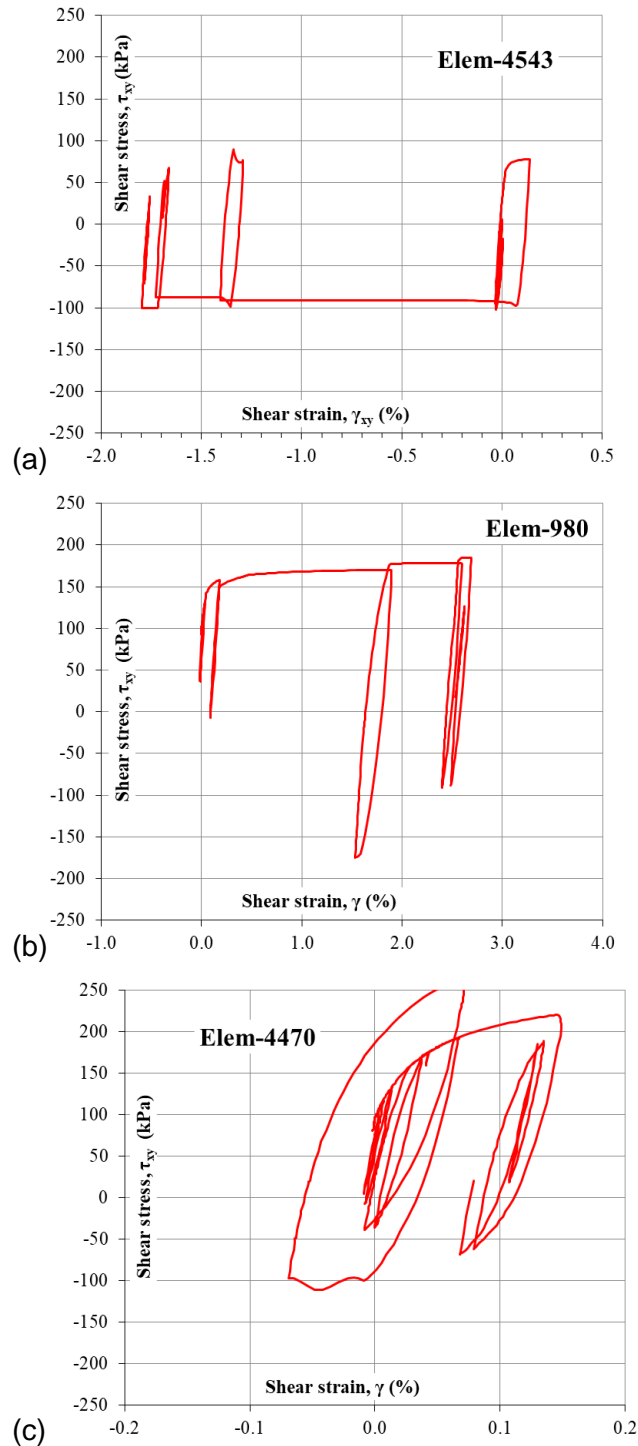


Fig. 14 Computed shear stress-strain histories under LEX-00°: (a) soil element 4543 (upstream saturated Zone 1); (b) soil element 980 (saturated lower core in Zone 2L); and (c) soil element 4470 (downstream unsaturated Zone 4).

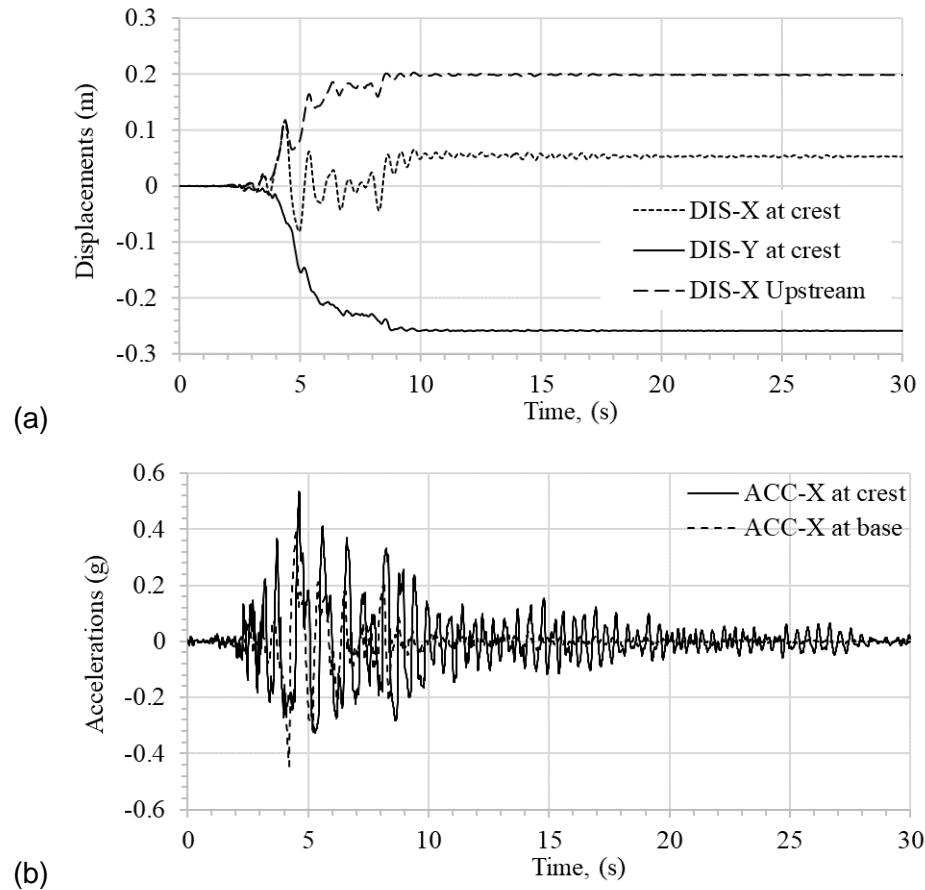


Fig. 15 Response histories of Section W-W' under LEX-00°: (a) horizontal (DIS-X) and vertical (DIS-Y) displacements at the dam crest and DIS-X at node 7943; (b) horizontal accelerations (ACC-X) at the dam crest and the input ACC-X at the base

6.2 Sensitivity Analyses: Effect of S_u and R_f

Parametric analyses of the Section W-W' included these scenarios: effect of viscous damping; the impact of S_u and R_f ; and the effect of dam foundation stiffness (i.e., shear wave velocity V_{s30}) on dynamic response of the dam. The results of these analyses are summarized in Table 3.

The effect of S_u and R_f on dam response in earthquake loading was studied using the following parameters:

- Middle S_u with $R_f = 1.0 \bullet K_g$: using the Middle strength line in Fig. 16 with $c = 40$ kPa and respective Ψ in equation [1]. The results of this study are reported as Case 2A(y) in Table 3.

The results of this sensitivity study are compared in Table 3 with Case 2A(g), in which the base-case parameters in Table 2 were used, i.e., $R_f = 0.75 \cdot K_g$ and the strength (S_u) line in Fig. 4 with $c = 20$ kPa and respective Ψ in equation [1]. As seen in Table 3, the dam crest settlements vary between 0.32-0.35 m [for Case 2A(y) with LEX 00°-90°] and 0.26-0.27 m [for Case 2A(g) also with LEX 00°-90°] when these two sets of parameters were used in analyses. For Section W-W' of Lenihan Dam, the R_f has a significant impact on dam deformations, 25% increase of R_f (i.e., a reduction of shear modulus at shear strain of 0.1% by about 13% for Zone 2L fill) resulted more dam crest settlement although the shear strength S_u has increased by 20 kPa for saturated soils in Zones 1 and 2L.

For comparison with studies by others (Hadidi et al. 2014), the S_u used in this sensitivity study are plotted in Fig. 17. It is seen that using the Middle strength line in Fig. 16, the S_u values are comparable with these calculated using the equations for S_u of Hadidi et al. (2014). Note that the vertical effective stress (σ'_y) used for Fig. 17(c) were calculated in this study using the VERSAT model in Fig. 6, a full reservoir level of El. 199 m and a higher (than in Fig. 6) phreatic surface in the dam (SCVWD 2012).

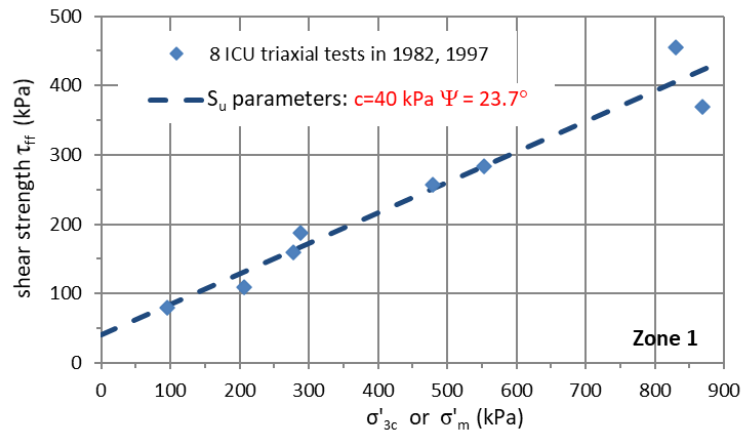
Table 3. Computed Accelerations (PGAs) and displacements of the Section W-W'

CASES	Details of Cases	Input Motions	Dam crest			Downstream DIS-X ^a , m
			ACC-X, g	DIS-X, m	DIS-Y, m	
CASE 2A: phreatic surface as in Dawson & Mejia (2021)	2A(g). Undrained strength S_u in Fig. 4	LEX-00	0.54	0.06	-0.26	0.20
		LEX-90	0.52	0.13	-0.27	0.24
	2A(h). As 2A(g), 2.5% viscous damping	LEX-00	0.51	0.03	-0.23	0.18
		LEX-90	0.47	0.09	-0.22	0.21
	2A(y). As 2A(g), Middle strength S_u in Fig. 16 ($c = 40$ kPa) and $R_f = 1.0 \cdot K_g$	LEX-00	0.47	0.20	-0.32	0.26
		LEX-90	0.46	0.28	-0.35	0.27
	2A(g2). As 2A(g), K_g in Table 2 reduced by 25%	LEX-00	0.56	0.05	-0.29	0.19
	2A_el(y). As 2A(y), elastic base $V_s = 1070$ m/s	LEX-00	0.39	0.16	-0.27	0.20

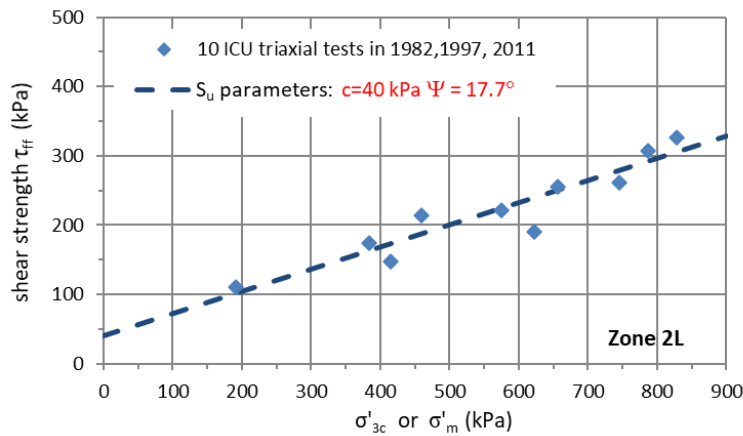
Note: The dam crest after the 1989 Loma Prieta earthquake settled 250 mm (10-in) on average by measurement and moved 62 mm (2.5-in) horizontally and towards the downstream; except noted otherwise, viscous damping of 2%, $R_f = 0.75 \cdot K_g$ and $DT = 0.001$ s were used in all dynamic analyses; for the rigid base model, vertical input accelerations were always applied with the horizontal input accelerations for both the 0° and 90° components.

^aDownstream DIS-X is the horizontal displacements at the finite element node No. 7943 located at X = 68.67 m and Y = 179.53 m in Fig. 6.

^bDT is the time increment (s) selected for numeric integration.

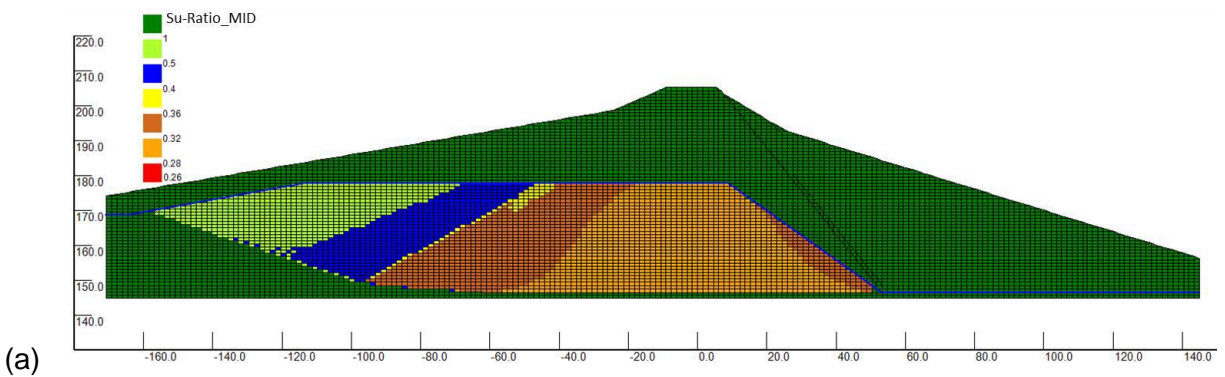


(a)



(b)

Fig. 16 Middle shear strengths and the mean consolidation pressure (σ'_m) derived from test data of the ICU triaxial test specimens from saturated soil samples of: (a) Zone 1; (b) Zone 2L.



(a)

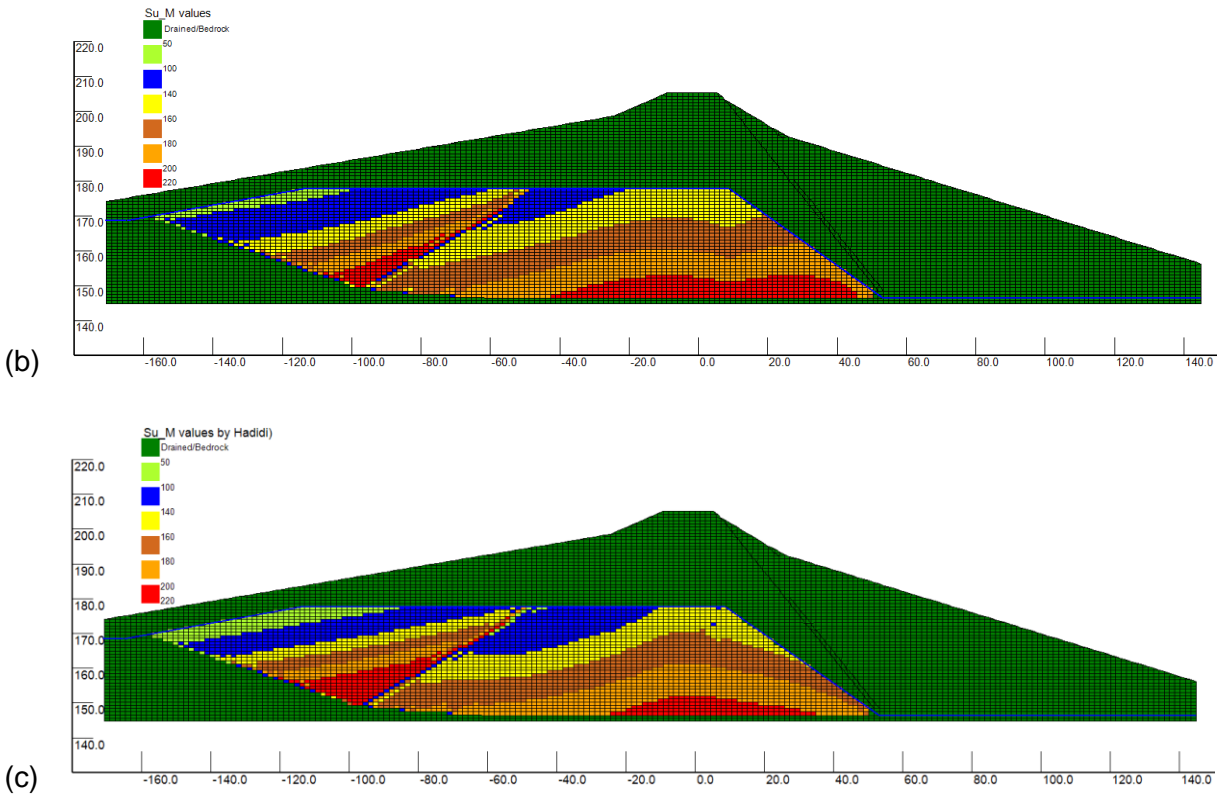


Fig. 17 Middle shear strength (S_u) of saturated Zone 1 ($c = 40$ kPa, $\Psi = 23.7^\circ$) & Zone 2L ($c = 40$ kPa, $\Psi = 17.7^\circ$): (a) distribution of S_u values; (b) distribution of S_u -ratios ($=S_u/\sigma'_y$); (c) calculated using equations by Hadidi et al. (2014) and stresses at full reservoir level (El. 199.0 m).

6.3 Dam Crest Acceleration Response Spectra

The 5% damped response spectra of the computed horizontal accelerations at the dam crest of Section W-W' and for Case 2A(y) (PGA of 0.47g for LEX-00°) in Table 3 are shown in Fig. 18; the results indicate a peak spectral acceleration (S_a) of 1.78g at 1.0 s and a second peak $S_a = 1.5$ g at 0.5 s. The spectral peaks agree well with these of the recorded accelerations (LEX-00° with a PGA of 0.45g) at the dam crest that have a peak $S_a = 2.25$ g at 1.0 s and a second peak $S_a = 1.1$ g at 0.5 s.

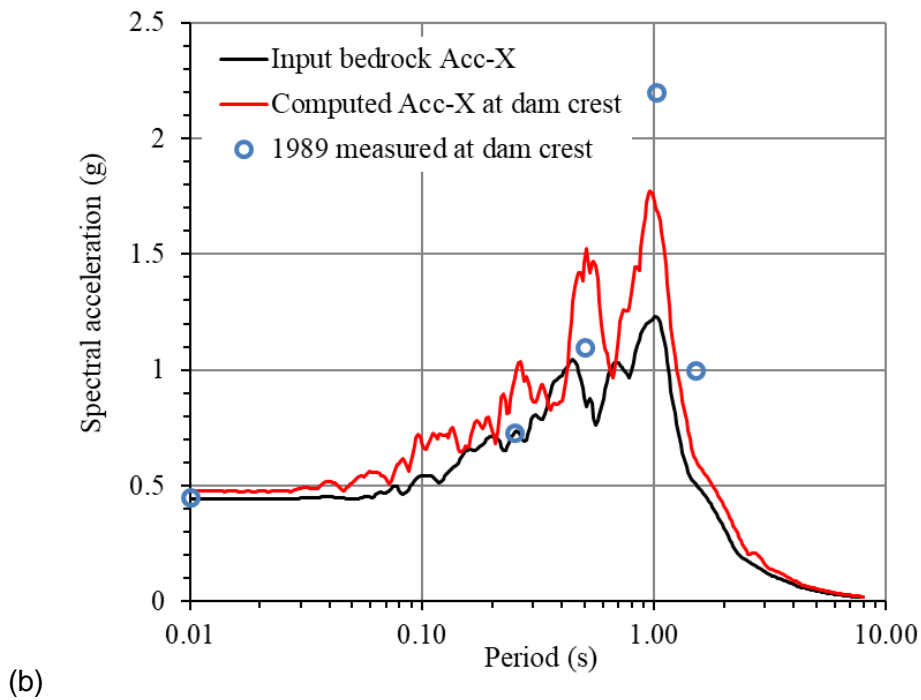
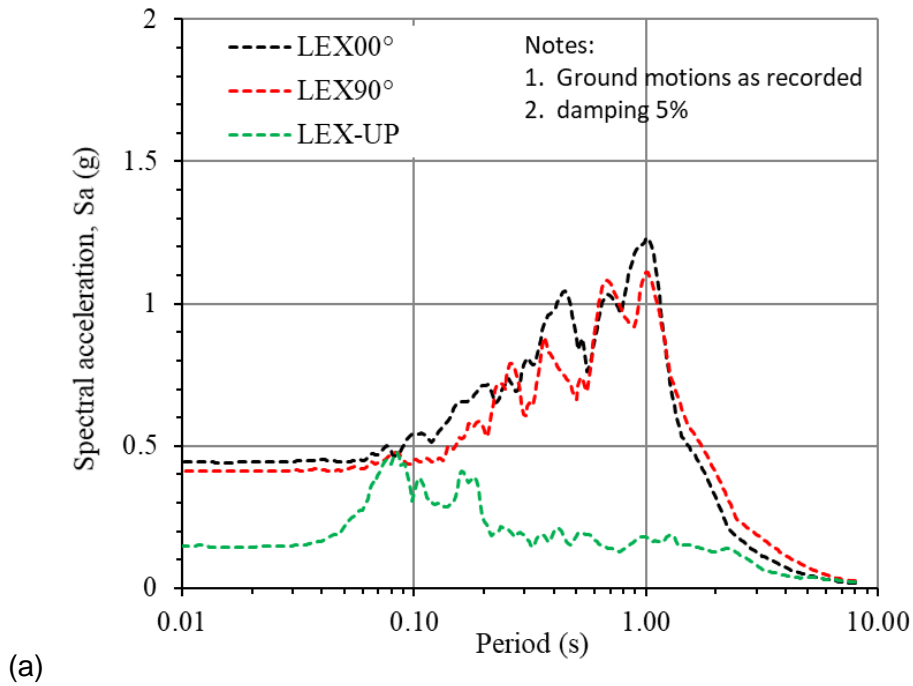


Fig. 18 Spectral accelerations (S_a - 5% damped): (a) input motions of LEX-00°, LEX-90° and LEX-UP recorded on bedrock at the left abutment of the dam; (b) calculated [Section W-W and Case 2A(y)] and recorded accelerations at the dam crest for LEX-00°

6.4 Effect of Dam Foundation Rock Stiffness

This sensitivity analysis of foundation bedrock stiffness was completed assuming that the input motion (LEX-00°) was the recorded ground motion on a free field surface of the same rock as the dam foundation. In here, a 1-m thick bedrock layer was included at the base of the model (see Fig. 6) to represent the elastic half space of bedrock with a shear wave velocity of 1070 m/s (i.e., assuming the Lenihan dam has bedrock V_{s30} of the Lexington dam rock foundation); the entire base (all finite element nodes on the base) was set to have a viscous boundary that is based on the formulations developed by Lysmer and Kuhlemeyer (1969). The “Outcropping Velocity” input option (WGI 2019) in VERSAT-2D program was turned on; the recorded horizontal velocities (also downloaded from the PEER website) were applied as outcropping input velocities.

The shaking intensity (PGA) and dam crest settlement for the elastic base case [i.e., Case 2A_el(g) reported in Table 3] are reduced to 0.27 m from 0.32 m; the latter was computed using the respective input accelerations but applied to the rigid base [i.e., Case 2A(g) in Table 3]. It is not a surprise that use of the elastic half space model have resulted in reduced shaking intensity (0.39g at the dam crest with an elastic base vs. 0.47g for a rigid base model) and dam crest settlement. The high stiffness of Zone 1 fill in the upstream slope and Zone 4 fill in the downstream slope has probably contributed to the reduction of shaking energy transmitted to the dam body; the shear wave velocities (V_s) in Zone 1 and Zone 4 are about 500-700 m/s (SCVWD 2012).

6.5 Effect of Shear Wave Velocity of the Dam Fills

In this sensitivity analysis on the shear wave velocity of the dam fills (Zones 1, 2L, 2U and 4), the low-strain shear modulus constant K_g is assigned values of 75% the corresponding values in Table 2 for each of the four zones, i.e., a reduction of shear stiffness of all dam fills by 25%. This sensitivity study is reported as Case 2A(g2) in Table 3.

The dam crest settlement increases to 0.29 m [Case 2A(g2) for LEX 00°] from 0.26 m (also for LEX 00°) for the corresponding Case 2A(g). The increase of settlement is likely caused by the decrease in the fundamental frequency of the dam due to a less stiff dam that brings the frequency of the dam closer to the predominant frequency of the input ground motions, see Fig. 18(a) for their response spectra.

6.6 Impact of Phreatic Surface in the Dam

Prior to adoption of the phreatic surface in the dam by Dawson and Mejia (2021), analyses were already performed using an assumed phreatic surface of the dam that was derived from the piezometer readings reported in Report LN-3 (SCVWD 2012). The VERSAT model and its assumed phreatic surface is shown in Fig. 19, where the reservoir level in the 1989 earthquake was assumed to be El. 174 m (570.7 ft). In addition, a portion of Zone 4 fill in the downstream is considered fully saturated and modelled using material Mat-7 in Fig. 19.

The undrained shear strengths (S_u) for the saturated Zone 4 fill, derived from results of ICU triaxial tests, are shown in Fig. 20, together with S_u for the upper core Zone 2U (although they are not used in this study of the phreatic surface effect, i.e., in the unsaturated zone).

The results of this sensitivity study are presented in Table 4. Although the downstream displacement at Node 7943 increases to 0.31 m for Case 2(g) in Table 4 from 0.20 m for Case 2A(g) in Table 3, the computed dam crest settlements are very much the same [0.27 m for Case 2(g) in here vs. 0.26 m for the base-case Case 2A(g)]. Similar comparison is also observed for Case 2(y) in Table 4.

Table 4. Summary of Results for Section W-W' with the assumed phreatic surface in Fig. 19

CASES	Details of Cases	Input Motions	Dam crest			Downstream DIS-X ^a , m
			ACC-X, g	DIS-X, m	DIS-Y, m	
CASE 2: phreatic surface assumed	2(g). Undrained strength S_u in Fig. 4	LEX-00	0.49	0.13	-0.27	0.31
	2(h). As 2(g), 2.5% viscous damping	LEX-00	0.49	0.10	-0.23	0.28
	2(y). As 2(g), Middle strength S_u ($c = 40\text{kPa}$) and $R_f = 1.0 \cdot K_g$	LEX-00	0.44	0.25	-0.32	0.35

Note: The dam crest after the 1989 Loma Prieta earthquake settled 250 mm (10-in) on average by measurement and moved 62 mm (2.5-in) horizontally and towards the downstream; except noted otherwise, viscous damping of 2%, $R_f = 0.75 \cdot K_g$ and $DT = 0.001$ s were used in all dynamic analyses; for the rigid base model, vertical input accelerations were always applied with the horizontal input accelerations for both the 0° and 90° components.

^aDownstream DIS-X is the horizontal displacements at the finite element node No. 7943 located at $X = 68.67$ m and $Y = 179.53$ m in Fig. 6.

^bDT is the time increment (s) selected for numeric integration.

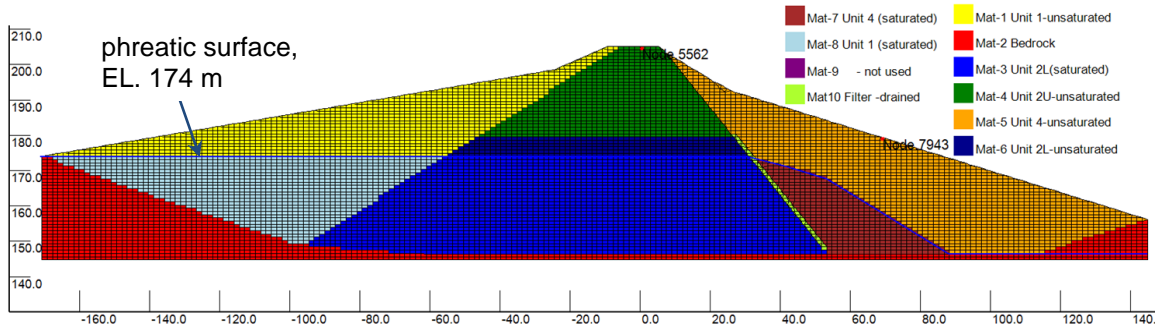
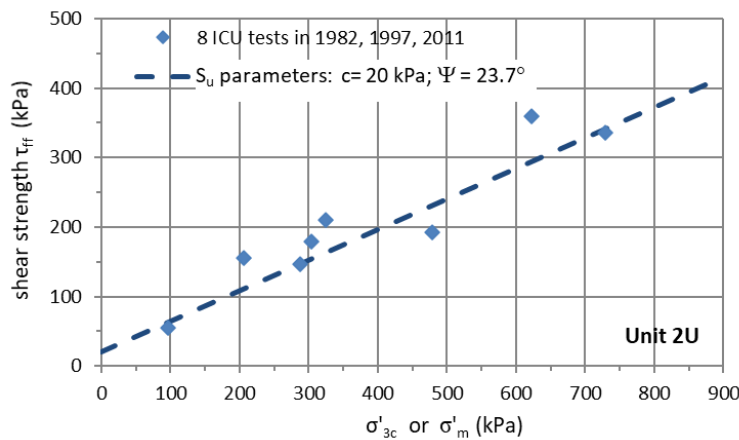
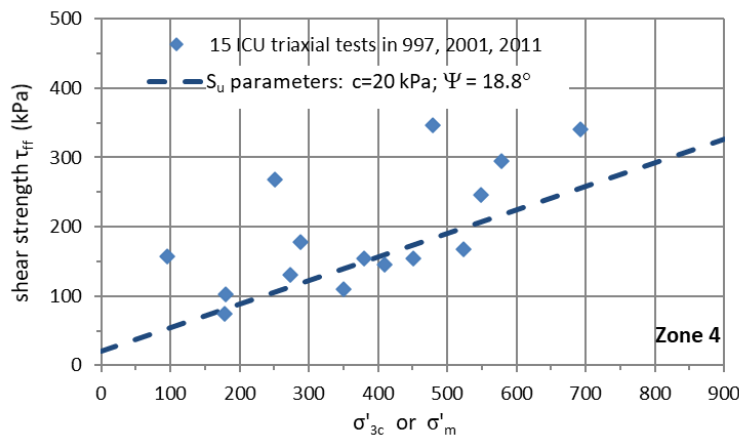


Fig. 19 Section W-W' Case 2 with an assumed phreatic surface in the dam for a reservoir level at EL. 174.0 m (570.7 ft): a portion of Zone 4 fill in the downstream is saturated [Mat-7]



(a)



(b)

Fig. 20. Shear strengths and the mean consolidation pressure (σ'_m) derived from test data of the ICU triaxial test specimens from saturated soil samples of: (a) Zone 2U; (b) Zone 4.

7.0 SEISMIC RESPONSE OF SECTION B-B

7.1 VERSAT Finite Element Model

The cross-section B-B' (see Fig. 2 for its alignment on the dam) of the dam is shown in Fig. 21. The VERSAT finite element model (9843 elements for soil and rock) and the assumed phreatic surface (same as Case 2 analyses of Section W-W') are shown in Fig. 22, where the reservoir level in the 1989 earthquake was assumed to be El. 174 m (570.7 ft). In addition, a portion of Zone 4 fill in the downstream is considered fully saturated and modelled using material Mat-7 in Fig. 22. The soil and model parameters used for Section B-B' are these listed on Table 2, i.e., the same as those used for Section W-W'.

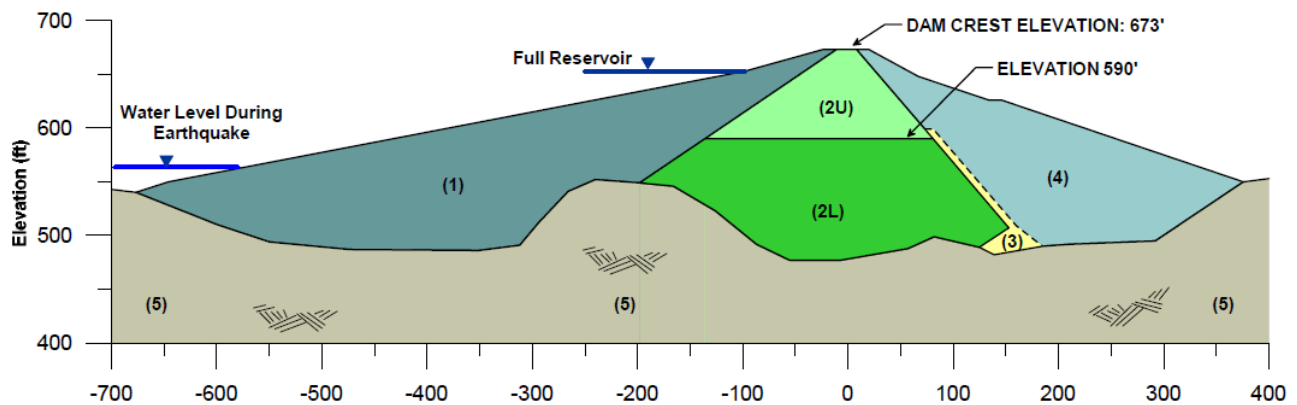


Fig. 21. Lenihan Dam: cross-section B-B' showing zones of dam fills and the foundation bedrock (after SCVWD 2012). Note: horizontal distance in ft.

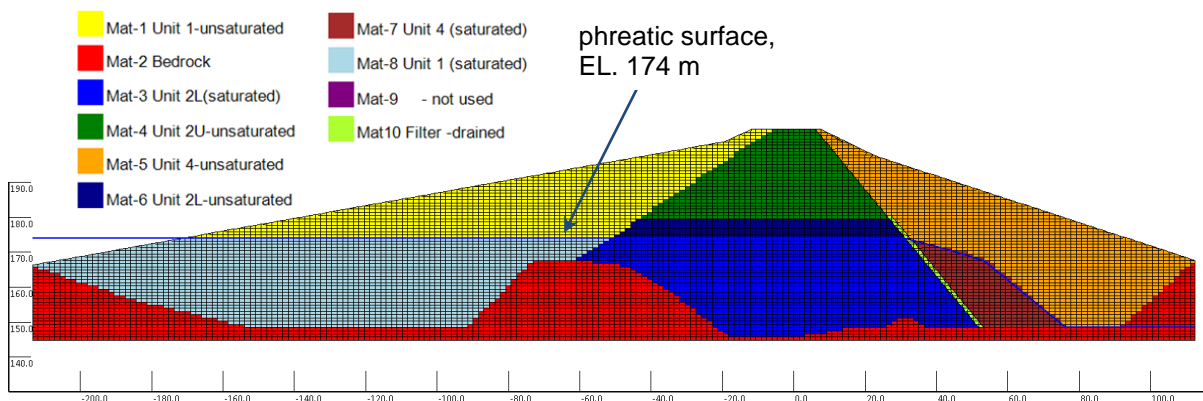


Fig. 22 VERSAT finite element model (9843 elements) of Section B-B': Assumed reservoir level at El. 174 m. Note: horizontal distance (X) and vertical elevation (Y) in m.

7.2 Seismic Deformation and Strain

The end-of-earthquake displacements and peak accelerations (PGA) at the dam crest are shown in Table 5; the computed dam crest settlements are about 0.10-0.22 m for Cases 1(n, q, k), all using input horizontal (LEX-00°) and vertical accelerations.

For Case 1(q), the end-of-earthquake deformations are shown in Fig. 23(a) and Fig. 23(b) for horizontal and vertical displacement contours, respectively; the corresponding values of shear strains are plotted in Fig. 23(c).

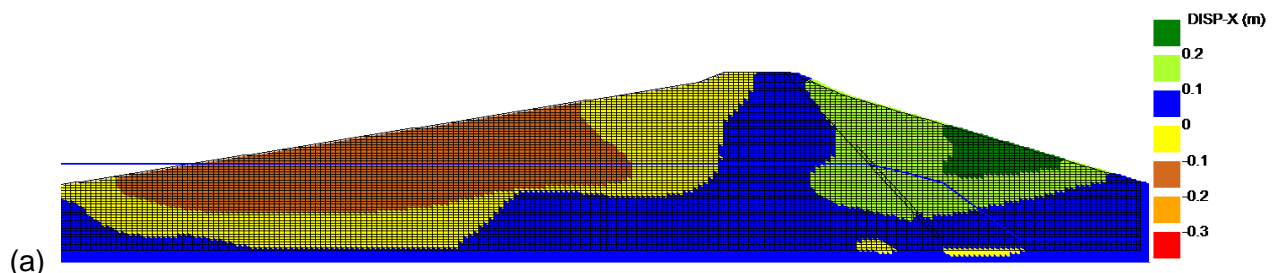
Obviously, the rock knob at about 60 m upstream of the dam crest and the relatively high bedrock elevation downstream of the crest have significantly impact on the shear strain and deformation pattern of the dam under the 1989 earthquake. The shear strains in soil elements near the bottom of the high plasticity soils (Zone 2L) under the downstream slope are predicted to be about 0.5-1.5%, which are much less than about 3-5% for Section W-W'.

Table 5. Displacements and accelerations (PGA) at the dam crest for Section B-B'

CASES	Details of Cases	Input Motions	Dam crest		
			ACC-X, g	DIS-X, m	DIS-Y, m
CASE 1: phreatic surface assumed	1(n). Undrained strength S_u in Fig. 4	LEX-00	0.40	0.0	-0.10
	1(q). As 1(n), $R_f = 1.0 \cdot K_g$	LEX-00	0.37	0.02	-0.15
	1(j). As 1(q), 1% viscous damping	LEX-00	0.34	0.04	-0.21

Note: The dam crest after the 1989 Loma Prieta earthquake settled 250 mm (10-in) on average by measurement and moved 62 mm (2.5-in) horizontally and towards the downstream; except noted otherwise, viscous damping of 2%, $R_f = 0.75 \cdot K_g$ and $DT = 0.001$ s were used in all dynamic analyses; for the rigid base model, vertical input accelerations were always applied with the horizontal input accelerations for both the 0° and 90° components.

^aDT is the time increment (s) selected for numeric integration.



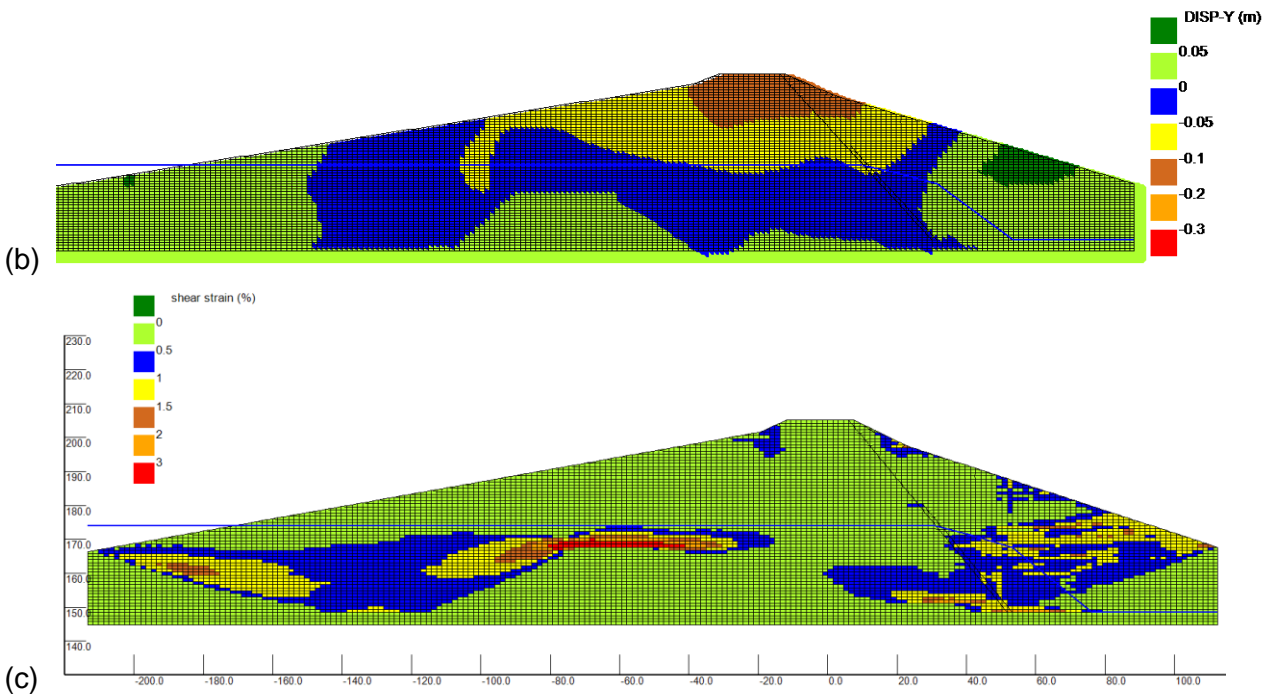


Fig. 23 Section B-B' Case 1(q) at end-of-earthquake for LEX-00°: (a) contours of horizontal (DIS-X) displacements; (b) contours of vertical (DIS-Y) displacements (negative sign represents settlement); (c) contours of absolute shear strain (%).

8.0 DISCUSSION

Uncertainties related to the case study of Lenihan Dam would include effect of the topography of the dam's rock foundation on ground motions propagating from the bedrock to the dam body. Previous studies by others (Hadidi et al. 2014; Dawson and Mejia 2021) appear to have significantly underpredicted the crest settlement of the dam under the 1989 earthquake. For the case of the 2D plane strain dynamic analyses by Hadidi et al. (2014), the underestimate of crest settlement could be the alignment of cross section B-B' in Fig. 2 adopted in their study; the bedrock surface there is noticeably higher in elevation and more irregular than the cross-section W-W'. Both Sections W-W' and B-B' have been analyzed in this study. For the case of the 3D dynamic analysis by Dawson and Mejia (2021), they suggested that it is possible that post seismic consolidation of the lower core (Zone 2L) contributed to the measured crest settlement.

9.0 CONCLUSIONS

Two-dimensional (2D) plane strain total stress dynamic analyses of the Lenihan dam under the 1989 Loma Prieta earthquake were conducted using the finite element program VERSAT-2D (WGI 2019) and its built-in soil constitutive models, the VERSAT-CLAY model, for simulation of the undrained response of saturated dam fills with a total stress approach; the VERSAT-SAND model was adopted for modelling the unsaturated dam fills above the phreatic surface. The 61-m high compacted earthen dam consisted primarily of low plasticity clayey sands and clayey gravels for Zones 1, 2U and 4, whereas the lower core (Zone 2L) of the dam was comprised of highly plastic sandy clays to silty sands or sandy silts. subjected to earthquake ground motions with estimated peak horizontal bedrock accelerations of 0.44g, the dam crest settled 0.25 m on average, developed longitudinal cracks on the dam faces.

The accelerations recorded on bedrock at the left abutment of the dam was directly applied as the input motion for the dynamic analyses of the dam. The VERSAT-2D dynamic analyses showed that the proposed S_u/σ'_m approach for calculating the undrained strengths of the saturated dam fills provides reasonably conservative approach for engineering analysis and design; the calculated dam crest settlements ranged from 0.22 to 0.35 m (among various sensitivity analyses on phreatic surface, soil stiffness and strength parameters) are in good agreement with the measured average of 0.25 m. The computed distribution of shear strains, using Section W-W', indicated that the dam experienced deep deformations with lateral spreading type of shear failure; shear strains about 3-5% were predicted to occur near the bottom of the high plasticity and saturated soils (Zone 2L) under the downstream slope.

The analyses also demonstrated that the computed accelerations at the dam crest agree well with the recorded ones; the computed crest horizontal accelerations have PGAs between 0.39 and 0.54g, while the recorded accelerations had PGAs of about 0.45g. The computed accelerations have a spectral peak of $S_a = 1.78$ g at 1.0 s while the recorded one has a similar peak of $S_a = 2.25$ g also at about 1.0 s.

ACKNOWLEDGMENTS 致谢

Any opinions, findings, conclusions, or recommendations expressed herein are those of the author and do not represent the views of any other parties. The anonymous

reviewers provided valuable comments and suggestions related to input ground motions and discussions on the undrained response of saturated clayey soils that significantly improved the paper. Engineers of the Santa Clara Valley Water District in California provided access to engineering data for Lenihan Dam. The author sincerely thanks them for their supports.

REFERENCE

Boulanger, R. W. 2019. "Nonlinear dynamic analyses of Lenihan Dam in the 1989 Loma Prieta earthquake." *J. Geotech. Geoenviron. Eng.* 145 (11). [https://doi.org/10.1061/\(ASCE\)GT.1943-5606.0002156](https://doi.org/10.1061/(ASCE)GT.1943-5606.0002156).

Bray, J. D., and J. Macedo. 2019. "Procedure for estimating shear-induced seismic slope displacement for shallow crustal earthquakes." *J. Geotech. Geoenviron. Eng.* 145 (12). [https://doi.org/10.1061/\(ASCE\)GT.1943-5606.0002143](https://doi.org/10.1061/(ASCE)GT.1943-5606.0002143).

Dawson, E. and L. Mejia. 2021. Three-dimensional analysis of the Lenihan dam for the Loma Prieta earthquake. In *Proc. 2021 Annual United States Society of Dams Conference*. Online

Duncan, J. M., and S. G. Wright. 2005. *Soil strength and slope stability*. New York: Wiley.

Finn, W. D. L, M. Yogendrakumar, N., Yoshida, and H. Yoshida. 1986. *TARA-3: A program for nonlinear static and dynamic effective stress analysis*. Vancouver, BC, Canada: Department of Civil Engineering, University of British Columbia.

Finn W. D. L and G. Wu. 2013. "Dynamic analyses of an earthfill dam on over-consolidated silt with cyclic strain softening." In *Proc., 7th Int. Conf. on Case Histories in Geotechnical Engineering*, Keynote paper, edited by S. Prakash. Chicago, US,

Hadidi, R., Y. Moriwaki, J. Barneich, R. Kirby, and M. Mooers. 2014. "Seismic deformation evaluation of Lenihan Dam under 1989 Loma Prieta Earthquake." In *Proc. 10th US National Conf. on Earthquake Engineering, Frontiers of Earthquake Engineering*. Oakland, CA: Earthquake Engineering Research Institute.

Harder, L. F., Jr., J. D. Bray, R. L. Volpe, and K. V. Rodda. 1998. "Performance of earth dams during the Loma Prieta earthquake." In *US Geological Survey Professional Paper 1552-D*, edited by T. L. Holzer, 3–26. Washington, DC: US Government Printing Office, USGS.

Ladd, C. C., and R. Foote. 1974. "New design procedure for stability of soft clays." *J. Geotech. Eng.* 100 (7): 763-786. US: ASCE.

Ladd, C. C. and D. J. DeGroot. 2004 revised. "Recommended practice for soft ground site characterization: Arthur Casagrande Lecture." In *Proc. 12th Pan-American Conference on Soil Mechanics*. Cambridge: US

Lysmer, J., and R. L. Kuhlemeyer. 1969. "Finite dynamic model for infinite media." *J. Eng. Mechanics*. 95 (4): 859-877. US: ASCE.

PEER (Pacific Earthquake Engineering Research Center). 2021 *PEER Ground Motion Database*. <https://ngawest2.berkeley.edu>. Berkeley, CA: PEER

SCVWD, 2012. *Seismic stability evaluations of Lenihan Dam: Site characterization, material properties, and ground motions*. Report No. LN-3, Santa Clara Valley Water District, California

Seed, H.B., and I. M. Idriss. 1970. Soil moduli and damping factors for dynamic response analyses. *Report UCB/ERRC-70/10, Earthquake Engineering Research Center*, Berkeley CA: University of California.

Sherstobitoff, J., D. Siu, I. Stewart, and Q. Chen. 2004. "First Narrows and Port Mann water supply crossings seismic vulnerability assessment." In *Proc. 13th World Conference on Earthquake Engineering*, Vancouver, Canada.

Sun, J. I., R. Golesorkhi, and H. B. Seed. 1988. Dynamic moduli and damping ratios for cohesive soils. *Report UCB/ERRC-88/15, Earthquake Engineering Research Center*, Berkeley CA: University of California.

Sweeney, N. and L. Yan. 2014. "Dam safety upgrade of the Ruskin dam right abutment." In *Proc. 2014 Annual Conference*. Alberta, Canada: Canadian Dam Association.

USBR (US Bureau of Reclamation). 2019. *Best Practices in Dam and Levee Safety Risk Analysis - Chapter D-5 Embankment Slope Instability*. Washington, US: USBR

Wu, G. 2001. "Earthquake induced deformation analyses of the Upper San Fernando dam under the 1971 San Fernando earthquake." *Can. Geotech. J.* 38 (1): 1-15. <https://doi.org/10.1139/t00-086>

Wu, G and S. Chan. 2002. "Design of the Russ Baker Way overpass on liquefiable sand - Vancouver Airport Connector - Sea Island, Richmond, B.C." In *Proc. 6th Int. Conf. on Short and Medium Span Bridges*, edited by P. Brett, N. Banthia, and P. G. Buckland, 579-586. Vancouver

Wu, G., T. Fitzell, and D. Lister. 2006. "Impacts of deep soft soils and lightweight fill approach embankments on the seismic design of the Hwy. 15 North Serpentine River bridges, Surrey, B.C." *Proc. 59th Canadian Geotechnical Conference*, 596-601. Vancouver: CGS (Canadian Geotechnical Society).

Wu, G. 2010. "Seismic soil pressures on rigid walls with sloped backfills." *Proc., 5th Int. Conf. on Recent Advances in Geotechnical Earthquake Engineering and Soil Dynamics*, edited by S. Prakash, Paper No. 6.20a. San Diego, US

Wu, G. 2015. "Seismic design of dams." In *Encyclopedia of Earthquake Engineering*, edited by M. Beer, I. A. Kougiumtzoglou, E. Patelli and I. S-K. Au. Berlin Heidelberg, Germany: Springer-Verlag

Wu, G. 2018. "Probabilistic approach to design of seismic upgrade to withstand both crustal and subduction earthquake sources." In *Proc., 25th Annual Symposium on Ground Improvement*. Vancouver, BC, Canada: VGS (Vancouver Geotechnical Society)

Wu, G. 2021. "Reliability-based dynamic analyses for seismic design optimization in British Columbia." In *Proc., 27th Annual Symposium on Risk and Liability*. Vancouver, BC, Canada: VGS (Vancouver Geotechnical Society)

WGI (Wutec Geotechnical International). 2019. *VERSAT-2D v.2019: A computer program for 2-dimensional static and dynamic finite element analysis of continua*. BC, Canada: WGI

WGI-220224. 2022. *Finite Element Dynamic Analyses of Austrian Dam*. Wutec Geotechnical Engineering Report No. 220224, February-22.

APPENDIX A BACKGROUND INFORMATION

The Loma Prieta, California, Earthquake of October 17, 1989—Earth Structures and Engineering Characterization of Ground Motion

THOMAS L. HOLZER, *Editor*

PERFORMANCE OF THE BUILT ENVIRONMENT
THOMAS L. HOLZER, *Coordinator*

U.S. GEOLOGICAL SURVEY PROFESSIONAL PAPER 1552-D

Prepared in cooperation with the National Science Foundation



APPENDIX A Background Information

UNITED STATES GOVERNMENT PRINTING OFFICE, WASHINGTON : 1998

LEXINGTON DAM (now the LENIHAN DAM)

Lexington Dam is a 205-foot-high dam located about 6 miles downstream of Austrian Dam and about 2 miles from the fault rupture associated with the earthquake (fig. 2). The dam was completed in 1953 as a zoned earth structure having a relatively thick sandy and gravelly clay core that is supported by upstream and downstream random shell zones of clayey sands and gravels. The dam also has relatively flat upstream (5.5:1) and downstream (3:1) slopes. A plan view and cross section are shown in figure 7. The embankment material properties are summarized in table 7. At the time of the earthquake, the reservoir was about 100 feet below the crest of the dam. Previous summaries of damage were presented by Bureau and others (1989), Seed and others (1990), and in the studies by R. L. Volpe & Associates (1990a).

Lexington Dam was instrumented with strong-motion instruments on the left abutment, left crest, and right crest. These accelerographs recorded transverse peak accelerations of 0.45, 0.39, and 0.45 g , respectively. This shaking was composed of about 6 to 7 s of relatively strong long-period motion. The left abutment or "bedrock" peak acceleration is within the range predicted by appropriate strong-motion attenuation relationships for a site approximately 2 miles from the nearest point on the fault rupture surface for a $M_s = 7.1$ event, but is a bit lower than the mean or expected value based on such relationships. In addition, there appears to be some spectral acceleration amplification at lower frequencies (0.9 to 1.2 Hz). This low frequency amplification may indicate that the recorded "bedrock" motion may have been affected by local topographic or geologic conditions.

The strong ground shaking produced transverse cracking on both the upstream and downstream sides of both abutments, oblique cracking on the crest about 150 feet in from the left abutment, longitudinal cracking on both the upstream and downstream slopes of the dam, and cracking of an access road on the right abutment upstream of the dam. The cracks, which were fairly isolated, were commonly less than 3/4 of an inch wide, and trenching indicated that they only extended to depths generally between 2 and 7 feet (R. L. Volpe & Associates, 1990a). The maximum earthquake-induced crest deformations were approximately 0.85 feet of vertical settlement, and 0.25 feet of lateral displacement in the downstream direction (R. L. Volpe & Associates, 1990a). An old slope indicator casing was found to have raised from beneath the crest to over 3 inches above the crest due to the embankment settling around it. The earthquake shaking and ground movements produced extensive cracking in the bridge abutment at the left abutment and ruptured a buried water line near the crest of the dam.

About 6 weeks after the earthquake, a relatively large seepage area developed high up on the downstream face of the dam. The seepage area was about 170 feet long and 35 feet wide and oriented at an oblique angle with the axis of the dam. This seepage area was really more of a wet or damp

area and never really flowed water. Although the cause of the seepage area is not definitively known, one explanation that has been offered is the fact that old exploration holes extending into the rock foundation lie within the area and that these old borings could have been acting as relief wells for earthquake-induced pore pressures within the lower portions of the embankment and bedrock (R. L. Volpe & Associates, 1990a). Another possible explanation is that the fill is relatively impervious at this elevation and that any surface water that infiltrates the dam becomes perched at this level.

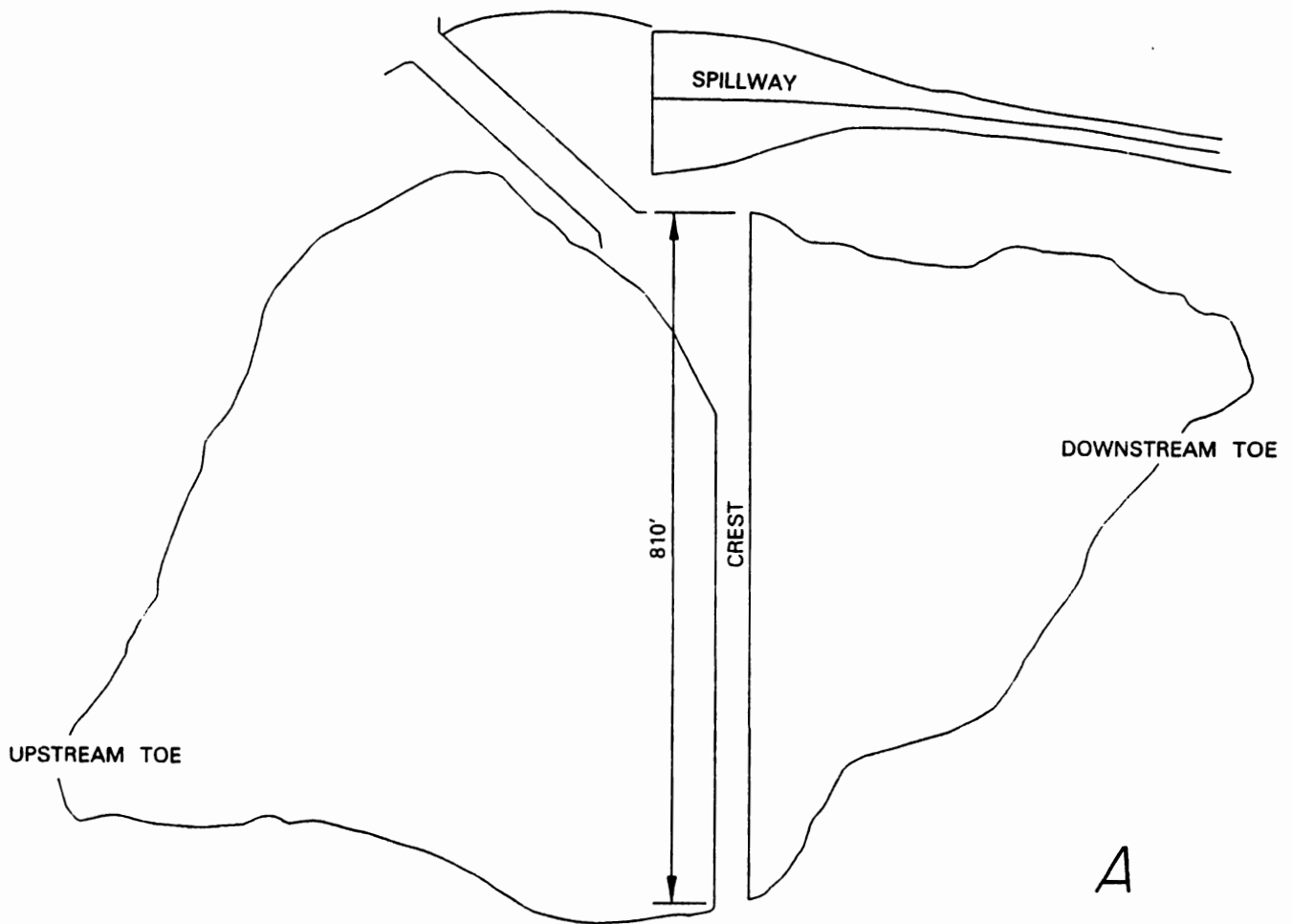
The repairs made to the dam consisted of trenching the cracked areas to depths ranging between 3 and 7 feet and compacting the excavated soil back into the trenches (R. L. Volpe & Associates, 1990b).

GUADALUPE DAM

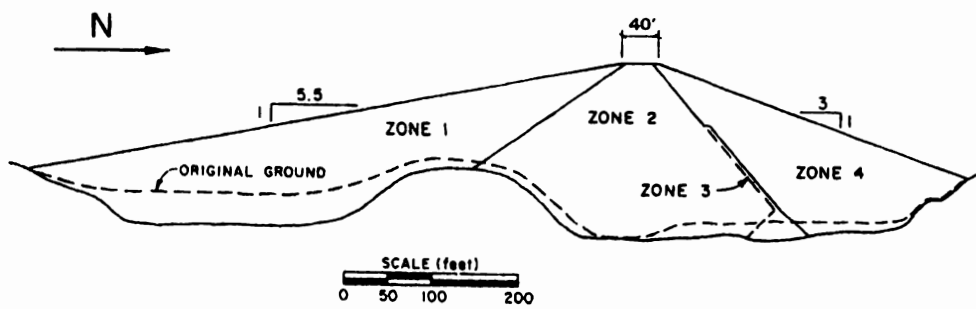
Guadalupe Dam is a 142-foot-high dam located about 6 miles from the Loma Prieta fault-rupture zone, and it probably experienced peak ground accelerations between 0.4 and 0.45 g (fig. 2). The dam was completed in 1935 as a rolled earth structure with an upstream facing of concrete panels for erosion protection. In a manner similar to that described for Austrian Dam, the embankment is apparently nearly homogeneous, as the selective borrowing to create upstream "impervious" and downstream "pervious" zones did not appear to be completely successful in creating distinctly different zones. In 1972, an upstream buttress was added to the dam to improve drawdown stability. A plan view and cross section are shown in figure 8. At the time of the earthquake, the reservoir was about 78 feet below the crest of the dam; however, the reservoir had been full up to about 3 months before the earthquake, and it is assumed that the upstream shell materials were nearly saturated at the time of the earthquake. Previous summaries of damage were presented by Bureau and others (1989), Seed and others (1990), and in the studies by R. L. Volpe & Associates (1990a).

The earthquake induced up to 0.64 feet of settlement and 0.15 feet of lateral displacement in the upstream direction as measured on the crest. Minor transverse cracking developed at the crest at both abutment contacts along with minor longitudinal cracking on the crest. The principal damage was to the upstream slope, where the upper portion of the buttress fill developed longitudinal cracking. Shortly after the earthquake, these cracks were observed to have a maximum width of less than 1 inch and extended across the entire face of the dam. About 5 weeks later, the cracks had widened to about 4 inches and extended to a depth of about 5 feet (R. L. Volpe & Associates, 1990a).

These cracks may have been caused by concentrations of dynamic stresses induced by the change in slope geometry. Alternatively, they may have resulted from possible past settlements caused by the placement of the berm. These past settlements may have created preexisting cracks which surfaced only after the development of strong ground motion.



A



B

Figure 7.—Plan view (A) and cross section (B) of Lexington Dam.

Table 7.—Characterization of Lexington Dam fill materials

Engineering Property	CORE (Zone 2)		SHELL (Zones 1 & 4)
Depth (ft)	0-80	>80	
Classification	SC, CL-CH		SC, GC, CL
Gradation: > No. 4 (%)	13-30	0-2	¹ 0-50
Gradation: < No. 200 (%)	29-52	86-97	² 18-97
Specific Gravity, <i>G_s</i>	2.67	- 2.73	2.73
Liquid Limit	31	- 37	33 - 39
Plasticity Index	14	- 18	14 - 24
<i>W_c</i> (in situ range and avg., %)	11.2-17.7 (14.4)	21.5-30.6 (25.6)	9.4-26.5 (15.3)
<i>γ_d</i> (in situ range and avg., pcf)	117.5-131.5 (120.9)	92.5-102.2 (96.6)	³ 95.2-134.8 (119.8)
<i>γ_{dmax}</i> , <i>W_{copt}</i> (20,000 ft-lb/ft ³)			131.7 pcf 8 %
<i>C</i> (psf)	400	0	0
<i>φ</i> (degrees)	36	25	36
<i>C</i> (psf)	1200	0	0
<i>φ</i> (degrees)	18	17	22
<i>K_{2max}</i>	100-150	~50	~100
<i>V_{smax}</i> (ft/sec)	1200-1600	1400-1600	1400-2200

Notes: ¹ Only one sample had less than 13 percent gravel.
² For 70 percent of the samples, <35 percent finer than No. 200.
³ Average dry unit weight was about 6 pcf lower at depths of 0-40', and 4 pcf higher at depths >40'.

The earthquake also caused the concrete panels on the upstream face above the berm to pound against each other, resulting in cracking and spalling in about 10 percent of the panels (R. L. Volpe & Associates, 1990a).

The repairs made to the dam consisted principally of excavating a 70-foot band of material (as measured along the slope, parallel to the crest) at the top of the upstream buttress to a depth of about 6 feet. The excavated material was temporarily stored in order to allow the material to dry to an acceptable water content and then recompacted into place. The cracks in the crest at the abutment contact were excavated to about 3 to 4 feet and the excavated material was recompacted back into place (R. L. Volpe & Associates, 1990b).

NEWELL DAM

Newell Dam is a 182-foot-high dam located about 6 miles from the Loma Prieta fault-rupture zone, and it probably experienced peak ground accelerations between 0.4 and 0.45 g (fig. 2). The dam was completed in 1960 as a zoned earth and rockfill dam generally composed of clayey zones except for an upstream zone of dirty rockfill. At the time of the earthquake, the reservoir was about 49 feet below the crest of the dam. Previous summaries of damage were presented by Bureau and others (1989), Seed and others (1990), and Creegan (1990).

Although the earthquake did not induce significant crest movements, a longitudinal crack was found on the 3:1 upstream slope running the entire width of the dam face at about the spillway elevation. This crack was generally between 1 and 9 inches in width. Trenching explorations of the crack indicated

that it was formed by tension within the zone 2 rockfill. The trenches, however, only extended to a maximum depth of 10 feet, and the crack, which was about 1 inch in width at the bottom of the trenches, extended farther to greater depths. There were also other minor cracks at various locations. Seepage through the dam and abutments, measured at the downstream toe, was also found to have increased from a normal 8 gpm to 41 gpm, but remained clear (Creegan, 1990). By early December 1989, the seepage had decreased back down to about 17 gpm.

The development of the longitudinal cracking was theorized to have resulted from settlement of the dirty rockfill upstream shell relative to the rest of the dam. This material consisted of quarried sandstone and shale and was placed in 5-foot lifts and compacted by sluicing. The other clayey zones were placed in thin lifts and compacted to about the maximum Standard Proctor dry density. Consequently, the upstream rockfill zone was relatively loose in comparison with the other zones in the embankment. There were indications that some of the cracking ran along the interface of the zone 2 rockfill and the clayey core. Further evidence of settlement of the zone 2 material was found at the bell toggle joints along the sloping intake tower where the embankment seemed to have pulled away from the structure by about 1 to 3 inches in a downstream direction (Creegan, 1990).

The repair of the longitudinal cracks consisted of using a large backhoe to excavate to a depth of about 6 feet along the alignment of the crack. The trench was then backfilled in 18-inch lifts with each lift being compacted with a vibrating shoe on the backhoe. The upstream slope was then rolled with a vibratory roller (Creegan, 1990).

ELMER J. CHESBRO DAM

The Elmer J. Chesbro Dam is a 95-foot-high embankment located about 8 miles from the Loma Prieta fault-rupture zone, and it probably experienced peak ground accelerations between 0.4 and 0.45 g (fig. 2). As for many of the embankment dams in this area, the embankment is a nearly homogeneous compacted fill, as selective borrowing to create upstream "impervious" and downstream "pervious" zones do not appear to be entirely successful in creating distinctly different materials. The upstream slope varies between 2:1 and 3:1. The downstream slope is about 2:1, but is fitted with a 45-foot-wide berm at about half the height of the dam. At the time of the earthquake, the reservoir was about 69 feet below the crest of the dam. Previous summaries of damage were presented by Bureau and others (1989), Seed and others (1990), and in the studies by R. L. Volpe & Associates (1990a).

Surveys of crest monuments showed that the earthquake induced up to 0.37 feet of settlement and 0.05 feet of lateral displacement in the upstream direction. The main area of cracking that developed at this dam occurred as longitudinal cracking near the upstream edge of the crest. This cracking extended about 240 feet and had a 4-inch width together with

SEISMIC STABILITY EVALUATIONS OF CHESBRO, LENIHAN, STEVENS CREEK, AND UVAS DAMS (SSE2)

PHASE A: STEVENS CREEK AND LENIHAN DAMS

LENIHAN DAM

SITE CHARACTERIZATION, MATERIAL PROPERTIES, AND GROUND MOTIONS (REPORT No. LN-3)

Prepared for

SANTA CLARA VALLEY WATER DISTRICT
5750 Almaden Expressway
San Jose, CA 95118

April 2012



TERRA / GeoPentech
a Joint Venture

core and one consolidation test on a sample from the upstream shell. These tests also indicate the maximum past pressure was approximately equal to the in-situ vertical effective stress and that the compressibility in the virgin compression range was as expected for normally consolidated clays. The three tests on the lower core had values of CR that ranged from 0.07 to 0.14 and the one test from the upstream shell had a CR value of 0.14.

5.5.3.3 Strength from Direct Simple Shear Tests

The primary embankment loading conditions due to seismic shaking are reasonably represented by the conditions simulated in direct simple shear testing. Thus, for seismic deformation analyses, undrained shear strengths measured under direct simple shear (DSS) loading conditions are of interest.

As part of the current laboratory investigations, TGP selected companion specimens from four samples so that triaxial compression and direct simple shear tests could be performed and the measured undrained shear strengths compared. The results of these tests are summarized below.

Boring	Sample	Dam Zone	Depth ft	TX $S_{u(max)}$ ksf	DSS $S_{u(max)}$ ksf	DSS / TX	σ_{v_o} (ksf)
LD-B-101	PB-4	Lower Core	88	4.96	2.93	0.59	9.6 (Fig.5-16)
LD-B-101	PB-8	Lower Core	131	5.90	3.99	0.68	13.7
LD-B-101	PB-12	Lower Core	171	6.05	3.61	0.60	15.5
LD-B-103	PB-5	Upper Core	52	4.50	2.66	0.59	6.3 (Fig.5-15)

These data are very consistent and indicate that the direct simple shear strengths of the compacted clay soils at Lenihan Dam are typically 60% of the strengths measured in triaxial compression tests.

All the DSS tests described above were conducted using a static loading rate; as a result, some adjustment in static strength for the rate of loading effects needs to be made in order to estimate the seismic undrained shear strength values to be used in seismic deformation analyses. We recommend using the static DSS undrained shear strengths (estimated as 60% of the triaxial compression strengths) and then adjusting these strengths for rate of loading effects. These adjustments would probably be on the order of a 20 to 40 percent increase in strength. We will evaluate this recommendation further through a refined analysis of the performance of the dam during the Loma Prieta earthquake that will be completed as part of our final seismic stability analyses.

5.5.3.4 Calibration of CPT Strengths using Laboratory Data

CPT probes were completed adjacent to each of the mud rotary borings as part of the current field and laboratory investigation by TGP. We compared the measured undrained strengths from our triaxial tests to the undrained strengths estimated from the adjacent cone data. In order to provide representative values of the cone tip resistance for calculating undrained shear strength, we considered median and 16% values (mean – 1 standard deviation). The 16% values were

**TABLE 5-2
MATERIAL CLASSIFICATION SUMMARY**

Zone ²	Idealized Material Description	Generalized USCS Classification	In-Situ Conditions ³			Gradation ³				Atterberg Limits ³	
			Dry Unit Weight, γ_d (pcf)	Moisture Content, W_c (%)	Compaction (%) ⁴	Gravel (%)	Sand (%)	Fines (%)	Clay Fraction, -2μ (%)	Liquid Limit LL	Plasticity Index PI
1	Upstream Shell	SC, CL	119.3 (95.2 - 132.3)	15.0 (10.3 - 26.5)	95 (76 - 106)	27 (0 - 43)	34 (3 - 44)	39 (19 - 97)	21 (12 - 44)	33 (30 - 39)	15 (6 - 24)
2U	Upper Core (Above El. 590 ft)	SC, GC	119.6 (108.0 - 131.5)	11.9 (6.0 - 17.7)	95 (81 - 112)	33 (3 - 58)	35 (23 - 48)	31 (16 - 53)	17 (13 - 30)	37 (30 - 48)	17 (14 - 29)
2L	Lower Core (Below El. 590 ft)	CH, SM-MH	99.9 (89.7 - 111.2)	24.1 (17.8 - 37.1)	101 (91 - 113)	6 (0 - 29)	15 (3 - 43)	79 (29 - 97)	42 (16 - 53)	62 (43 - 70)	35 (15 - 48)
4	Downstream Shell	SC, GC	124.3 (100.6 - 143.3)	11.9 (6.2 - 19.9)	89 (72 - 102)	32 (13 - 56)	38 (16 - 60)	30 (15 - 63)	17 (11 - 26)	33 (22 - 46)	15 (6 - 29)

Notes:

1. Data in this table are averages with minimum and maximum values in parentheses. No data is available for Drain Material (Zone 3).
2. See Figure 5-1.
3. In-situ conditions, gradation and Atterberg limits are summarized based on laboratory testing performed by Wahler (1981), Geomatrix (1996), Harza (1997), RLVA (1999), Frame and Volpe (2001), and Terra / GeoPentech (2011c).
4. Per D1557 modified, 20,000 ft-lbs.

**TABLE 5-3
SUMMARY OF ENGINEERING PROPERTIES**

Zone	Moist Unit Weight (pcf) γ_t	Effective Friction Angle ⁽¹⁾ ϕ'	Triaxial Undrained Strength Parameter ⁽²⁾ S_u/σ_{vc}'	Stress-Strain Strength Relationship ⁽³⁾ E_{u50} / S_u	Dynamic Properties ⁽⁴⁾		
					V_s		G/G_{max} and Damping Ratio
					K (ft/sec)	n	
1	138	37.5 °	$e^{-0.22 \cdot \ln(\sigma_{vc}') + 0.12}$	140	1305	0.25	Figure 5-20
2U	132	35.5 °	$e^{-0.20 \cdot \ln(\sigma_{vc}') - 0.01}$	180	1190	0.25	Figure 5-20
2L	124	25.5 °	$e^{-0.27 \cdot \ln(\sigma_{vc}') - 0.15}$	170	680	0.25	Figure 5-20
4	140	35 °	$e^{-0.21 \cdot \ln(\sigma_{vc}') - 0.12}$	180	1550	0.25	Figure 5-20

Notes:

⁽¹⁾ Effective Friction Angle, ϕ' (with no cohesion)

⁽²⁾ σ_{vc}' in ksf; minimum S_u for all soils = 2.0 ksf; also see Figures 5-14 to 5-17

⁽³⁾ Stress-Strain Strength Relationship

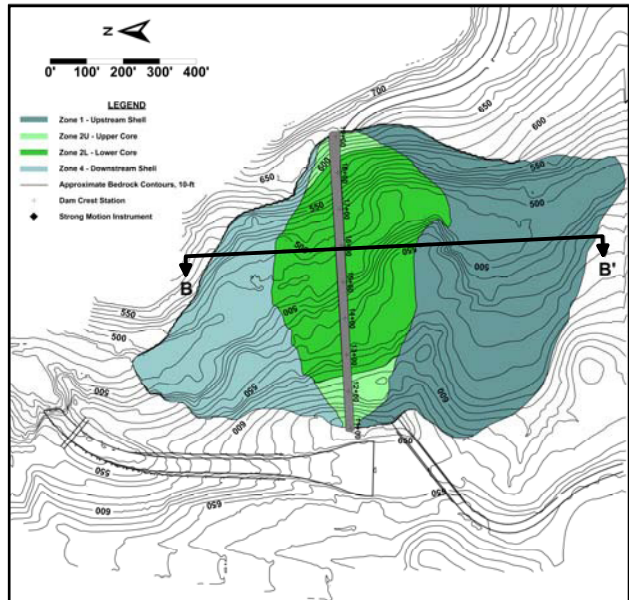
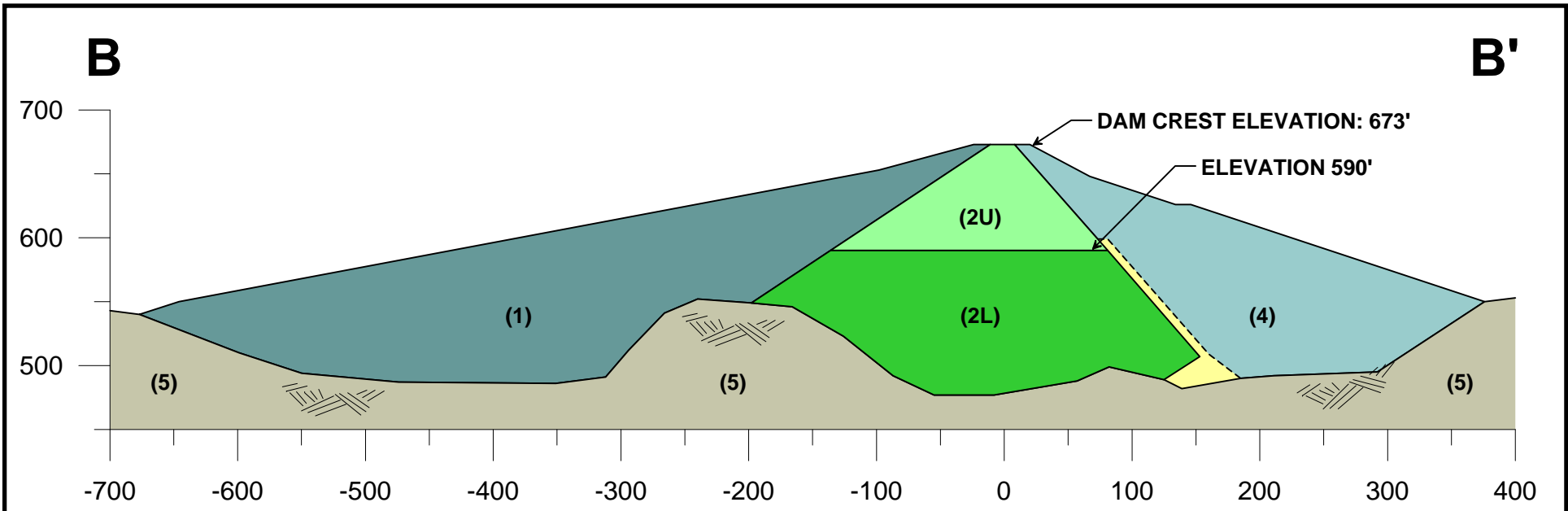
E_{u50} = Undrained Secant Modulus at 50% S_u

⁽⁴⁾ Dynamic Properties, V_s (shear wave velocity), G/G_{max} (shear modulus) and Damping Ratio

$V_s = K \cdot (\sigma_{vc}'/p_a)^n$ where K is in ft/sec

**TABLE 5-4
COMPARISON OF LABORATORY AND CPT UNDRAINED STRENGTHS**

Boring No.	Sample No.	Dam Zone	Depth ft	TX $S_{u(max)}$ ksf	CPT (50%) S_u ksf	CPT (16%) S_u ksf	CPT S_u / TX $S_{u(max)}$	
							50%	16%
LD-B-101	PB-4	Lower Core	88	4.96	5.76	5.05	1.15	1.02
LD-B-101	PB-8	Lower Core	131	5.90	7.48	6.42	1.27	1.09
LD-B-101	PB-12	Lower Core	171	6.05	4.73	4.25	0.78	0.70
LD-B-103	PB-5	Upper Core	52	4.50	7.95	5.17	1.77	1.15
LD-B-103	PB-6	Upper Core	59	5.41	6.71	6.00	1.24	1.11
LD-B-102	PB-1	Downstream Shell	36	6.84	31.90	18.50	4.66	2.70
LD-B-102	PB-6	Downstream Shell	100	7.57	15.00	10.60	1.98	1.40



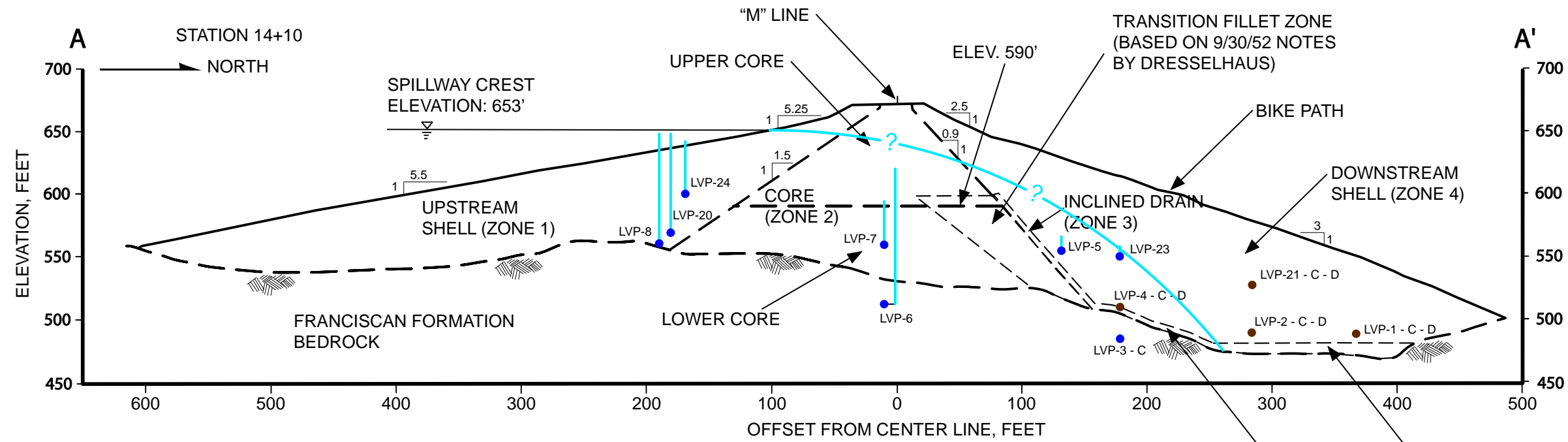
Zone	Color Code	Material Description	Predominant Soil Classification
1	[Blue-Grey]	Upstream Shell	Gravely Clayey Sands (SC) to Sandy Clays (CL)
2U	[Light Green]	Upper Core (Above El. 590)	Gravely Clayey Sands (SC) to Clayey Gravels (GC)
2L	[Dark Green]	Lower Core (Below El. 590)	Sandy Highly Plastic Clays (CH) to Silty Sands-Sandy Highly Plastic Silts (SM/MH)
3	[Yellow]	Drain Material	N/A
4	[Light Blue]	Downstream Shell	Gravely Clayey Sands (SC) to Clayey Gravels (GC)
5	[Brown]	Bedrock	Franciscan Complex

Rev. 1 12/08/2011 SSE2-R-4LN



MAXIMUM CROSS SECTION B-B'
 LENIHAN DAM
 SEISMIC STABILITY EVALUATIONS (SSE2)

Figure
 2-6

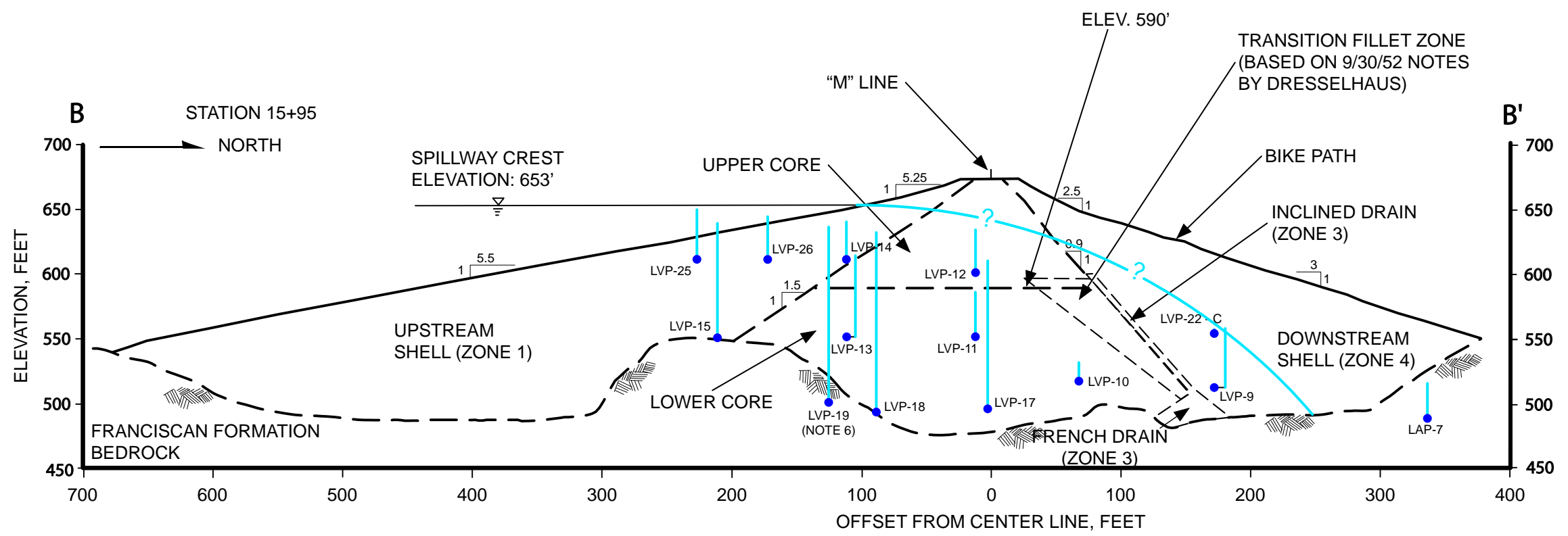


LEGEND

LOCATION AND NUMBER OF PIEZOMETER TIP

NOTES

- 1) ELEVATION OF THE TOP OF BLUE BAR REPRESENTS MEASURED TOTAL HEAD AT FULL RESERVOIR LEVEL.
- 2) HEIGHT OF BLUE BAR REPRESENTS MEASURED PRESSURE HEAD.
- 3) C INDICATES TOTAL HEAD IS INDEPENDENT OF RESERVOIR LEVEL.
- 4) D INDICATES THE PIEZOMETER TIP IS DRY. A BROWN TIP IS SHOWN AT THESE LOCATIONS.
- 5) TOP FLOW LINE SHOWN IS APPROXIMATE, PARTICULARLY IN VICINITY OF CHIMNEY DRAIN, AND IS AT THE SAME LOCATION ON BOTH SECTIONS.
- 6) LVP-19 IS PROJECTED 30 FT WEST AND IS SCREENED IN EMBANKMENT

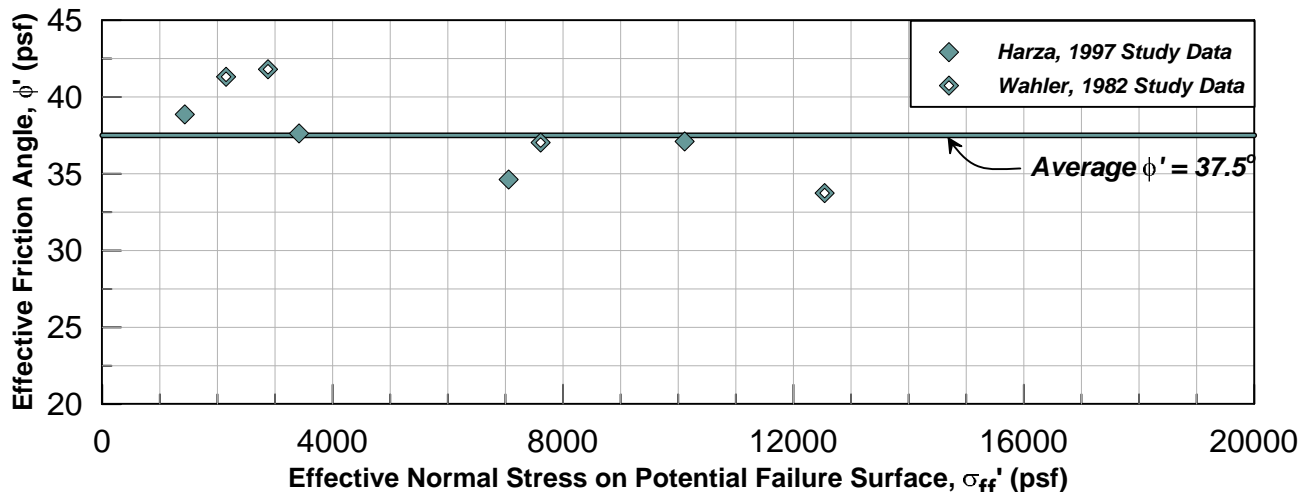


Rev. 0 11/18/2011 SSE2-R-3LN

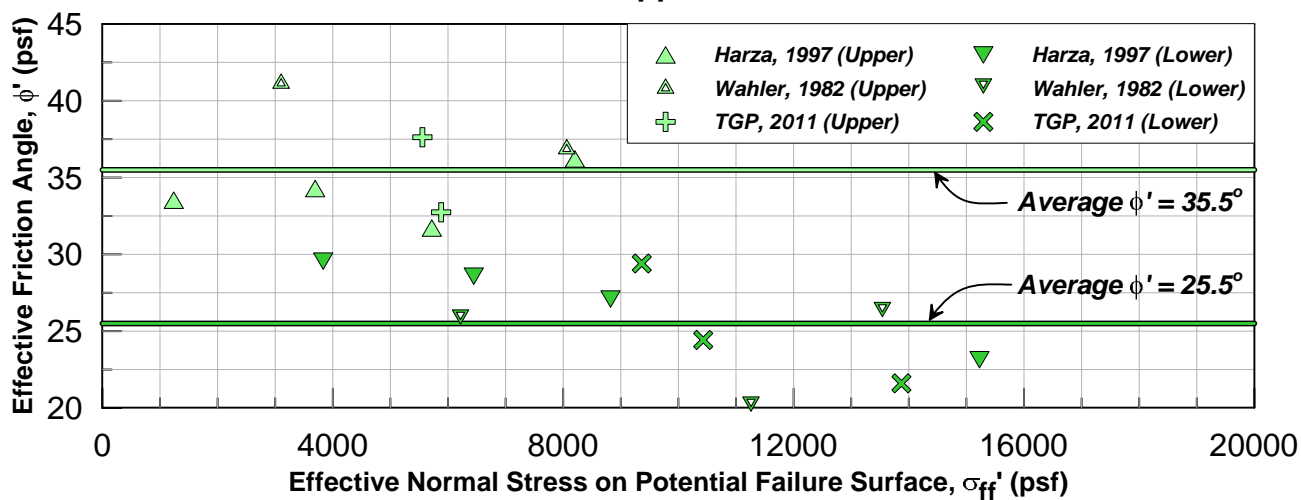


CROSS SECTIONS AND MEASURED PIEZOMETRIC LEVELS - LENIHAN DAM SEISMIC STABILITY EVALUATIONS (SSE2)

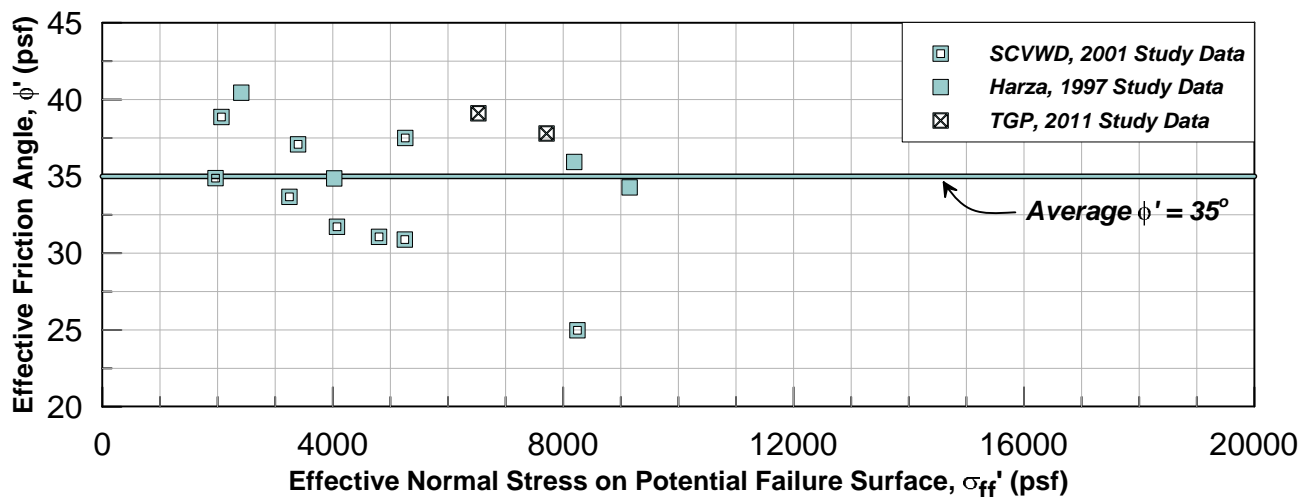
Zone 1 - Upstream Shell

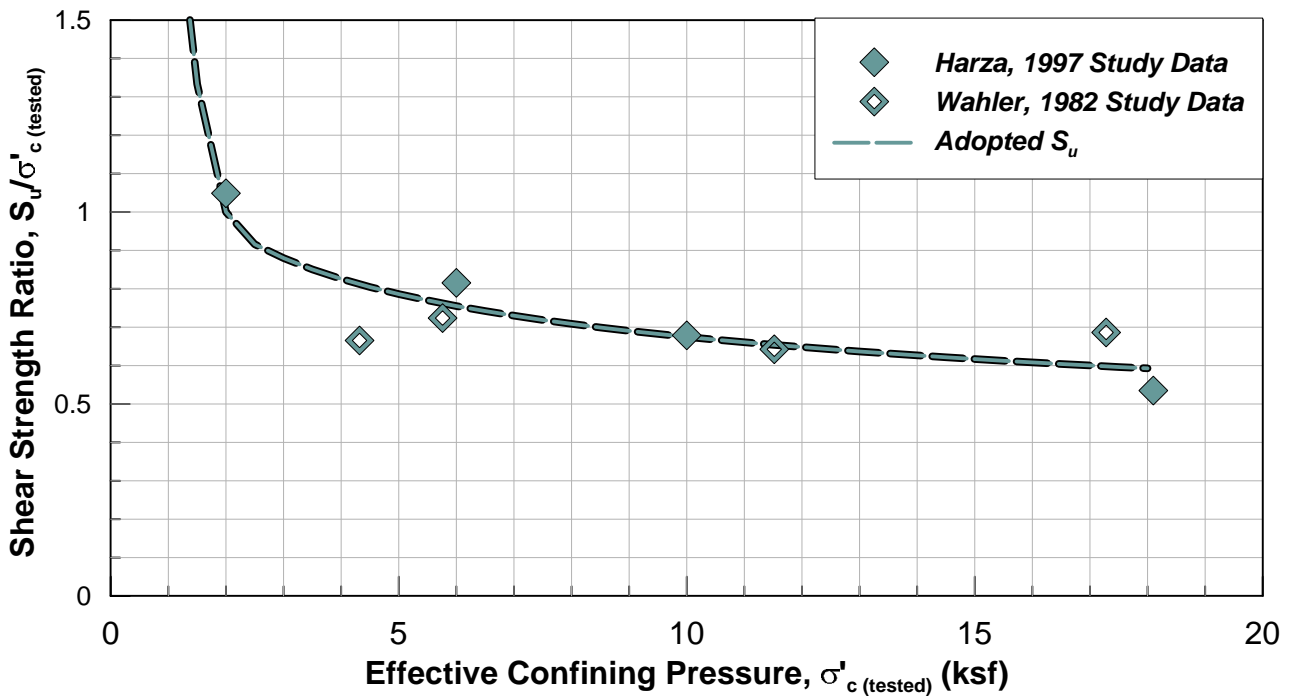
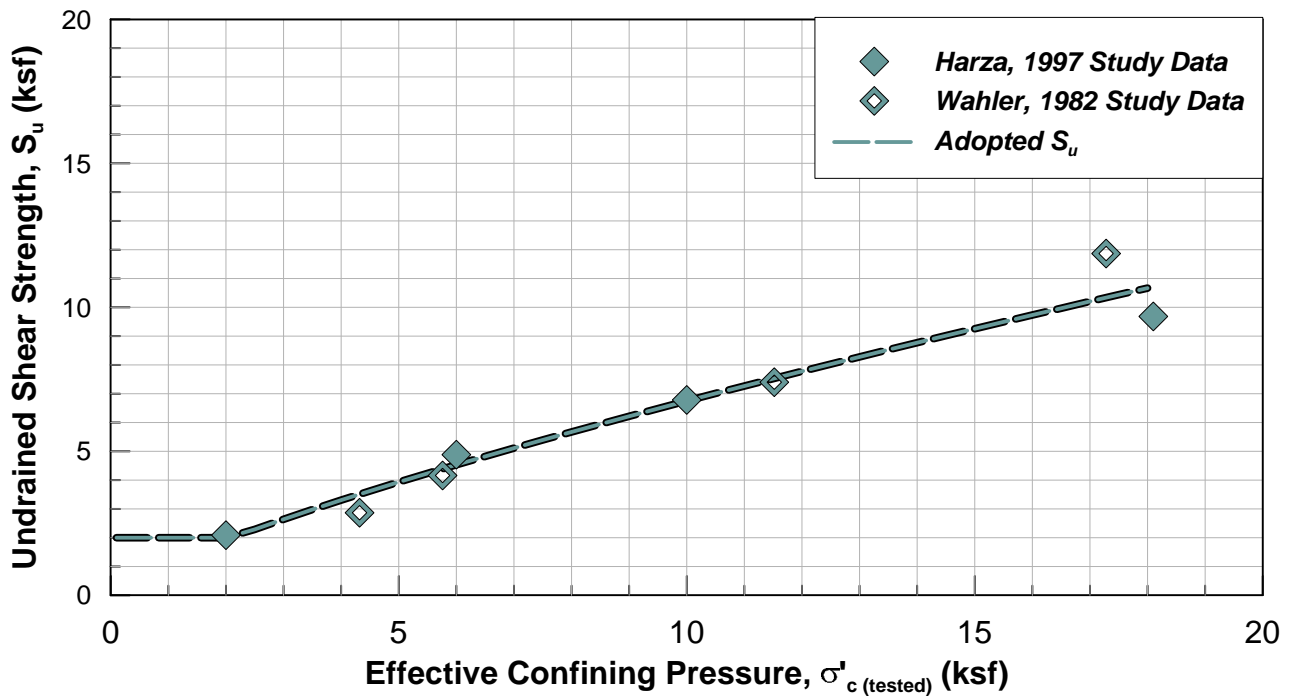


Zone 2U and 2L - Upper and Lower Core



Zone 4 - Downstream Shell



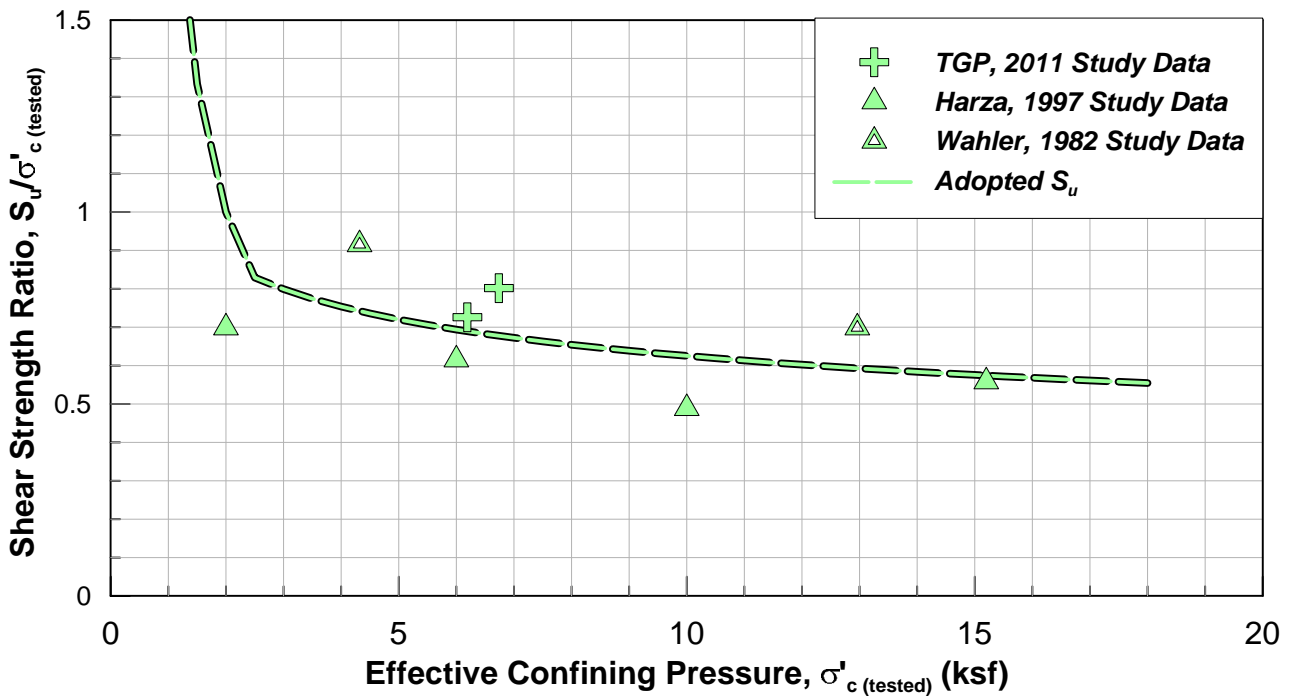
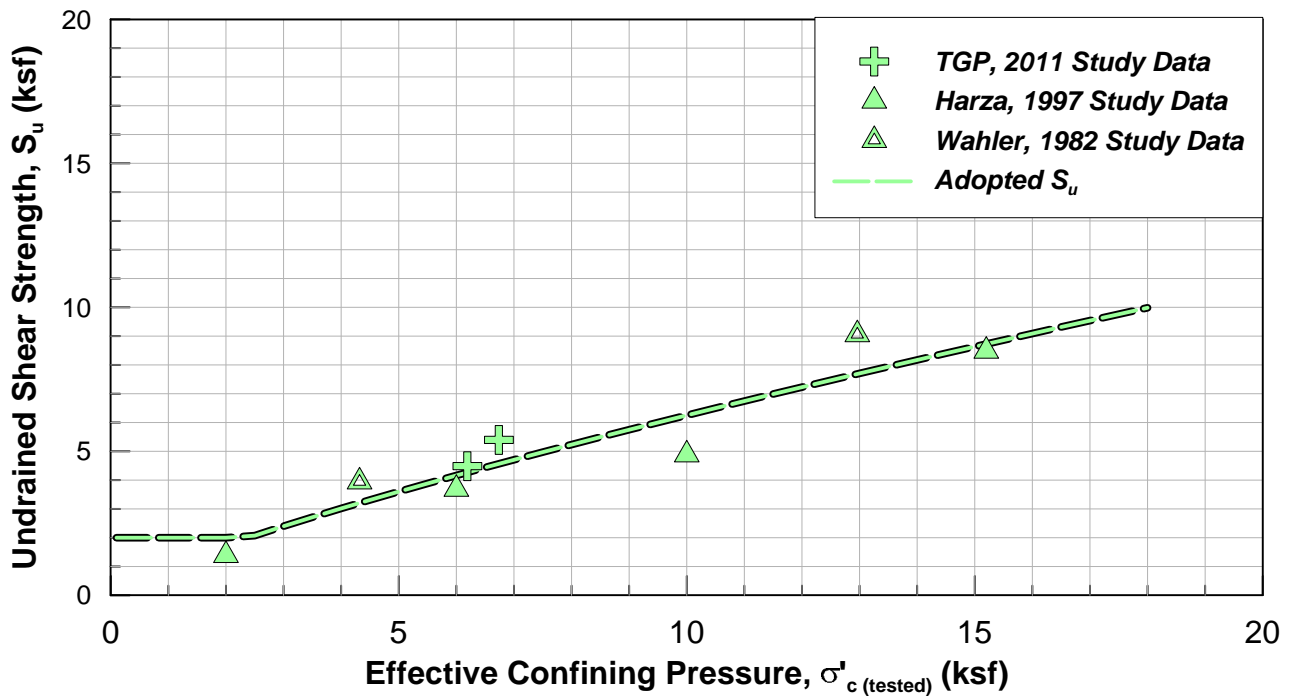


Note: All data from ICU'TXC Triaxial Tests

Adopted Parameter

$$S_u / \sigma'_{vc} = e^{[-0.22 \cdot \ln(\sigma'_{vc}) + 0.12]}, S_u \geq 2.0 \text{ ksf}$$



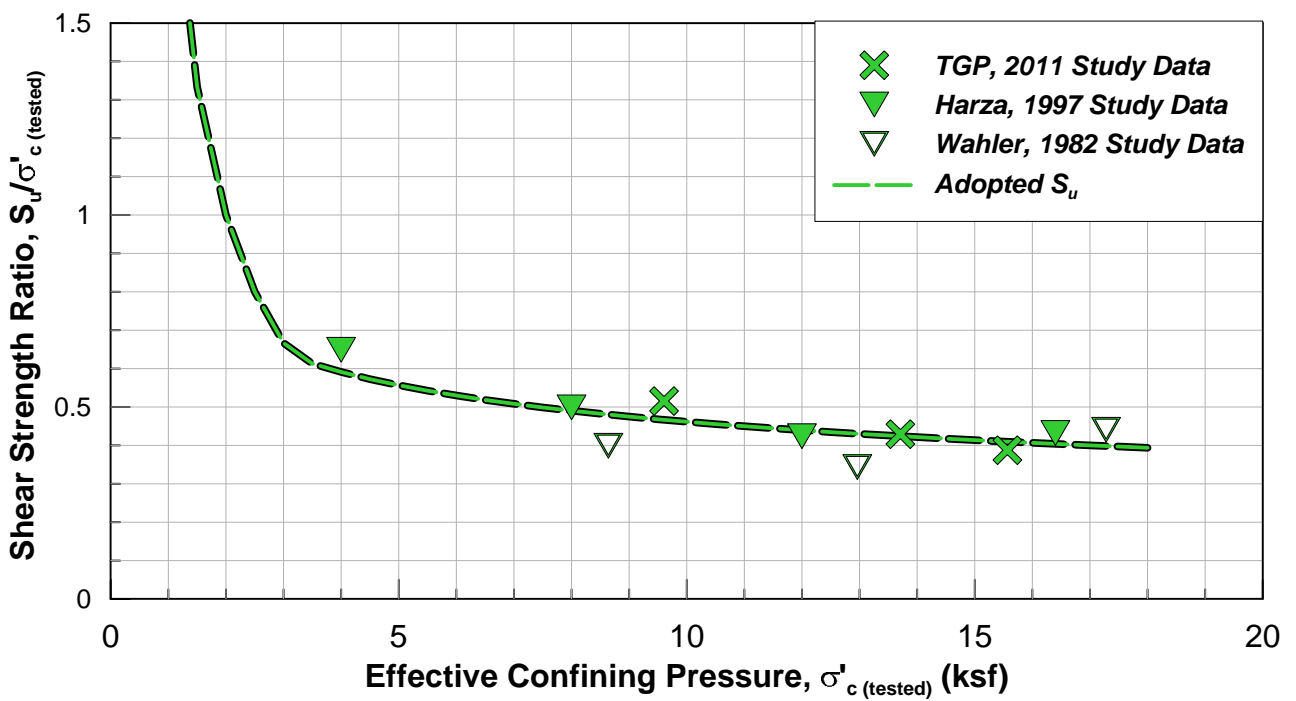
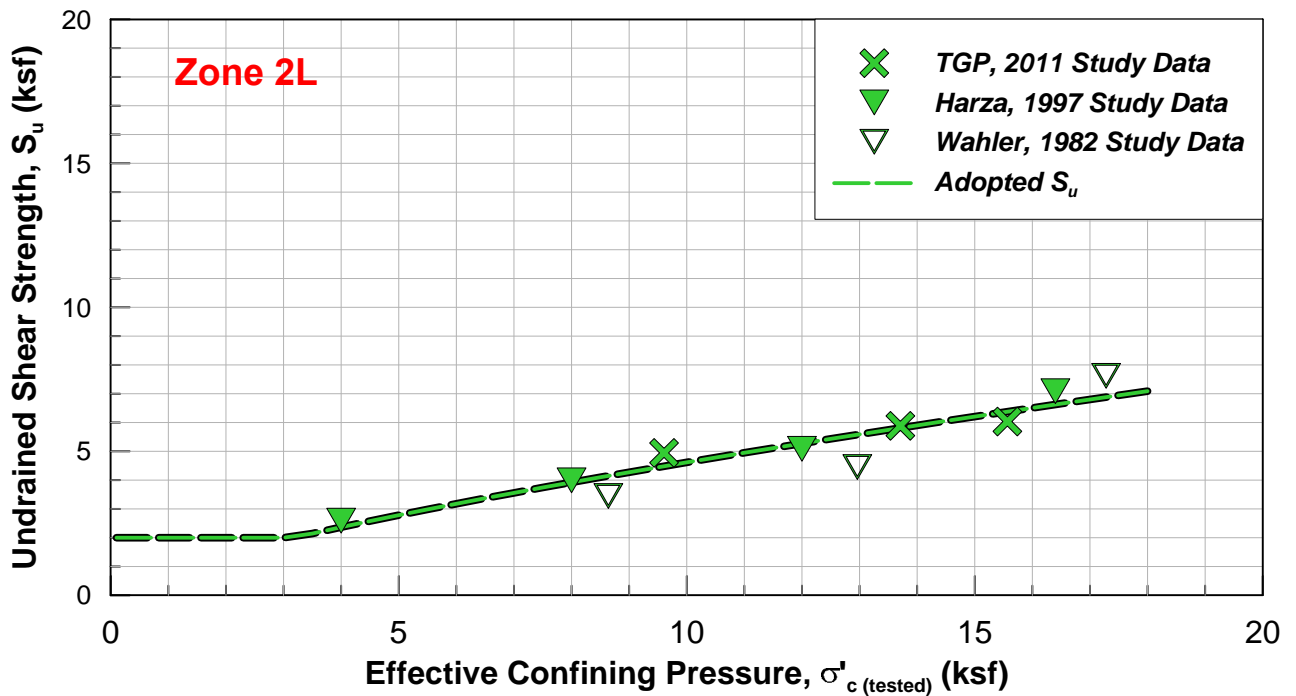


Note: All data from ICU'TXC Triaxial Tests

Adopted Parameter

$$S_u / \sigma'_{vc} = e^{-0.20 \ln(\sigma'_{vc}) - 0.01}, S_u \geq 2.0 \text{ ksf}$$



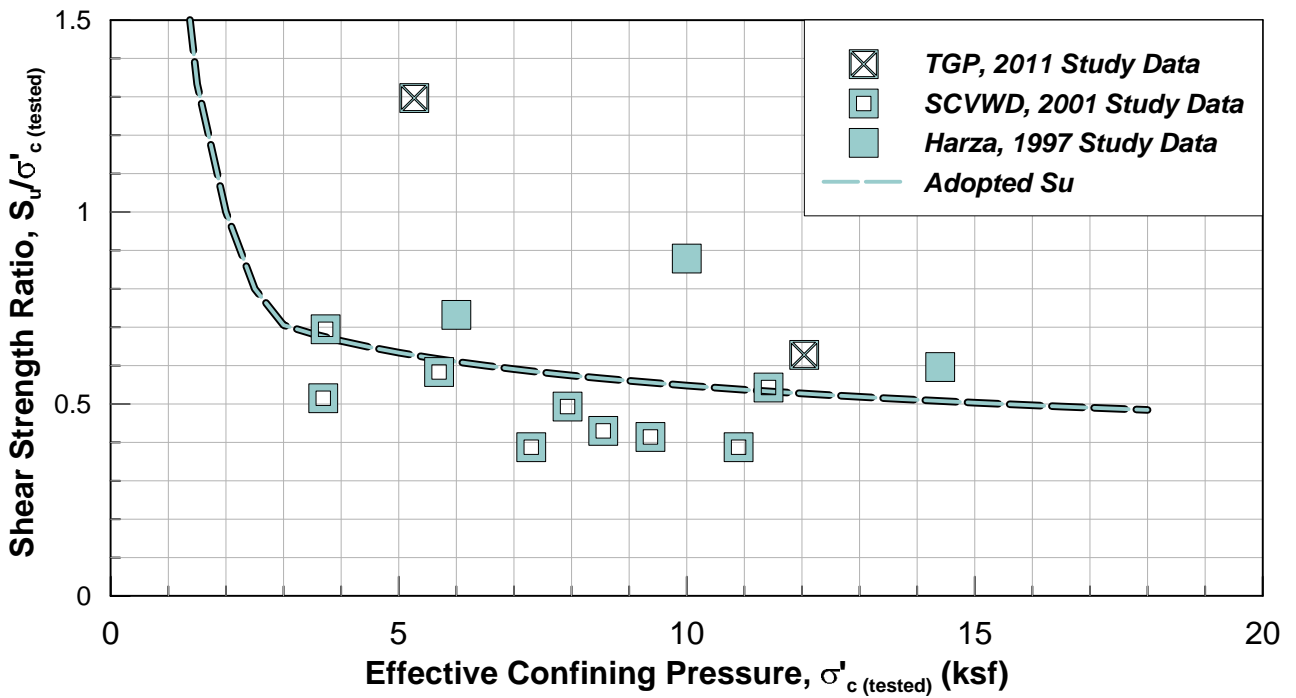
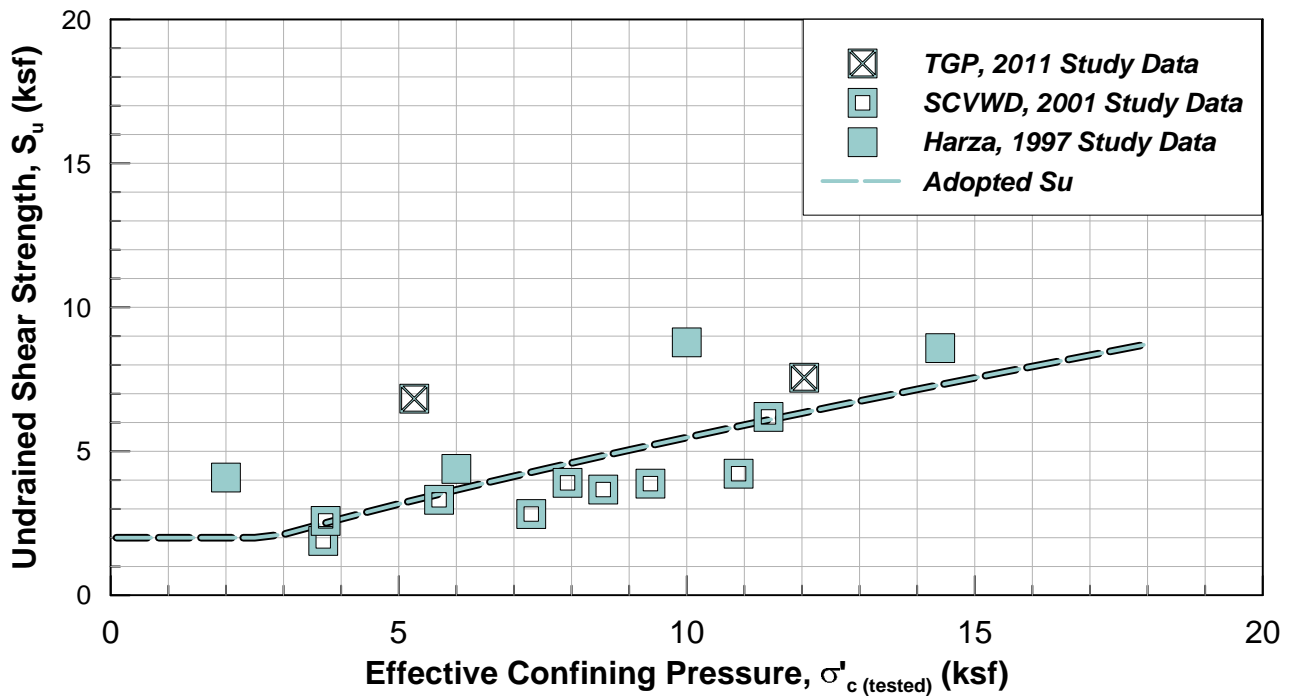


Note: All data from ICU'TXC Triaxial Tests

Adopted Parameter

$$S_u / \sigma'_{vc} = e^{[-0.27 \cdot \ln(\sigma'_{vc}) - 0.15]}, S_u \geq 2.0 \text{ ksf}$$



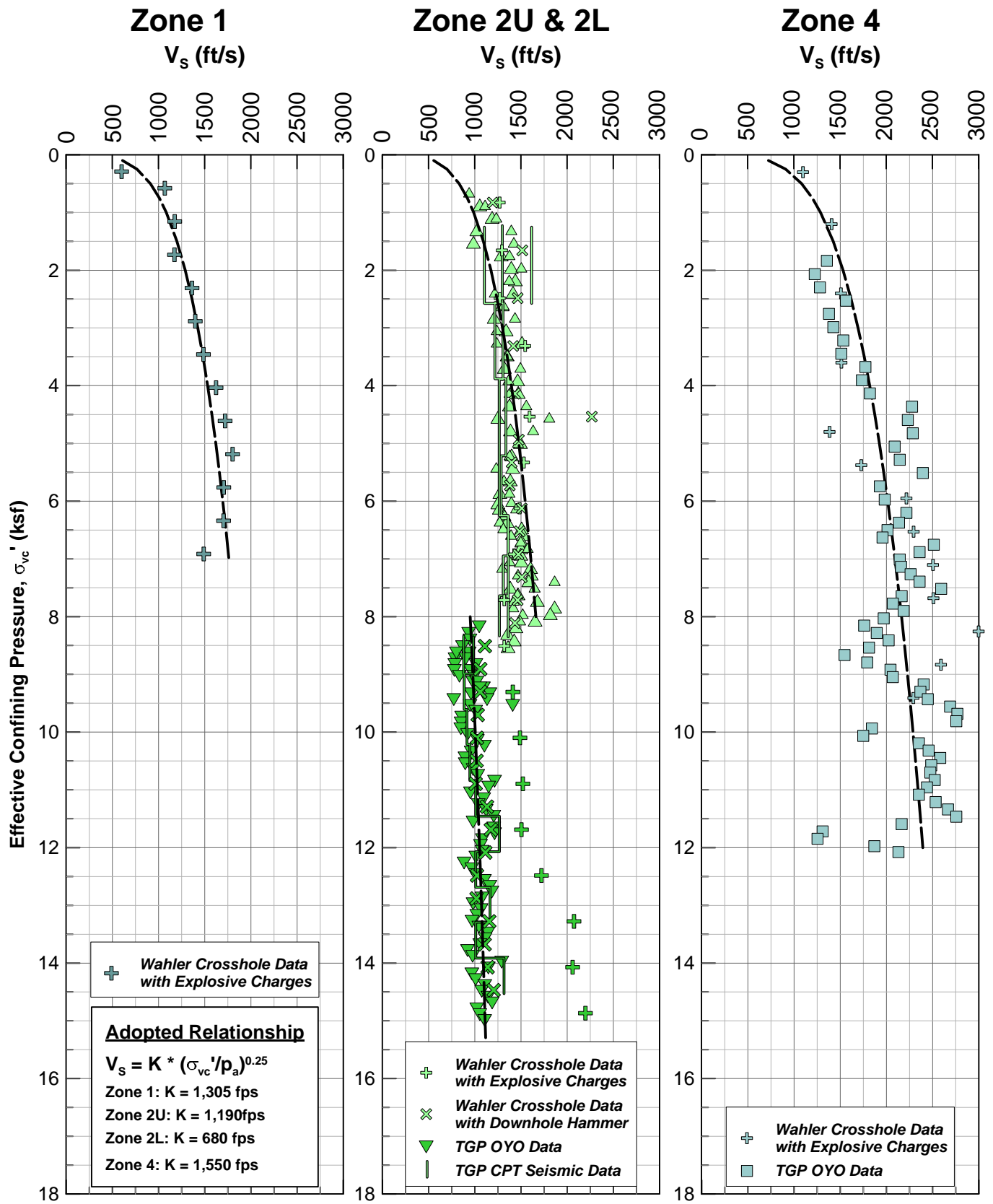


Note: All data from ICU'TXC Triaxial Tests

Adopted Parameter

$$S_u / \sigma'_{vc} = e^{[-0.21 \cdot \ln(\sigma'_{vc}) - 0.12]}, S_u \geq 2.0 \text{ ksf}$$



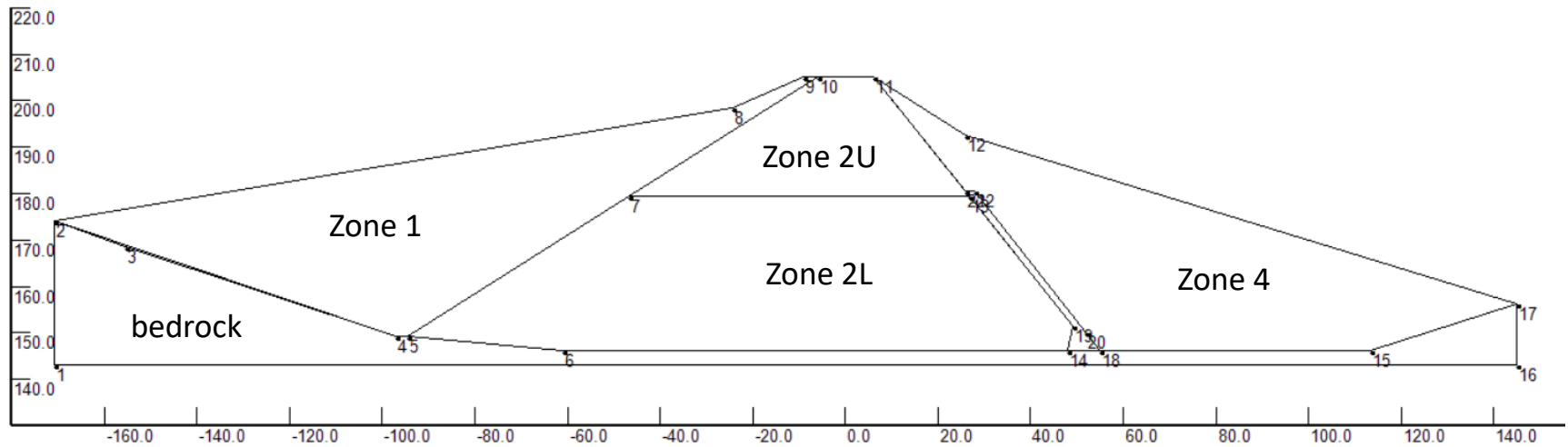


APPENDIX B SECTION W-W AND S_U FOR ZONE 2L

Report No. WGI-220301
March 1, 2022

Lenihan Dam - cross-section W-W'

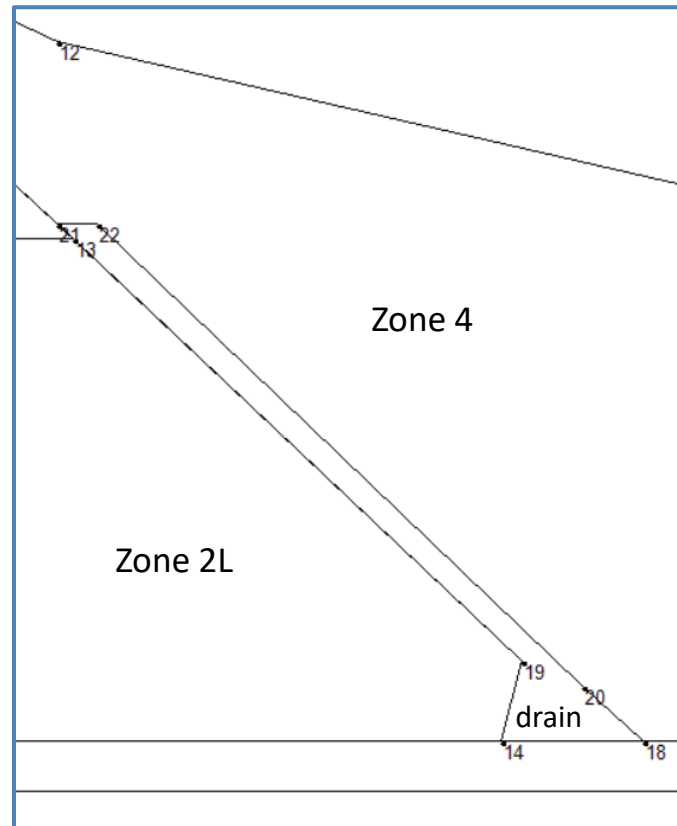
- Showing control points of the section



Lenihan Dam - cross-section W-W'

- Showing X and Y for control points, and a detail of the section

point No.	X	Y
1	-170.69	143
2	-170.69	174.09
3	-155.45	168.55
4	-96.9	149.4
5	-94.5	149.4
6	-61	146.3
7	-46.65	179.53
8	-24.38	198.53
9	-9.14	205.13
10	-6	205.13
11	6	205.13
12	25.91	192.6
13	26.71	179.53
14	48	146.3
15	113.4	146.3
16	145	143
17	145	156.2
18	55	146.3
19	49	151.6
20	52	150
21	25.93	180.5
22	27.93	180.5



Source: 2012 Lexington Dam SSE2 Rpt LN-3 Final

#2, 7, 8 ICU completed in Wahler (1982)

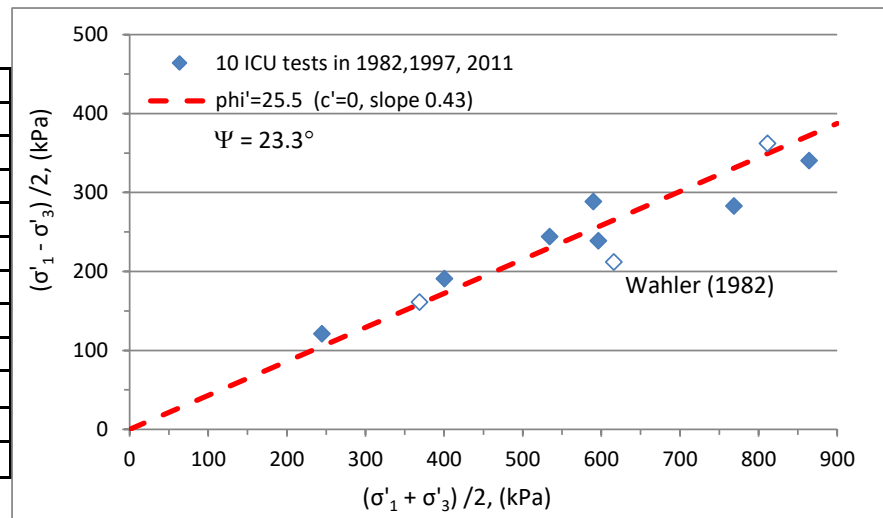
#5, 6, 9 done in 2011

	slope 0.43		slope 0.292		slope 0.32		slope 0.32		
1 kPa = 20.885 psf	0	0	0	0	0	20	40		
phi φ' (°) = 25.5	0.45	0.43	900	387.46	1200	350.4	900	308	328

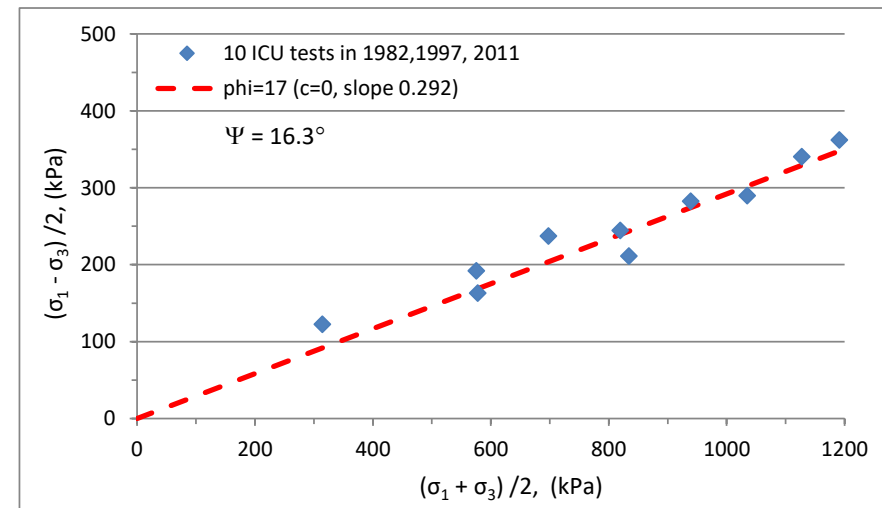
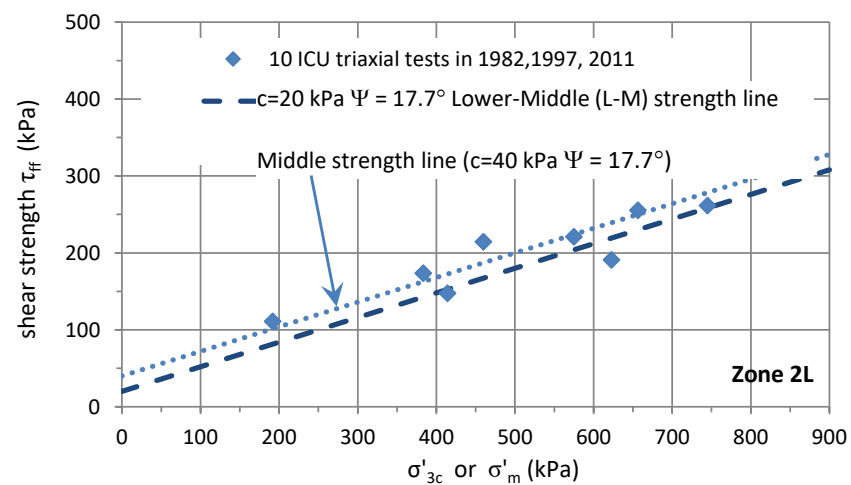
Effective stress

Zone 2 L core

Tests	sig'f (psf)	sig'f (kPa)	phi	phi (rad)	tau_ff	tau_max (kPa)	0.5*(s'1+s'3)	Kf
No.82-1	6230	298.4	25.9	0.45	144.90	161.08	368.78	2.55
No.82-2	11340	543.2	20.1	0.35	198.78	211.67	615.93	2.05
No.82-3	13570	650.0	26.5	0.46	324.08	362.13	811.58	2.61
No.97-1	3850	184.4	29.7	0.52	105.19	121.10	244.41	2.96
No.97-2	6450	309.0	28.5	0.50	167.75	190.88	400.04	2.83
No.97-3	8820	422.5	27.2	0.47	217.12	244.12	534.06	2.68
No.97-4	15240	730.0	23.2	0.40	312.88	340.40	864.09	2.30
No.11-1	10450	500.6	23.6	0.41	218.69	238.65	596.10	2.34
No.11-2	13870	664.4	21.6	0.38	263.04	282.91	768.52	2.17
No.11-3	9360	448.3	29.3	0.51	251.60	288.51	589.53	2.92



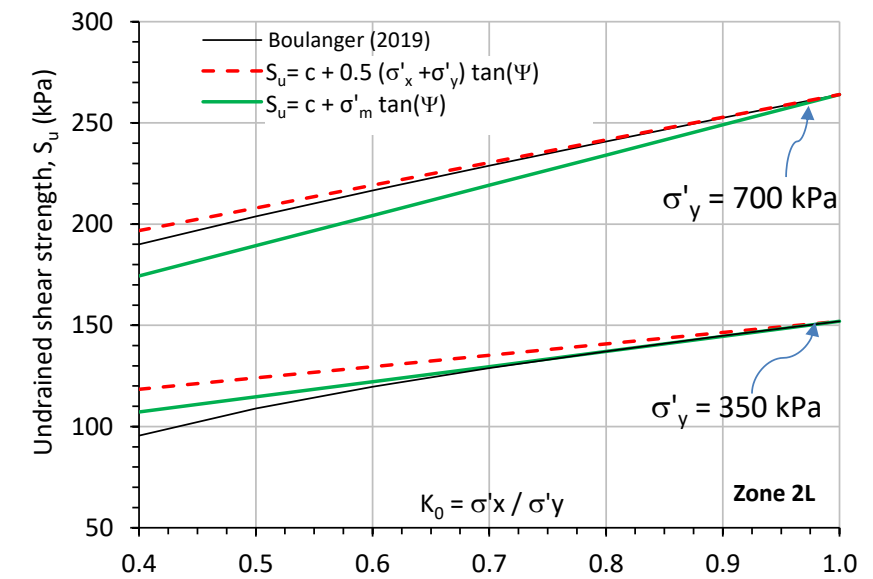
Tests	sig'c		tau_max (kPa)		At failure plane		tau_max (kPa)	Cross-Check OK
	sig'c	sig'c - kPa	(s1-s3)/2	(s1-s3)/2, kPa	tau_ff (kPa)	(s1+s3)/2		
No.82-1	8650	414.3	3410	163.3	147.4	577.7	1.4%	
No.82-2	13000	622.7	4410	211.2	190.7	833.9	-0.2%	
No.82-3	17300	828.7	7560	362.1	326.8	1190.8	0.0%	
No.97-1	4000	191.6	2560	122.6	110.7	314.2	1.2%	
No.97-2	8000	383.2	4010	192.1	173.4	575.3	0.6%	
No.97-3	12000	574.8	5110	244.8	220.9	819.6	0.3%	
No.97-4	16420	786.5	7110	340.6	307.4	1127.1	0.0%	
No.11-1	9600	459.8	4960	237.6	214.4	697.4	-0.4%	
No.11-2	13700	656.2	5900	282.6	255.1	938.8	-0.1%	
No.11-3	15550	744.8	6050	289.8	261.6	1034.6	0.4%	



K_f=2.5 used below

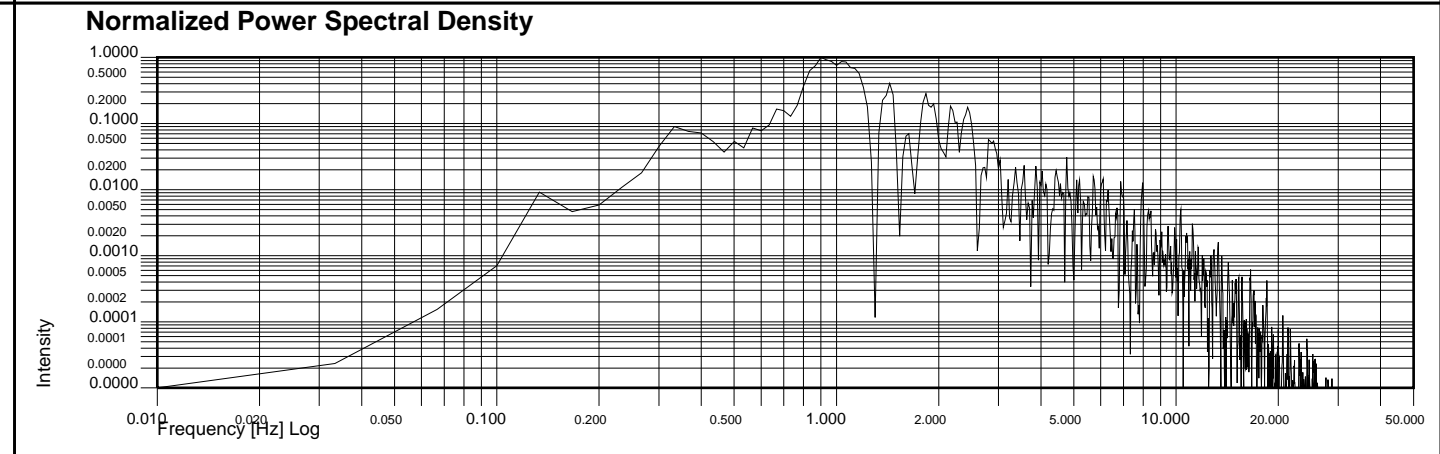
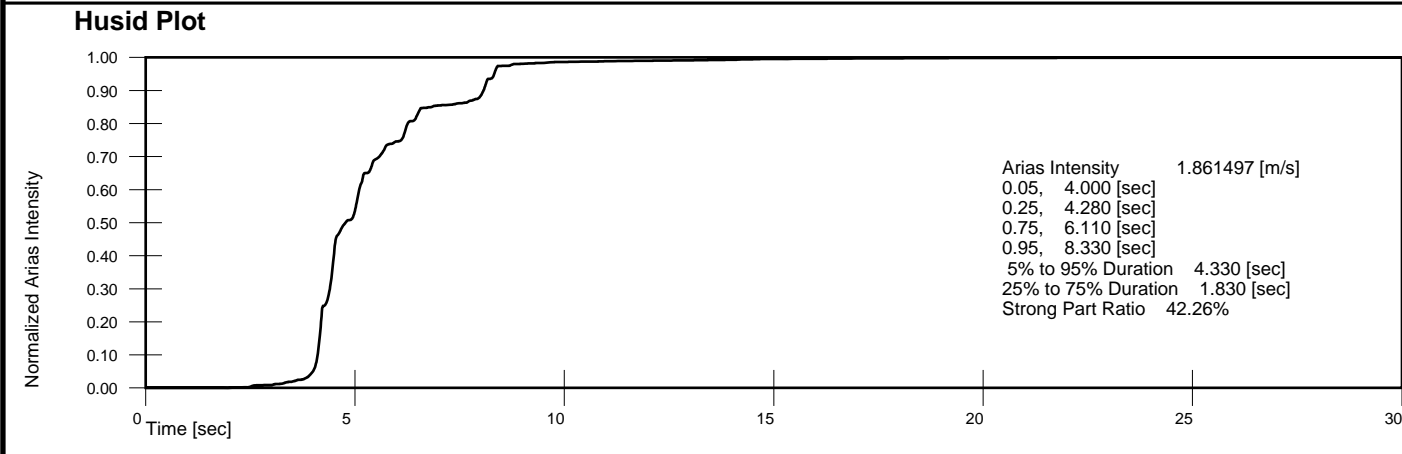
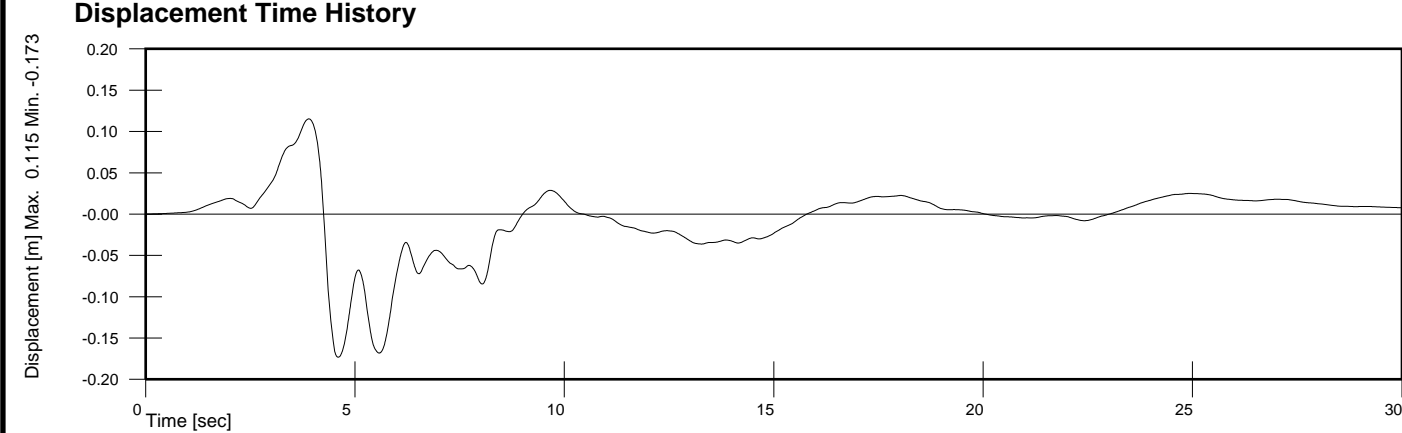
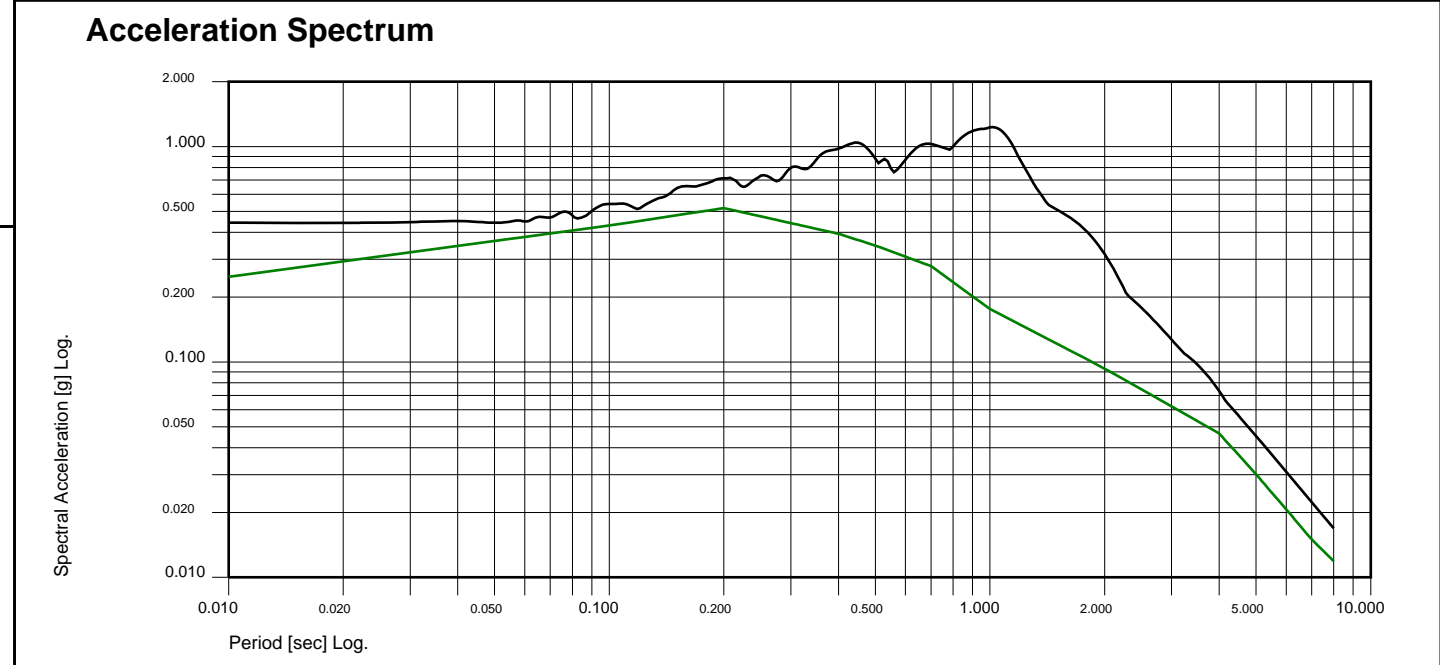
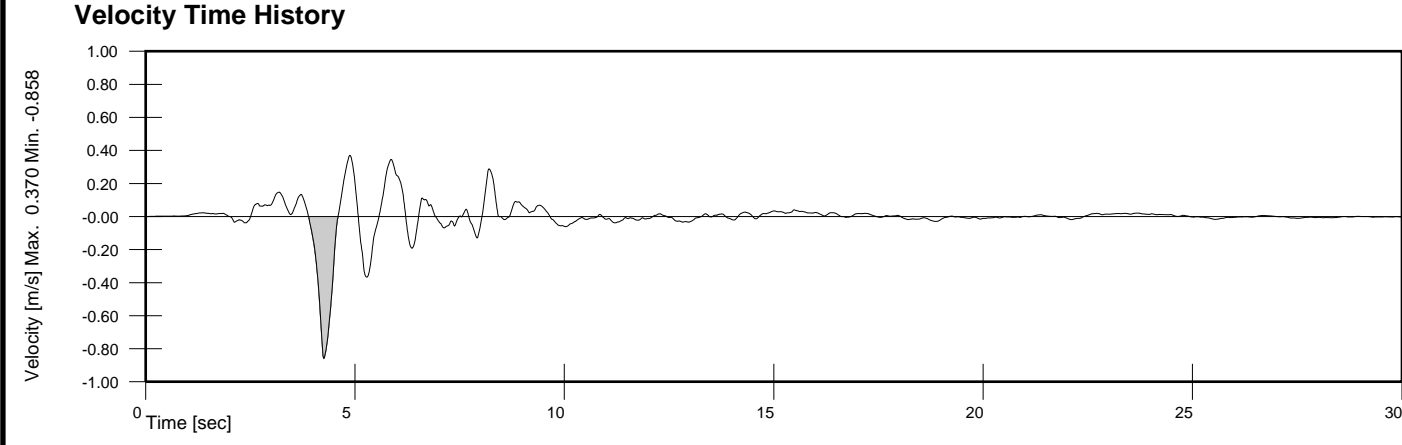
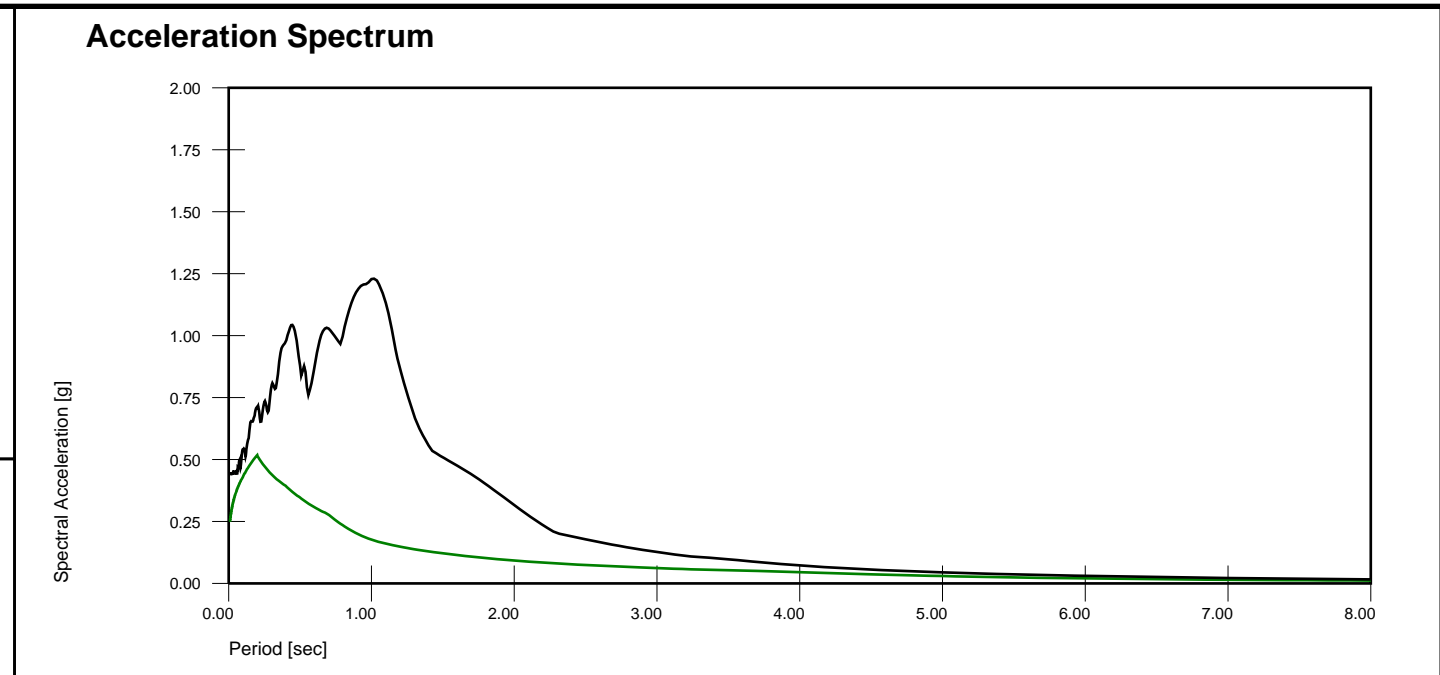
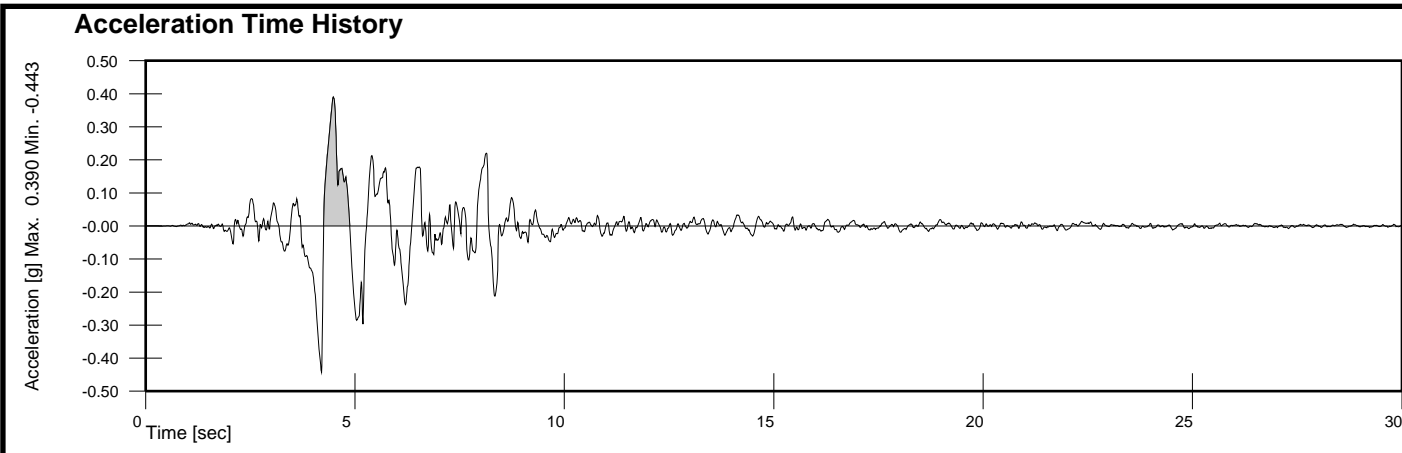
sig'1=	K0=	Kc=	sig'3	sig'fc	tau_ff_Kc=1	tau_ff_Kf	tau_ff_at Kc	Wu: sigma'_m	Wu: sigma'_p	Su_ratio	Su_ratio Boulanger (2019)
700	0.40	2.50	280	399.6	167.9	190.6	190.0	174.4	196.8	0.25	0.27
	0.50	2.00	350	449.7	183.9	214.5	203.8	189.3	208.0	0.27	0.29
	0.60	1.67	420.0	499.7	199.9	238.4	216.6	204.3	219.2	0.29	0.31
	0.70	1.43	490.0	549.8	215.9	262.2	228.8	219.2	230.4	0.31	0.33
	0.80	1.25	560	599.9	232.0	286.1	240.7	234.1	241.6	0.33	0.34
	0.90	1.11	630	649.9	248.0	310.0	252.5	249.1	252.8	0.36	0.36
	1.00	1.00	700	700.0	264.0	333.9	264.0	264.0	264.0	0.38	0.38

sig'1=	K0=	Kc=	sig'3	sig'fc	tau_ff_Kc=1	tau_ff_Kf	tau_ff_at Kc	Wu: sigma'_m	Wu: sigma'_p	Su_ratio	Su_ratio Boulanger (2019)
350	0.40	2.50	140	199.8	103.9	95.3	95.5	107.2	118.4	0.31	0.27
	0.50	2.00	175	224.8	111.9	107.2	108.9	114.7	124.0	0.33	0.31
	0.60	1.67	210	249.9	120.0	119.2	119.6	122.1	129.6	0.35	0.34
	0.70	1.43	245	274.9	128.0	131.1	128.8	129.6	135.2	0.37	0.37
	0.80	1.25	280	299.9	136.0	143.1	137.1	137.1	140.8	0.39	0.39
	0.90	1.11	315	325.0	144.0	155.0	144.8	144.5	146.4	0.41	0.41
	1.00	1.00	350	350.0	152.0	166.9	152.0	152.0	152.0	0.43	0.43



**APPENDIX C RSN3548_LOMAP_LEX(X, Y, Z) & CREST
ACCELERATION**

- Earthquake accelerations recorded on bedrock at the left abutment of the Lenihan Dam: RSN3548_LOMAP_LEX000, 090, -UP downloaded from PEER database (PEER 2021).
- Computed horizontal accelerations at the dam crest for Case-2A(g), Case-2A(h), and Case-2A(y) in Table 3



Set:001, Dir:X, File: C:\2021\THS\Base-acc-00.aaa

Desc.: BaseACCx

Incremental Velocity 1.227 [m/s], Incremental Displacement 0.289 [m]
 PGA Ratio 0.560, Area Ratio 0.477 [1.000 Hz to 10.000 Hz], MSE 0.248661

not target spectrum - sample only

BChydro

unscaled LEX00,90,-UP

1989 Loma Pieta EQ

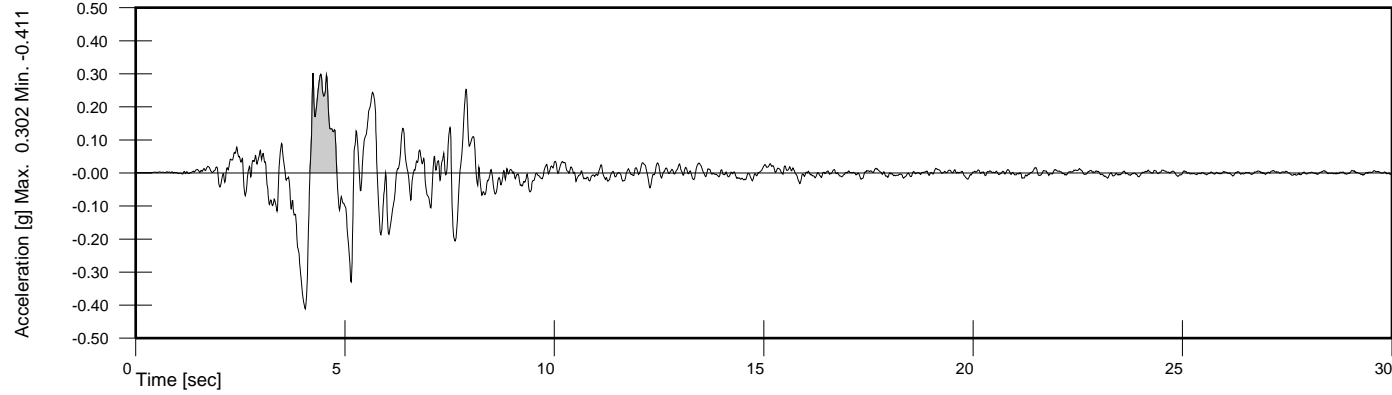
THS by A. Felber, Program Version 0.01, 2010 June 15

Date: 2022, March, 14

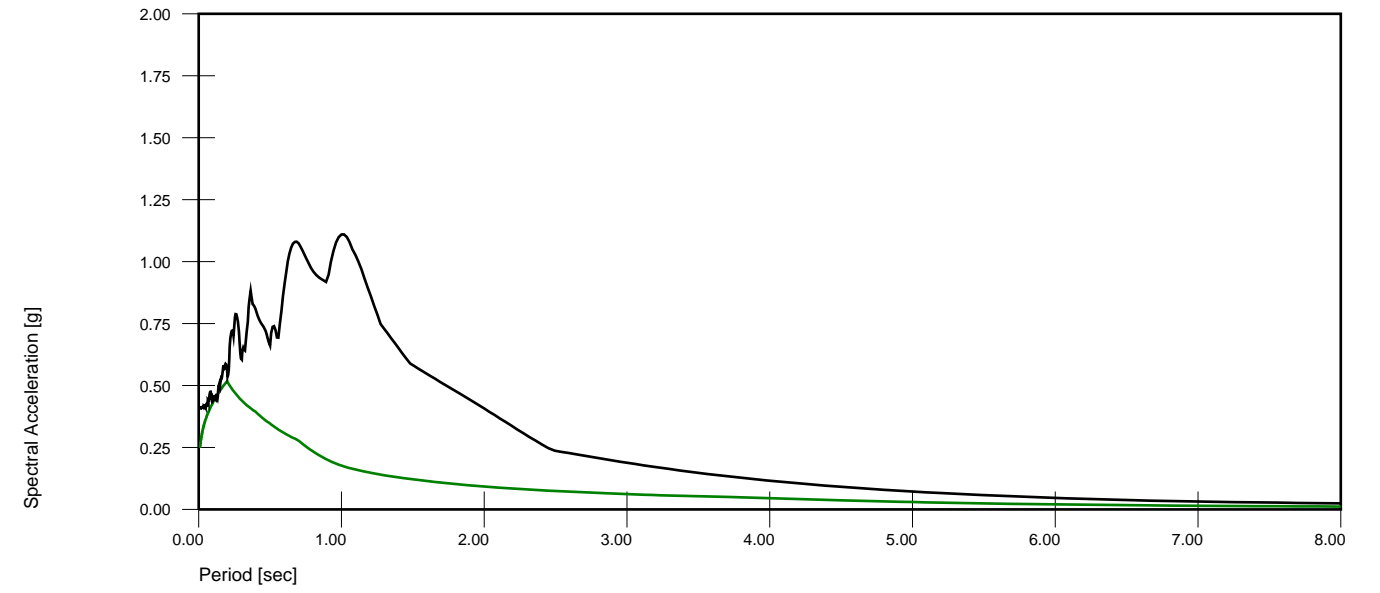
Time: 16:56:04

Page 7 of 12

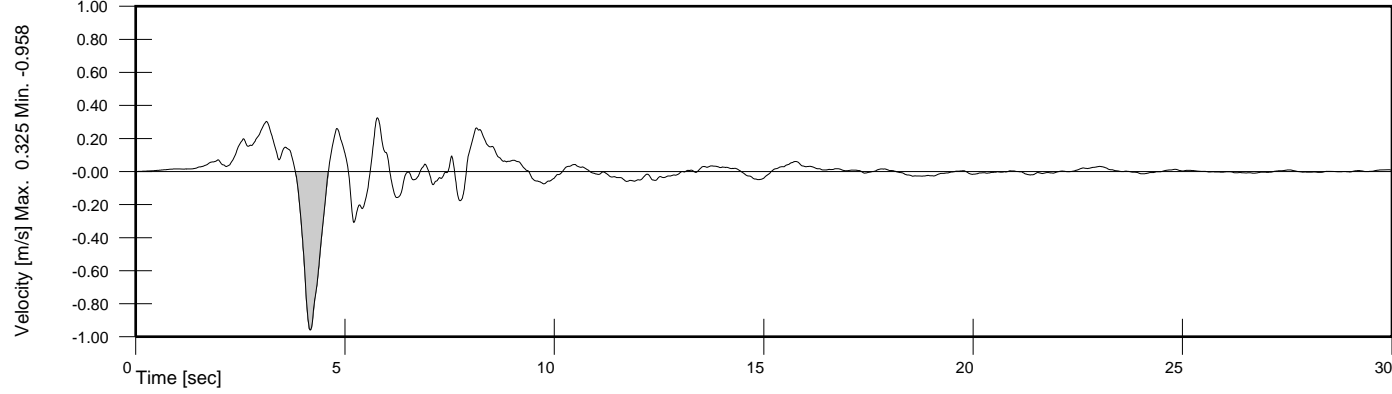
Acceleration Time History



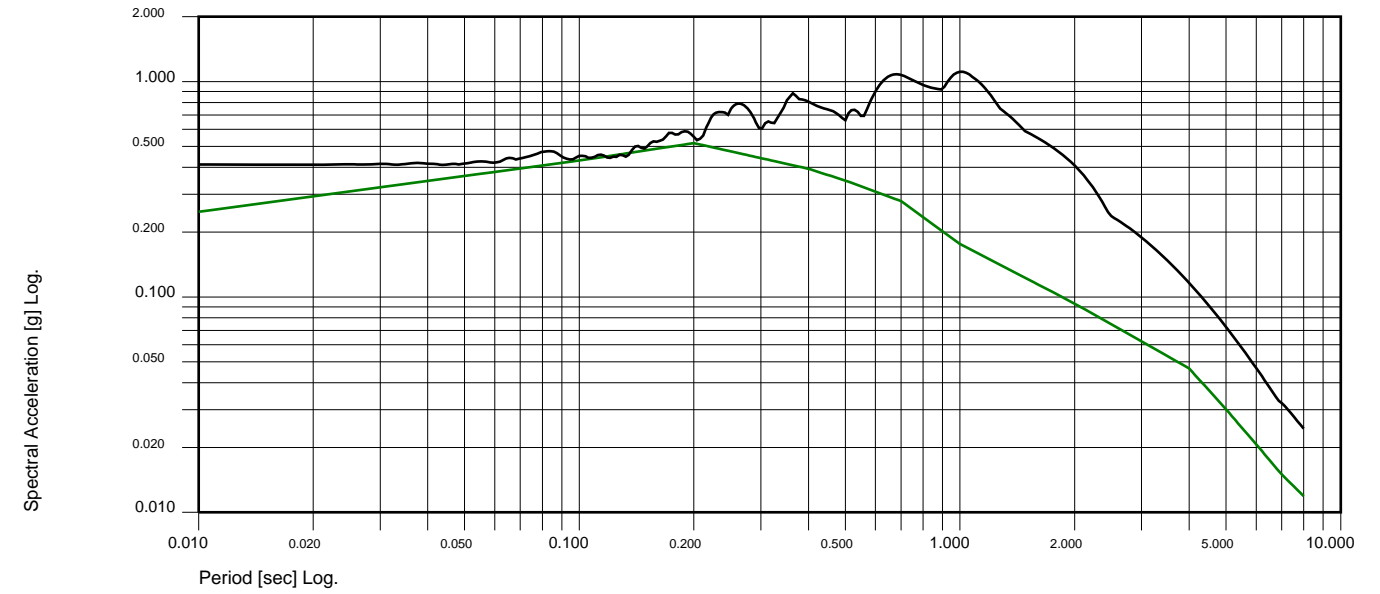
Acceleration Spectrum



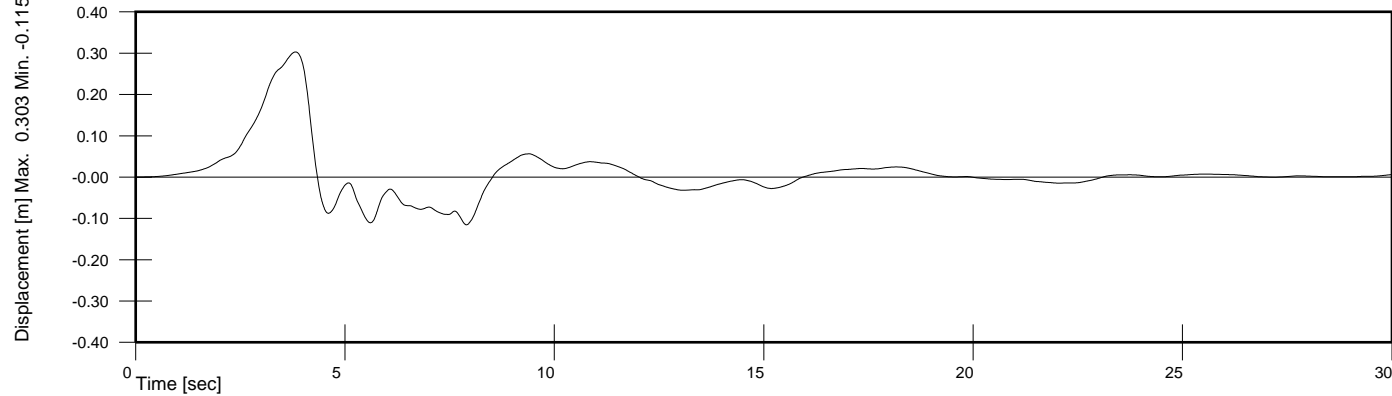
Velocity Time History



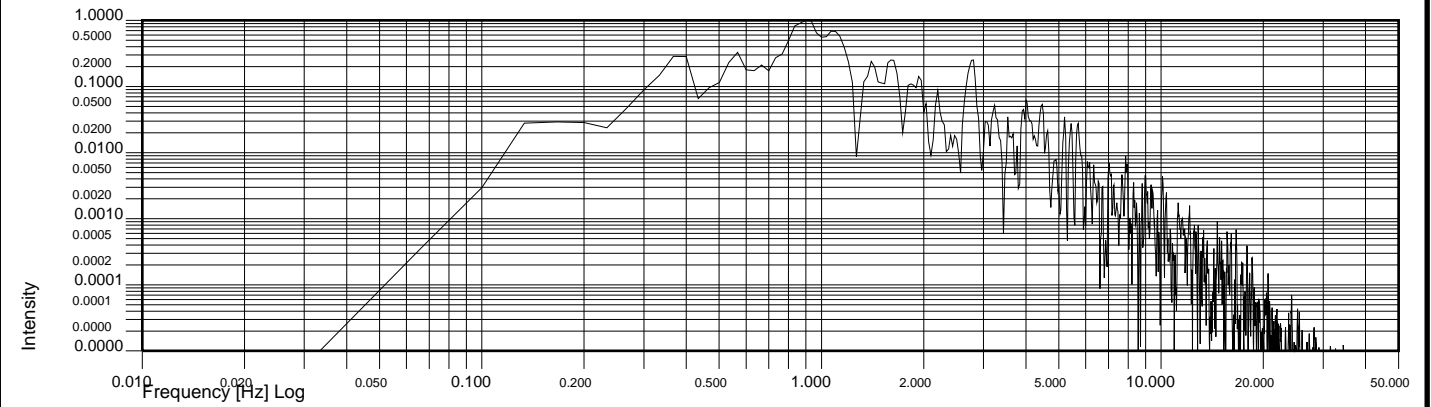
Acceleration Spectrum



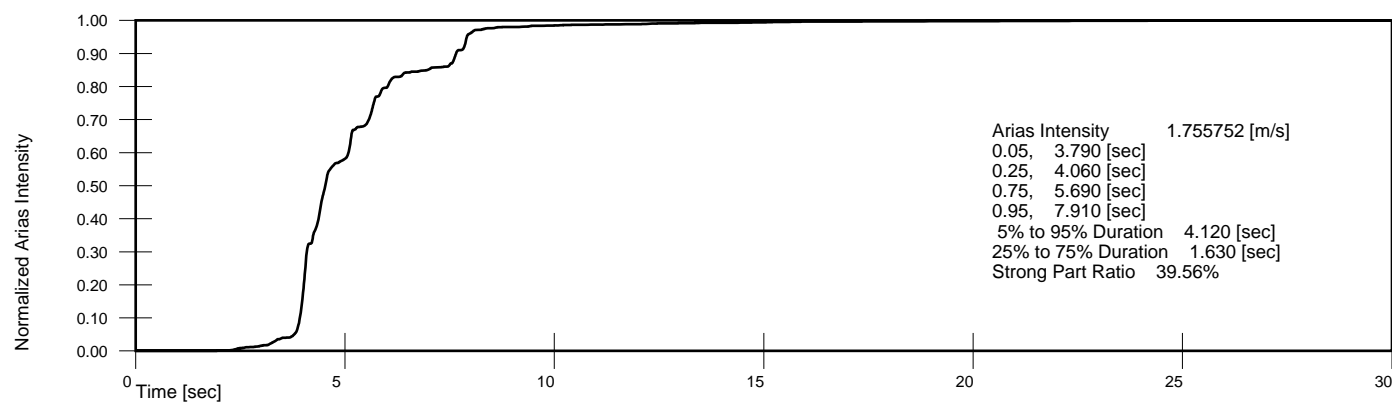
Displacement Time History



Normalized Power Spectral Density



Husid Plot



Set:001, Dir:Y, File: C:\2021\THS\Base-acc-90.aaa

Desc.: BaseACC090

Incremental Velocity 1.219 [m/s], Incremental Displacement 0.391 [m]
 PGA Ratio 0.603, Area Ratio 0.543 [1.000 Hz to 10.000 Hz], MSE 0.277735

not target spectrum - sample only

BChydro

unscaled LEX00,90,-UP

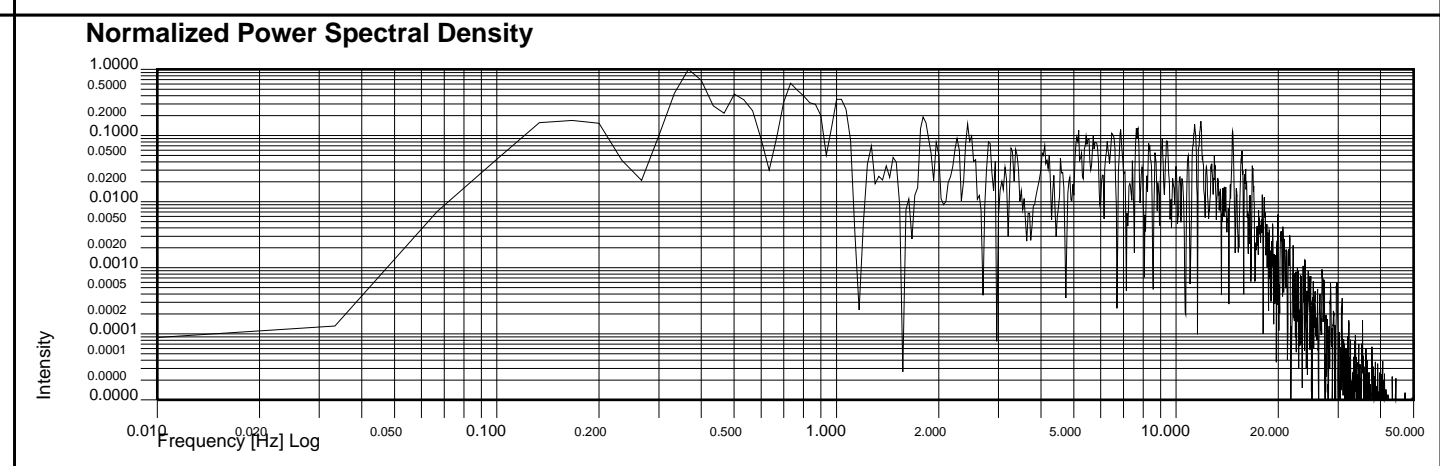
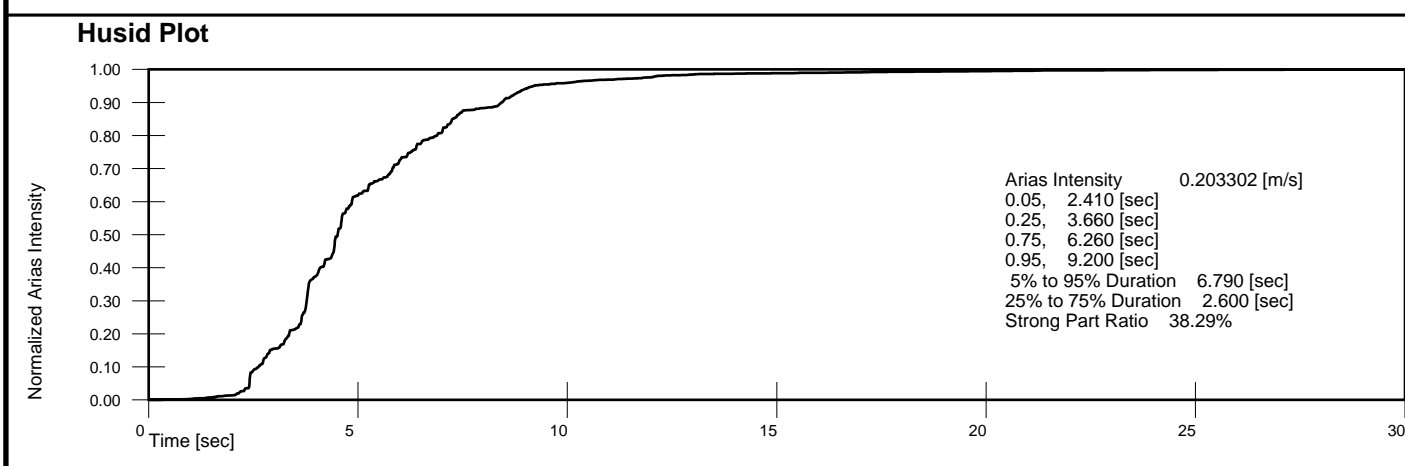
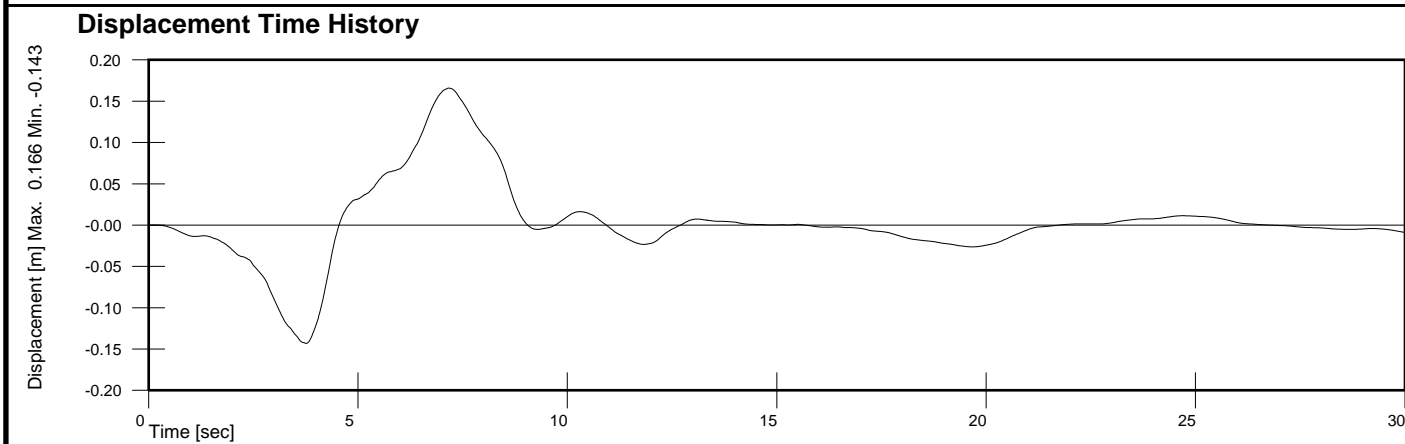
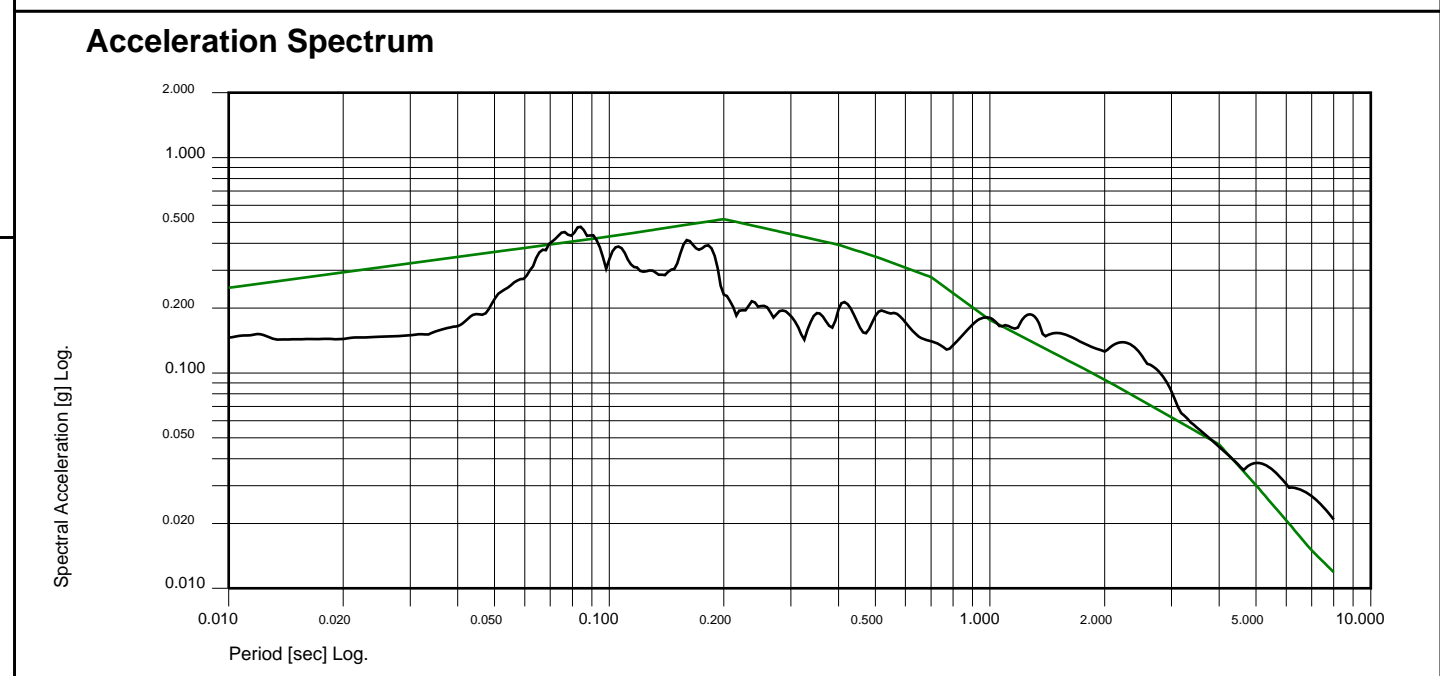
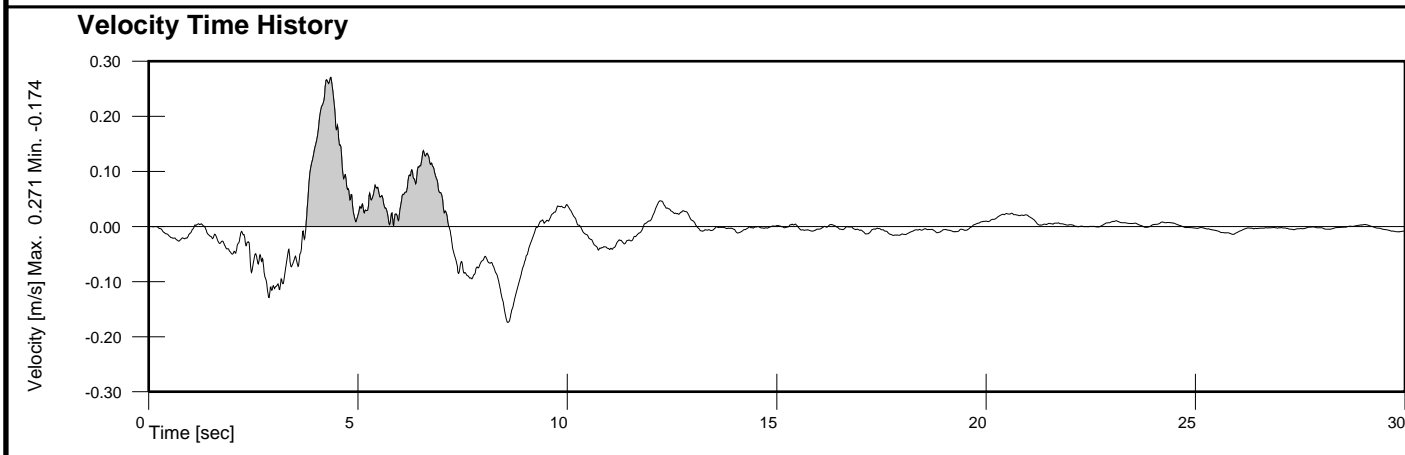
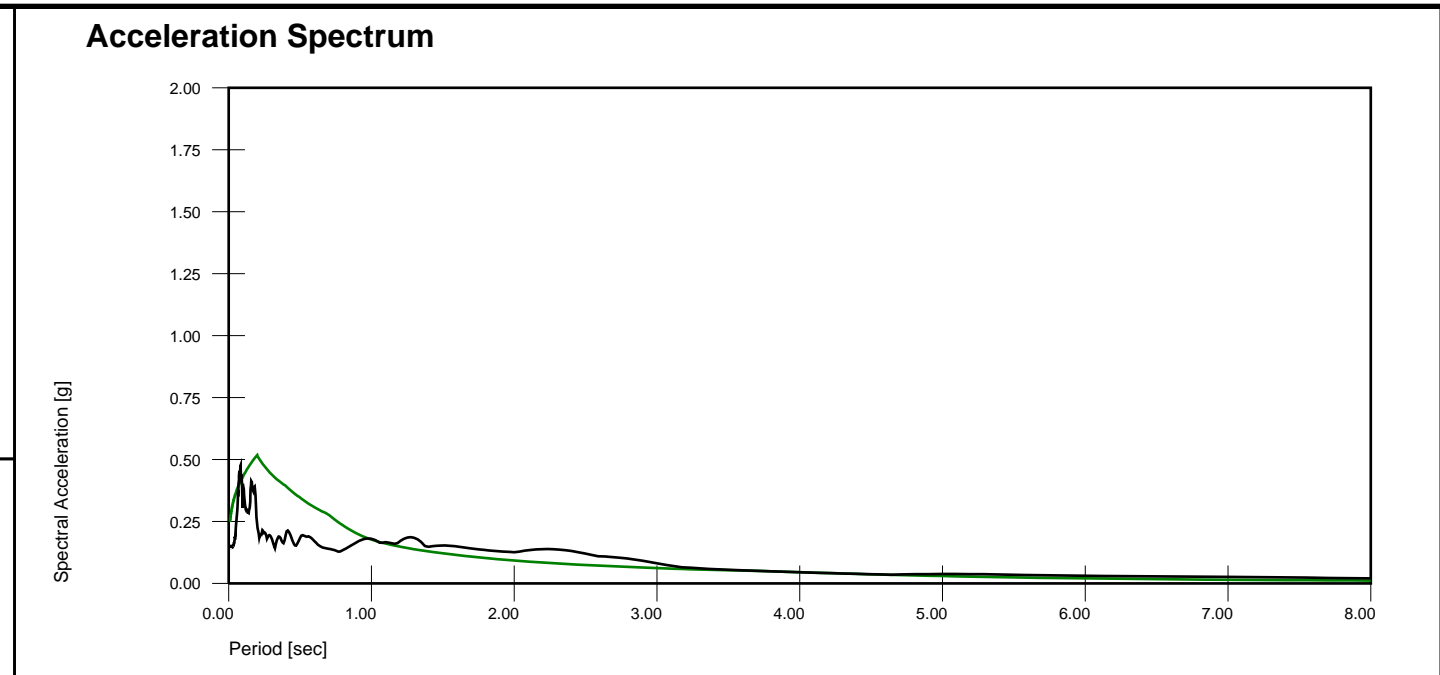
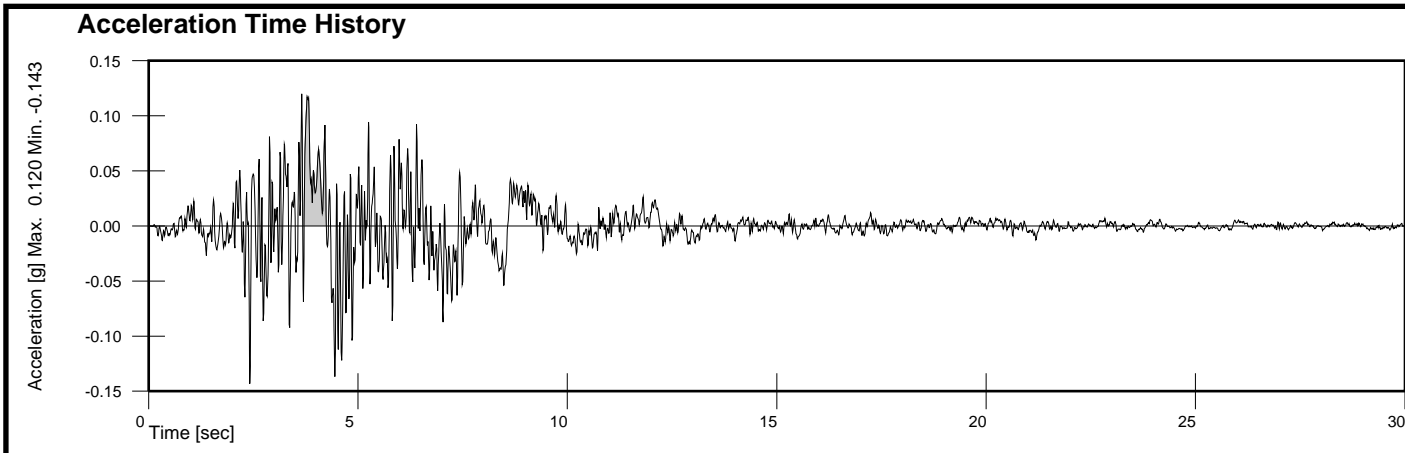
1989 Loma Pieta EQ

THS by A. Felber, Program Version 0.01, 2010 June 15

Date: 2022, March, 14

Time: 16:56:04

Page 8 of 12



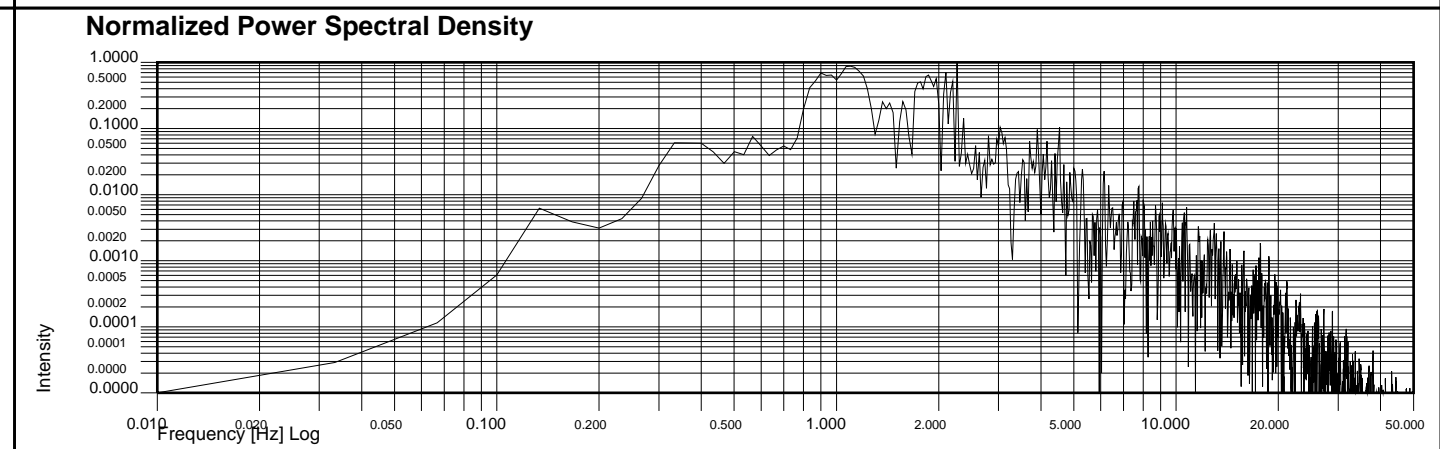
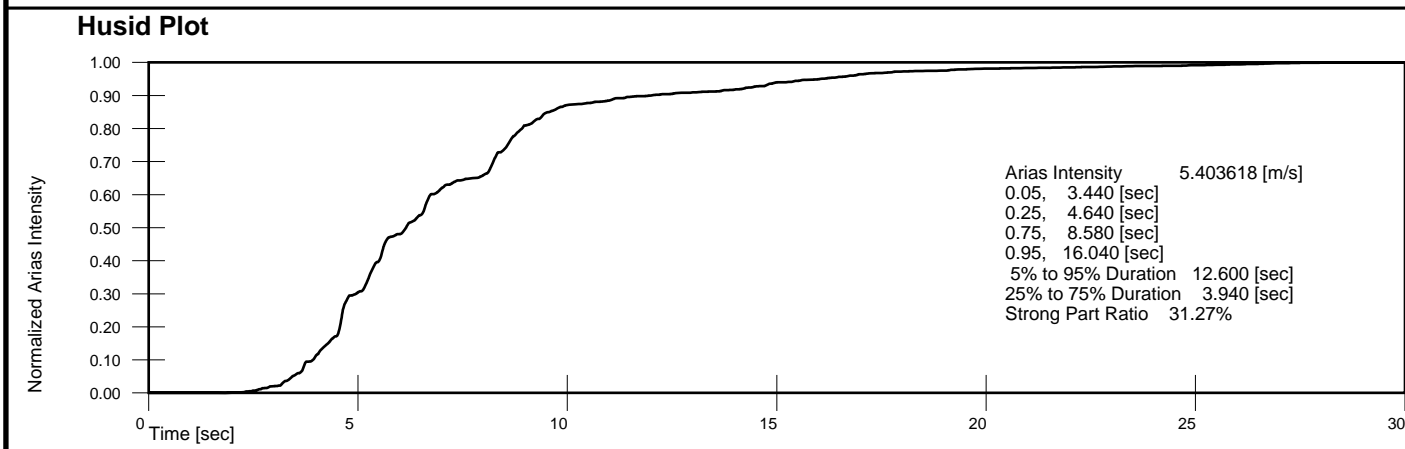
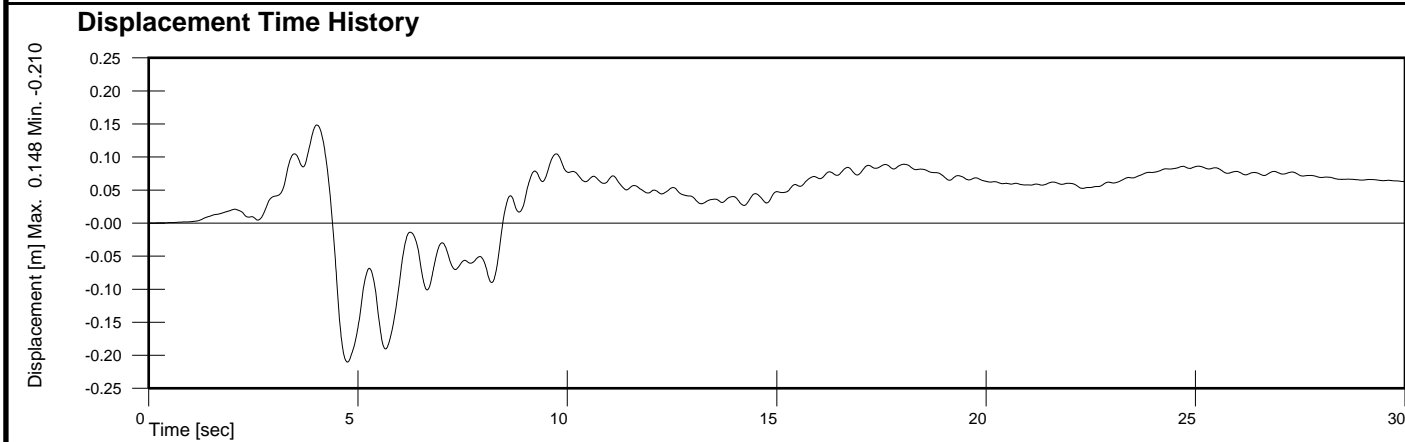
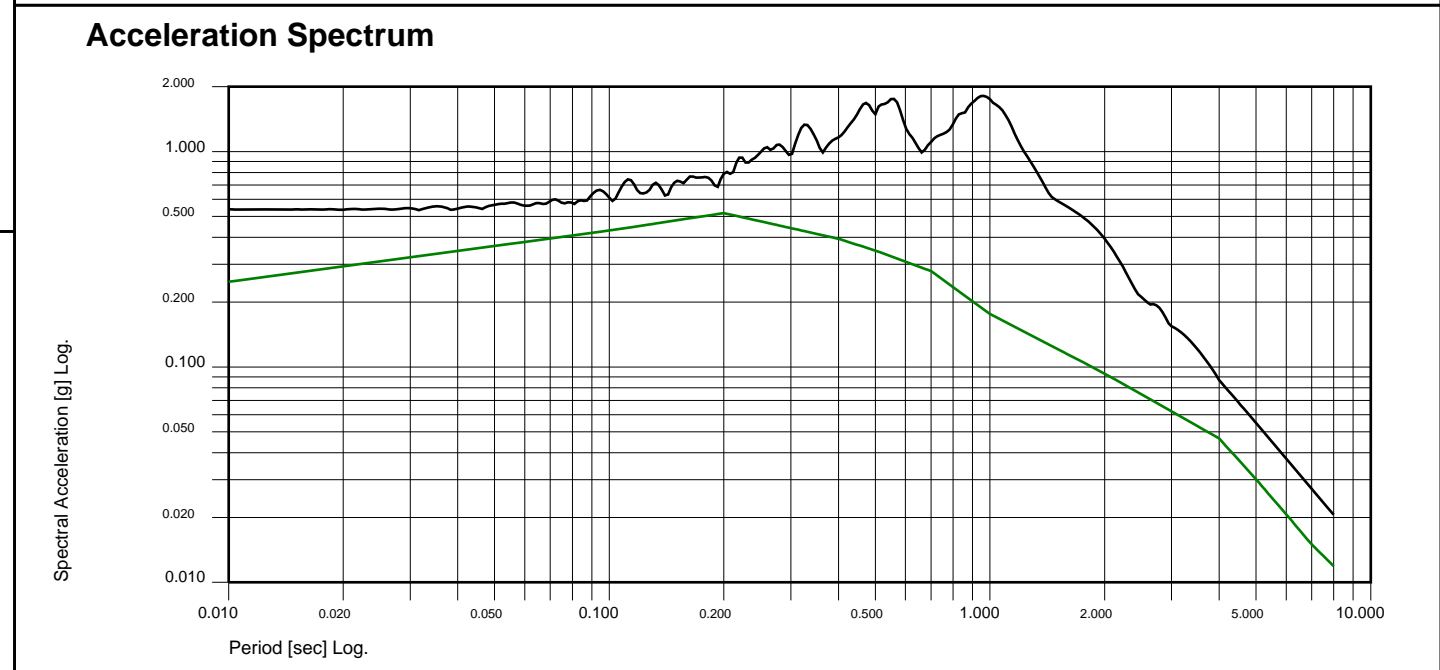
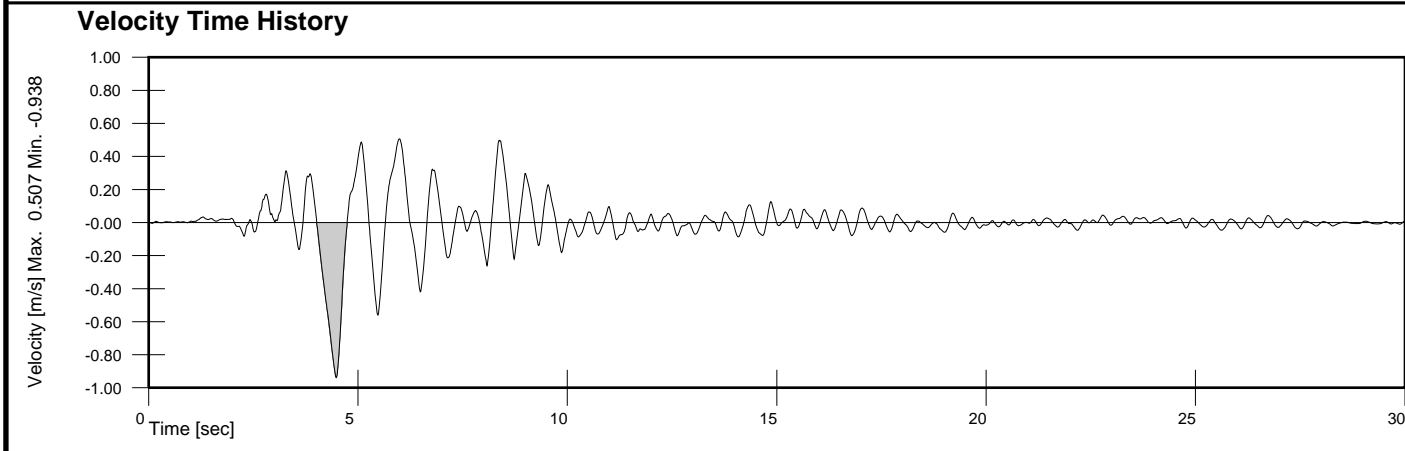
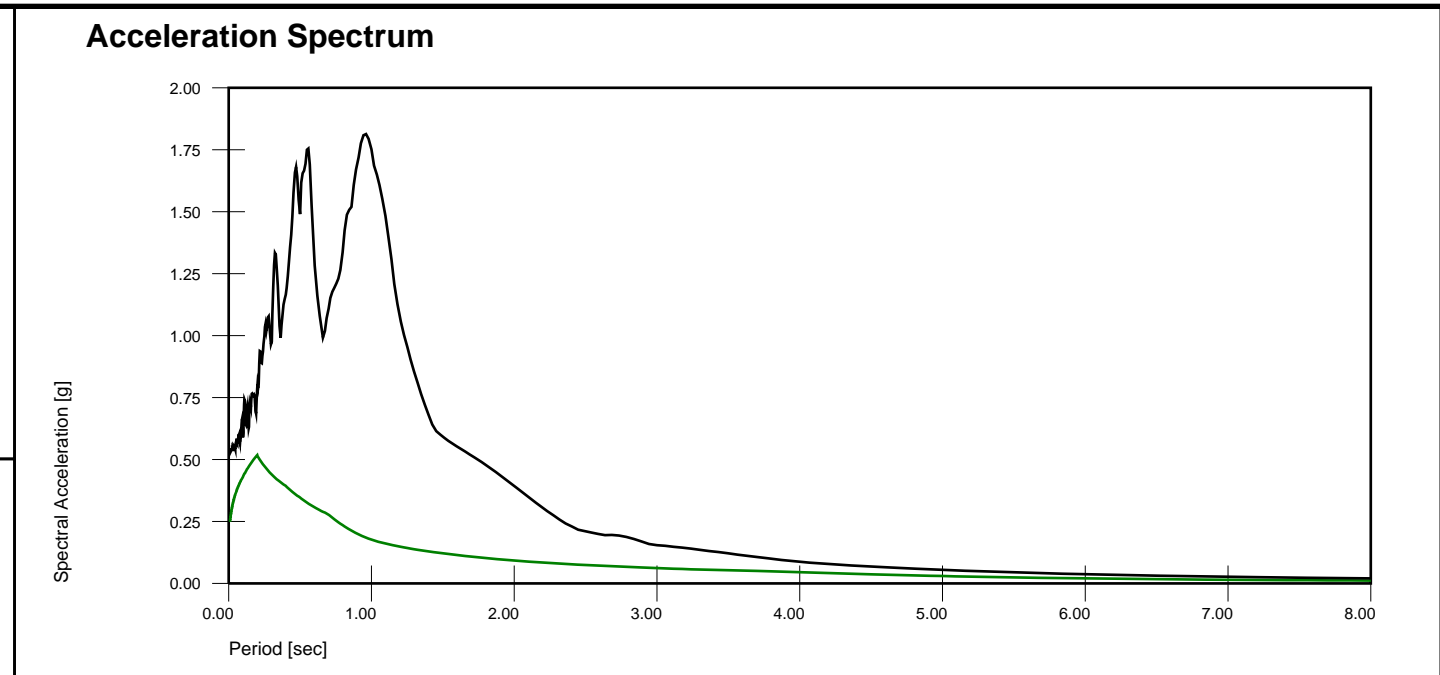
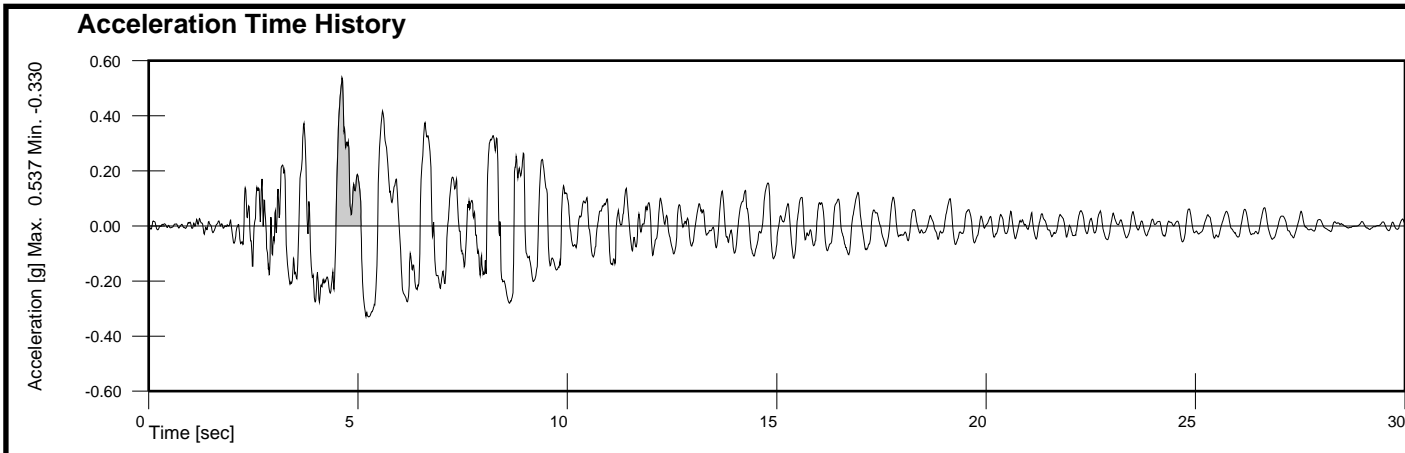
Set:001, Dir:X, File: C:\2021\THS\Base-acc-UP.aaa
 Desc.: BaseACC-y

Incremental Velocity 0.289 [m/s], Incremental Displacement 0.309 [m]
 PGA Ratio 1.704, Area Ratio 1.801 [1.000 Hz to 10.000 Hz], MSE 0.070255

not target spectrum - sample only

BChydro
 unscaled LEX00,90,-UP
 1989 Loma Pieta EQ

THS by A. Felber, Program Version 0.01, 2010 June 15
 Date: 2022, March, 14 Time: 16:56:05 Page 9 of 12

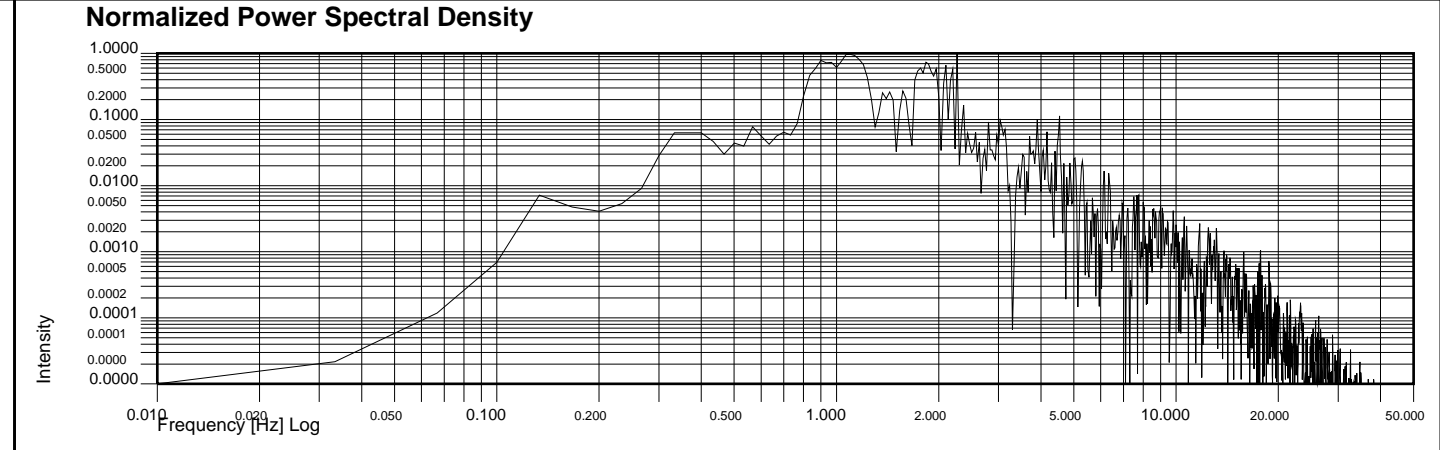
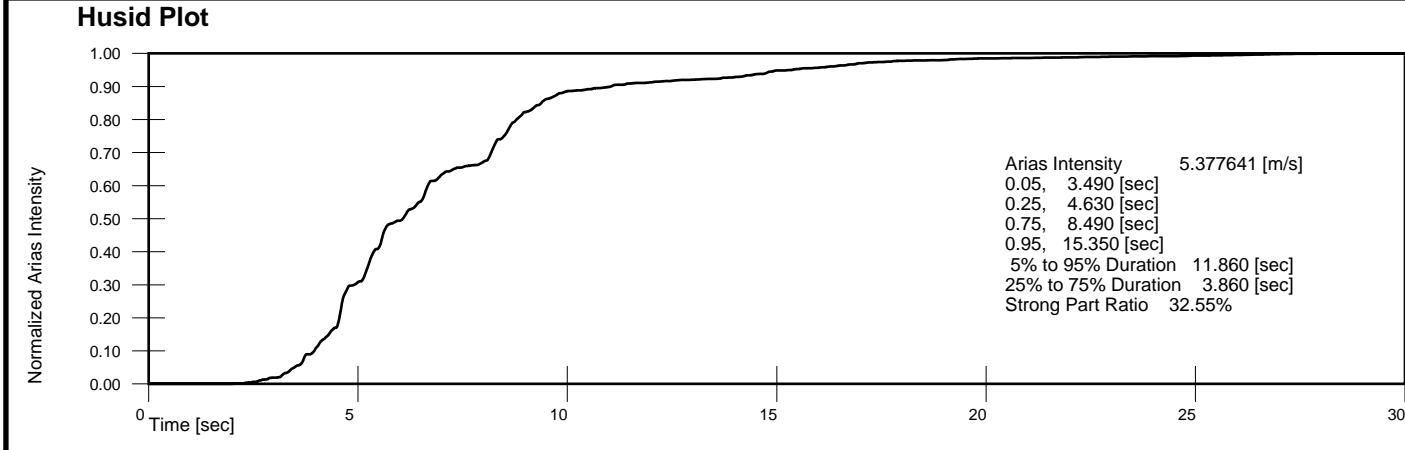
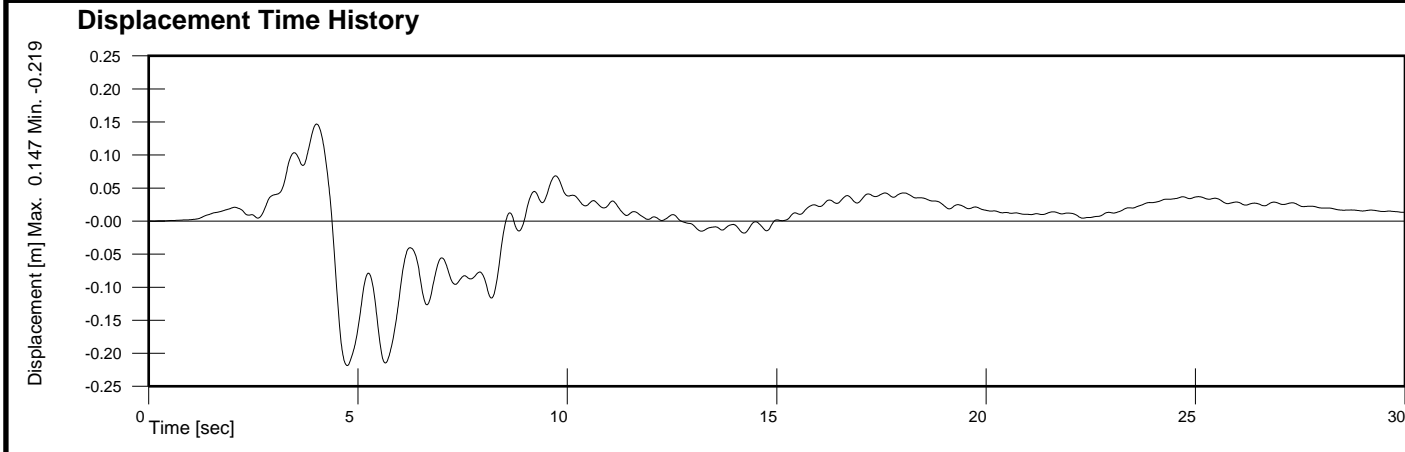
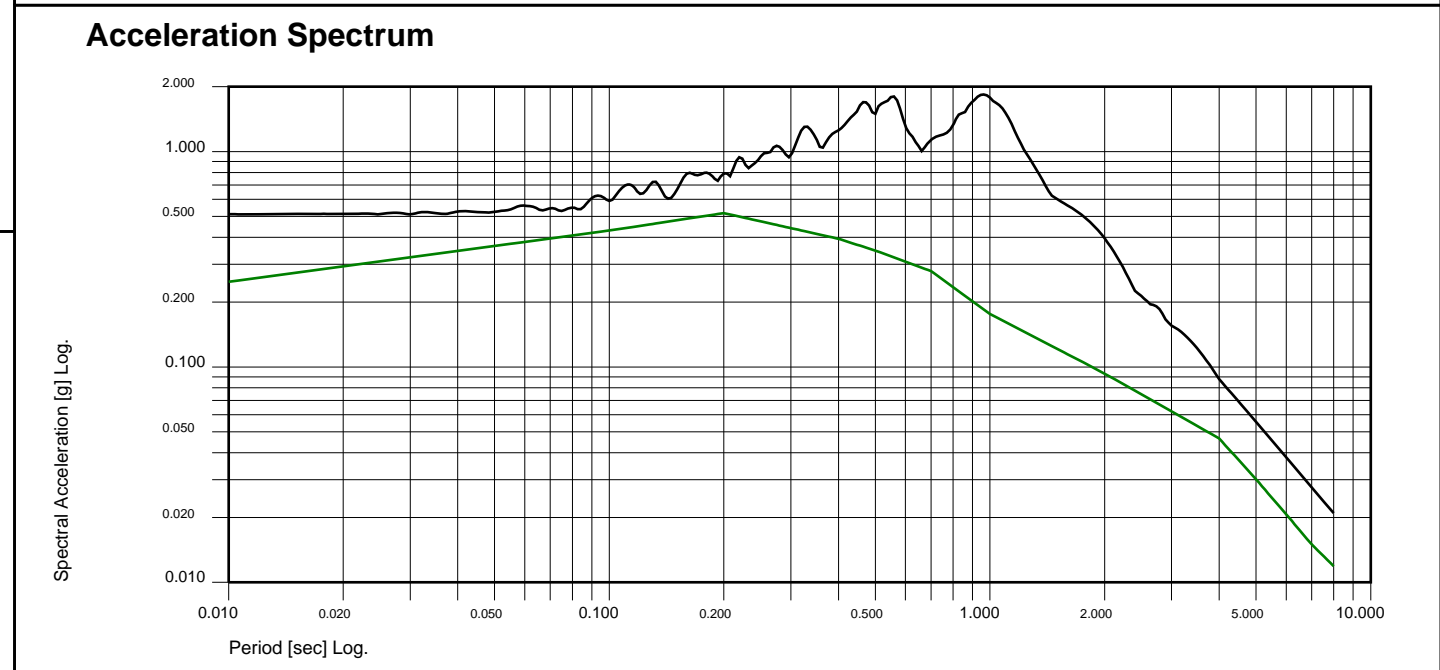
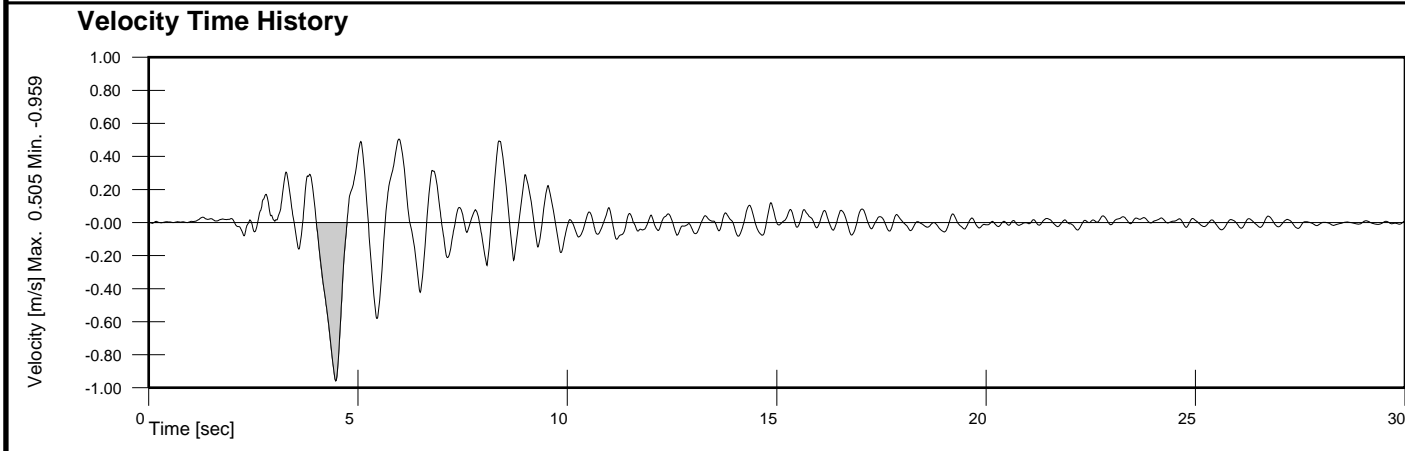
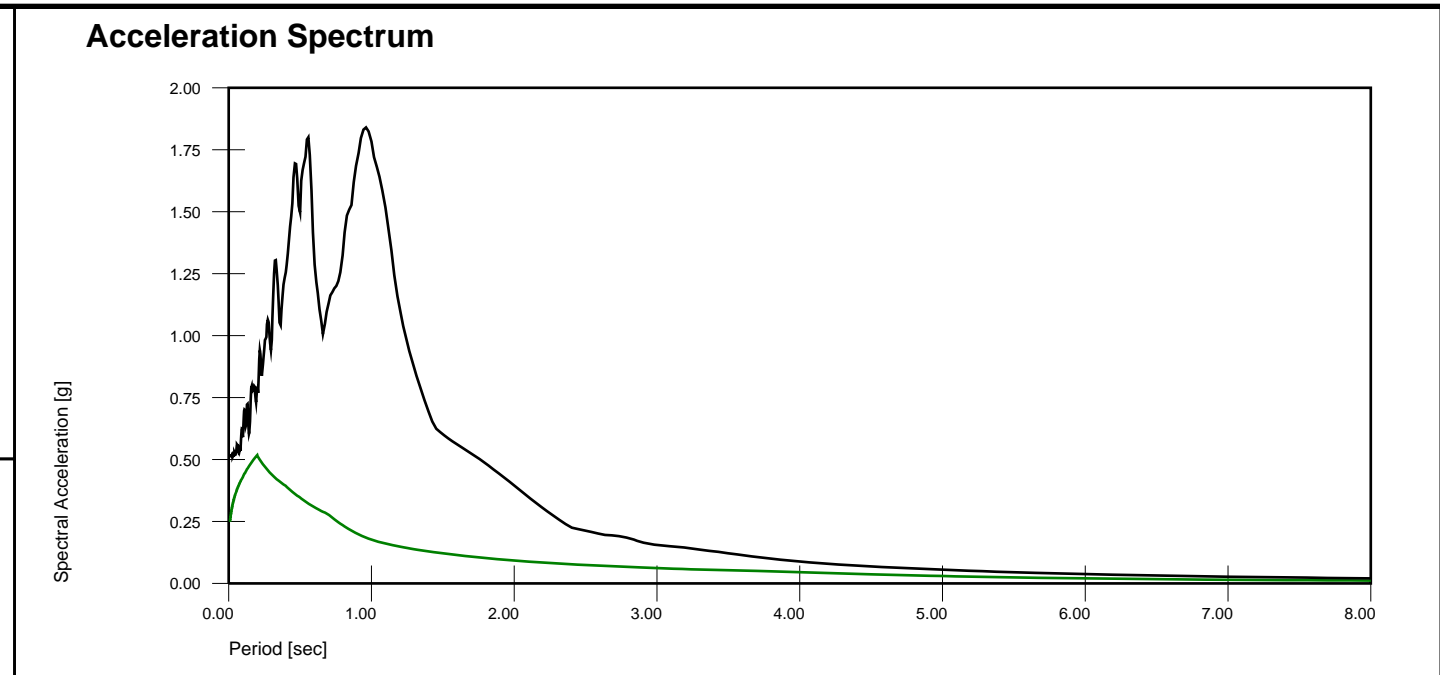
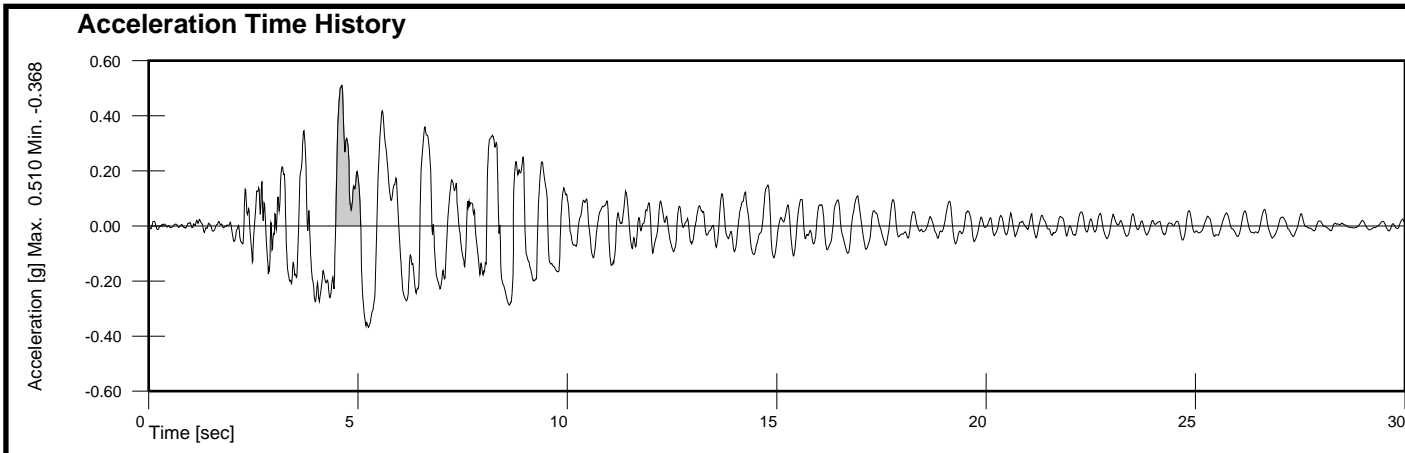


Set:001, Dir:X, File: C:\2021\THS\2A-g_00.aaa
 Desc.: aaa

Incremental Velocity 1.423 [m/s], Incremental Displacement 0.359 [m]
 PGA Ratio 0.461, Area Ratio 0.361 [1.000 Hz to 10.000 Hz], MSE 0.323385

not target spectrum - sample only

BChydro
 unscaled LEX00,90,-UP
 1989 Loma Pieta EQ
 THS by A. Felber, Program Version 0.01, 2010 June 15
 Date: 2022, March, 14 Time: 16:56:05 Page 10 of 12



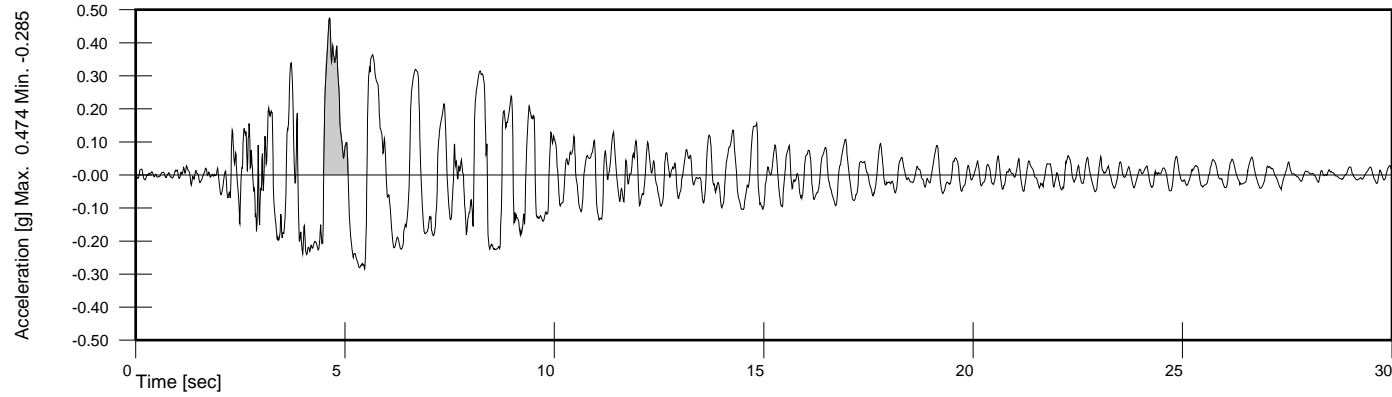
Set:001, Dir:X, File: C:\2021\THS\2A-h_00.aaa
 Desc.: aaa

Incremental Velocity 1.448 [m/s], Incremental Displacement 0.365 [m]
 PGA Ratio 0.486, Area Ratio 0.359 [1.000 Hz to 10.000 Hz], MSE 0.331160

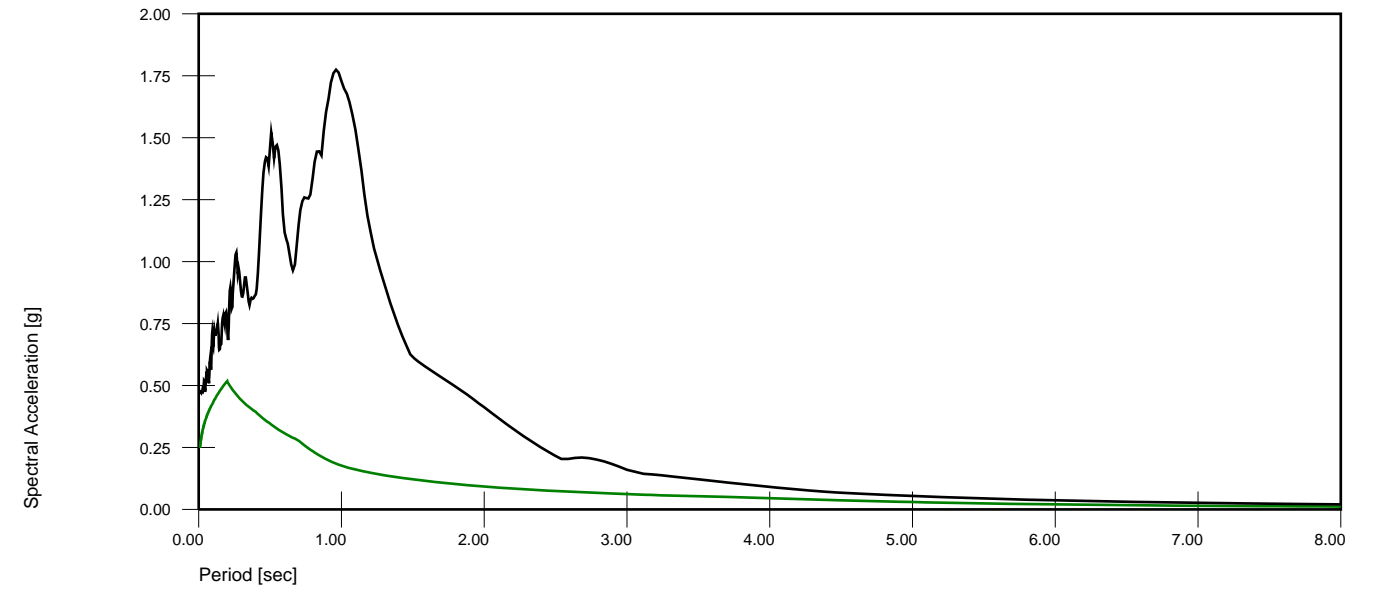
not target spectrum - sample only

BChydro
 unscaled LEX00,90,-UP
 1989 Loma Pieta EQ

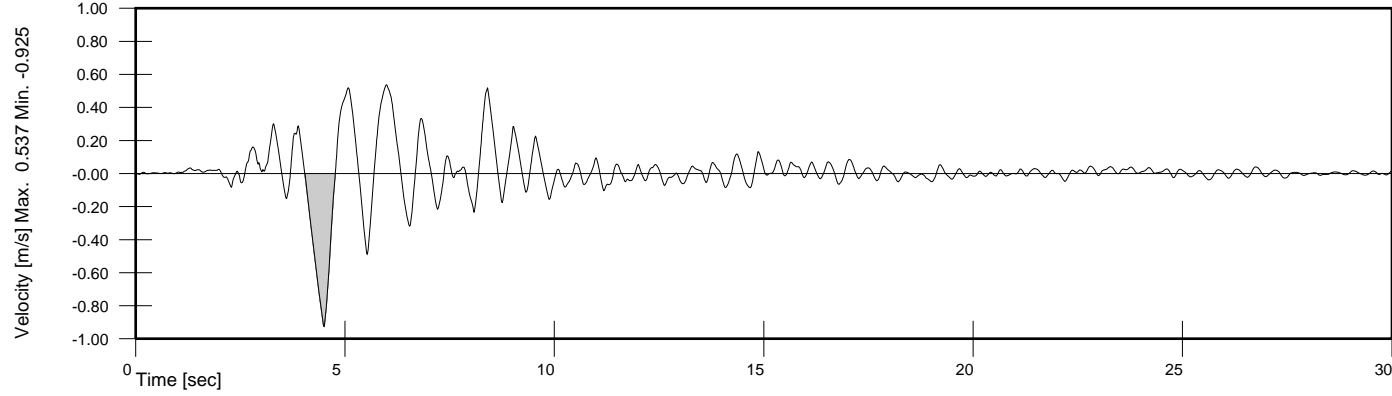
Acceleration Time History



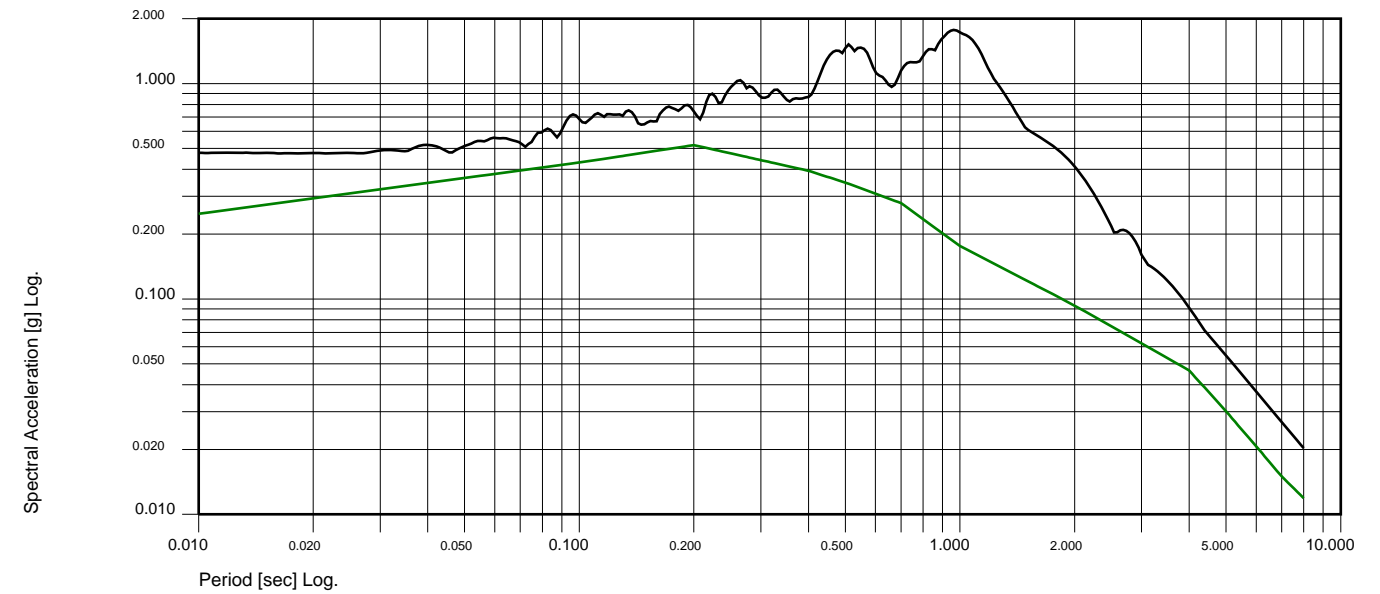
Acceleration Spectrum



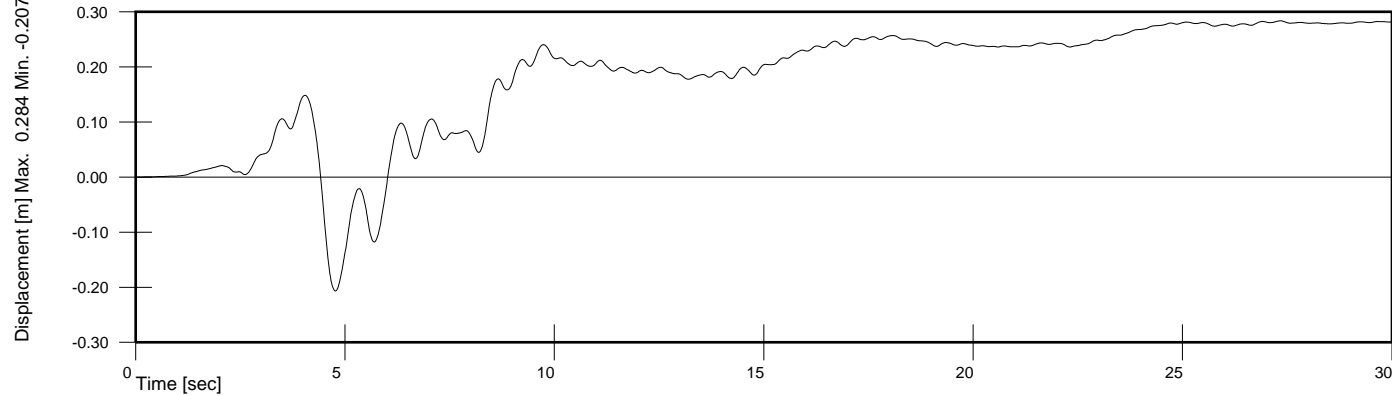
Velocity Time History



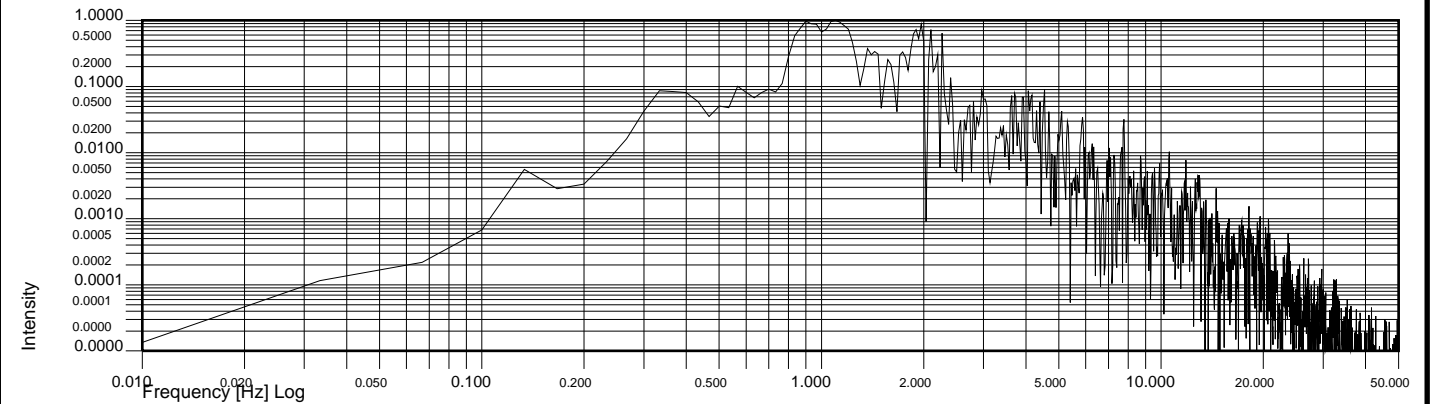
Acceleration Spectrum



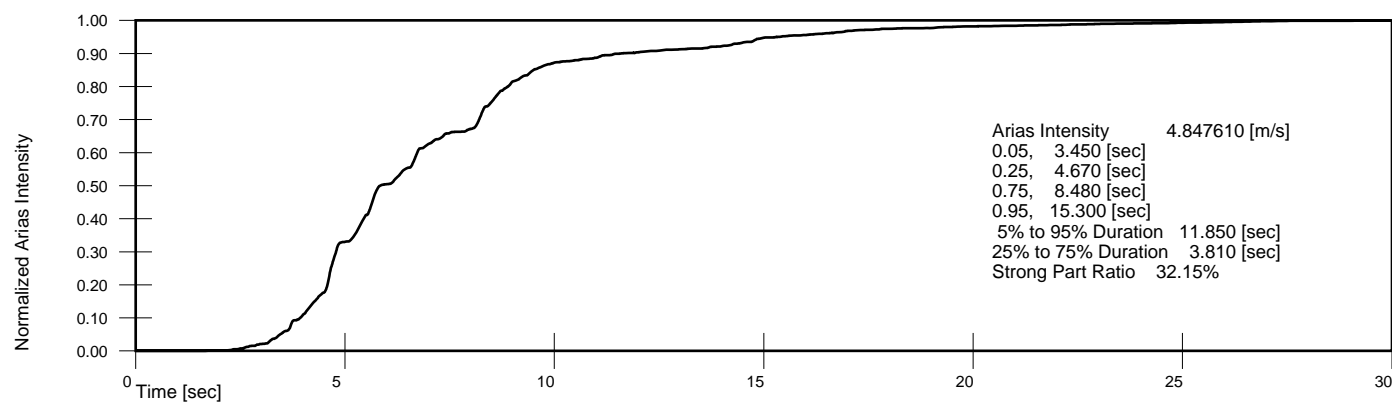
Displacement Time History



Normalized Power Spectral Density



Husid Plot



Set:001, Dir:X, File: C:\2021\THS\2A-y_00.aaa

Desc.: aaa

Incremental Velocity 1.442 [m/s], Incremental Displacement 0.355 [m]
PGA Ratio 0.522, Area Ratio 0.390 [1.000 Hz to 10.000 Hz], MSE 0.303698

not target spectrum - sample only

BChydro

unscaled LEX00,90,-UP

1989 Loma Pieta EQ

THS by A. Felber, Program Version 0.01, 2010 June 15

Date: 2022, March, 14

Time: 16:56:05

Page 12 of 12

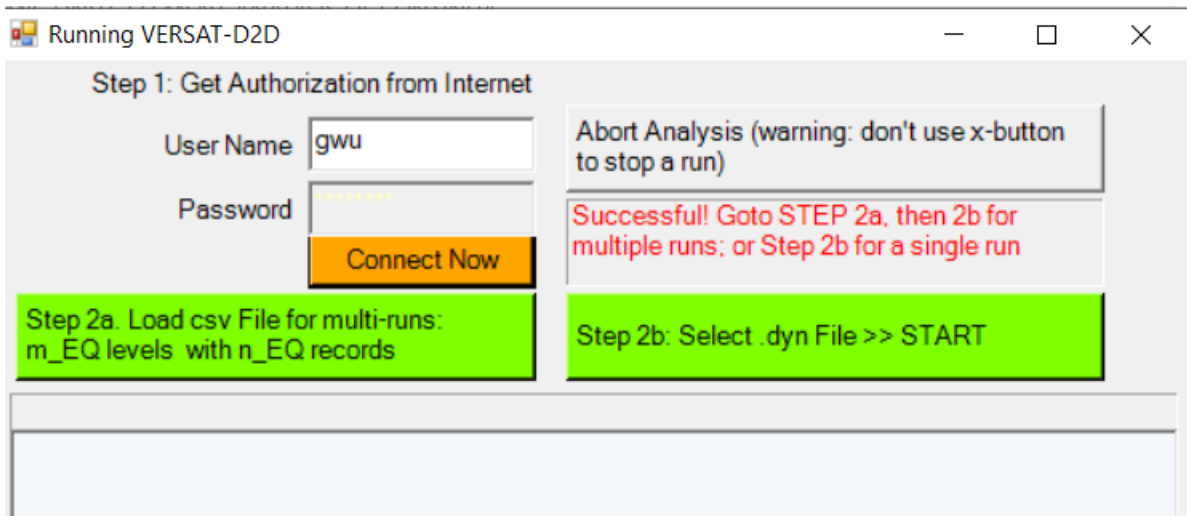
APPENDIX D VERSAT-2D INPUT AND OUTPUT FILES

Notes:

- All input files are in text format so they are convenient for import/export. See VERSAT-2D Technical and User Manuals for details.
- The node and element information (or data) are essentially the same for Input File 1, Input File 2 and Input File 4. However, when needed for modelling of special problems, the MAT data and the PWP data for each element can change in various stages of modelling.

Steps:

1. Run 'VERSAT-S2D' using Input File 1: LEX-2A_dry.sta
2. Rename the stress output "LEX-2A_dry.pr4" as "LEX-2A_add-w.t.prx"
3. Run 'VERSAT-S2D' using Input File 2: LEX-2A_add-w.t.sta
4. Rename the stress output "LEX-2A_add-w.t.pr4" as "LEX-2A(g).prx"
5. Run "VERSAT-D2D" (see below interactive window)
 - a. Click Step 2a and load Input File 3: LEX-2A(g).PSPA.csv; then
 - b. Click Step 2b and load Input File 4: LEX-2A(g).dyn
6. Output of Step 5 above are saved in folder: ".\output" that will contain the following files
 - a. "LEX-2A(g)_LomaPrietaEQ.LX_dam_0.oud": main output with captions for quantities
 - b. "LEX-2A(g)_LomaPrietaEQ.LX_dam_0.csv": time histories at selected node/element
 - c. "LEX-2A(g)_LomaPrietaEQ.LX_dam_0.o21": modal frequencies with time
 - d. "LEX-2A(g)_LomaPrietaEQ.LX_dam_0.dis": displacement and acceleration for plotting
 - e. "LEX-2A(g)_LomaPrietaEQ.LX_dam_0.sig": stresses and strains output for plotting



Input File 1 Build the Dam in Dry

File name: LEX-2A_dry.sta

```
1 Lexington Dam -Section W-W step 2A construct in Layers - no w.t.
2 0,9.81,9.81,101.3,1
3 9262,9122,4,0
4 25,0.5,0
5 NMAT=,10
6 1,1
7 3100,0.5,619,0.5,18.8,0
8 0,37.5,0,0,3,0
9 2,3
10 60000,30000,25.5,0,0,0
11 0,0,0,0,0,0
12 3,1
13 1290,0.5,258,0.5,19.5,0
14 0,25.5,0,0,3,0
15 4,1
16 3065,0.5,613,0.5,18.8,0
17 0,35.5,0,0,3,0
18 5,1
19 3370,0.5,674,0.5,19.5,0
20 0,35,0,0,3,0
21 6,1
22 1290,0.5,258,0.5,19.5,0
23 0,25.5,0,0,3,0
24 7,1
25 3370,0.5,674,0.5,22,0
26 0,35,0,0,3,0
27 8,1
28 3100,0.5,619,0.5,21.7,0
29 0,37.5,0,0,3,0
30 9,1
31 3065,0.5,613,0.5,20.7,0
32 0,35.5,0,0,3,0
33 10,1
34 3370,0.5,674,0.5,22,0
35 0,35,0,0,3,0
36 NLAY=,9
37 1664,1255,1595,1471,1147,875,669,310,136,0
38 SOLVE,***** RUN 1 *****
39 END,****
40 1,2,-170.69,144.78,0,0,0
41 2,2,-170.69,145.69,0,0,1
42 ... node input continues
43 9261,2,145.00,154.84,0,0,1
44 9262,2,145.00,156.20,1,0,1
45 1,5,2,0.00,1,34,35,2
46 2,5,2,0.00,34,68,69,35
47 ... element input continues
48 9121,5,4,0.00,5762,5830,5764,5763
49 9122,5,1,0.00,5093,5159,5160,5160
**End of File: LEX-2A_dry.sta"
```

Input File 2 Add Reservoir Water

File Name: LEX-2A_add-w.t.sta

1	Lexington Dam -Section W-W step 2A (Dawson-Mejia 2021 - add phreatic surface water table (M3,M8 saturated)
2	0,9.81,9.81,101.3,1
3	9262,9122,4,9122
4	25,0.5,0
5	NMAT=,10
6	1,1
7	3100,0.5,619,0.5,18.8,0
8	0,37.5,0,0,3,0
9	2,3
10	60000,30000,25.5,0,0,0
11	0,0,0,0,0,0
12	3,1
13	1290,0.5,258,0.5,19.5,0
14	0,25.5,0,0,3,0
15	4,1
16	3065,0.5,613,0.5,18.8,0
17	0,35.5,0,0,3,0
18	5,1
19	3370,0.5,674,0.5,19.5,0
20	0,35,0,0,3,0
21	6,1
22	1290,0.5,258,0.5,19.5,0
23	0,25.5,0,0,3,0
24	7,1
25	3370,0.5,674,0.5,22,0
26	0,35,0,0,3,0
27	8,1
28	3100,0.5,619,0.5,21.7,0
29	0,37.5,0,0,3,0
30	9,1
31	3065,0.5,613,0.5,20.7,0
32	0,35.5,0,0,3,0
33	10,1
34	3370,0.5,674,0.5,22,0
35	0,35,0,0,3,0
36	NLOD=,1
37	33,177.70,0.00
38	1,0.0000,0.0000,0.0000
39	NWAT=,7
40	33
41	1,-171,168.5
42	2,-165,168.5
43	3,-114,177.7
44	4,9,177.7

45 5,53.34,146.3
46 6,88.4,146.3
47 7,145,146.3
48 SOLVE,***** RUN 1 *****
49 END,****
50 1,2,-170.69,144.78,0,0,0
51 2,2,-170.69,145.69,0,0,1
52 ... node input continues
53 9261,2,145.00,154.84,0,0,1
54 9262,2,145.00,156.20,1,0,1
55 1,5,2,0.00,1,34,35,2
56 2,5,2,0.00,34,68,69,35
57 ... element input continues
58 9121,5,4,0.00,5762,5830,5764,5763
59 9122,5,1,0.00,5093,5159,5160,5160

End of File: LEX-2A_add-w.t.sta

Output from Input File 2

File Name: LEX-2A_add-w.t.out

```

1          *****
2          |
3          | versat-s2d: static 2-dimensional
4          |         finite element analysis of continua
5          |
6          |         Versions 1998/2001/2005/2008/2009/2011
7          |         2012/2013/2021.11.18
8          |
9          |         copyright (c) 1998-2021 Dr. G. Wu
10         |         copyright (c) 1998-2021 w.g.i.
11         |         wutec geotechnical international
12         |
13         | input: *.sta; *.prx(optional)
14         | output: *.out; .pr4; .oug; .dis; .sig
15         |
16         | *****
17
18         compiled v.2022.01.15; 130 MB; max size of [K], variables= 25600000 50400
19
20         Lexington Dam -Section W-W step 2A (Dawson-Mejia 2021 - add phreatic surface water table (M3,M8 saturated)
21
22         *****
23         gravity is on (0=yes; 1=no)      0
24         gravity acceleration=           9.81
25         unit weight of water=          9.81
26         atmospheric pressure=           101.30
27         ichang=1: elastic non-linear analysis
28
29         total number of nodes           9262
30         total number of elements        9122
31         maximum number of nodes in an element4
32         number of elements having stresses 9122
33
34         maximum number of iterations =   25
35         residual (unbalanced) force allowed 0.50
36         imsh=0: small strain application
37
38         total number of materials 10
39         =====
40         ky      area  i  Unit. W  rr      (beam)
41         kb      k-sh  Unit. W      (elas)
42         SOIL   kb  n  kg  m  Unit. W  c  phi/-k  Soil Model
43         -----
44         SAND 1 3100.00 0.50 619.00 0.50 18.80 0.00 37.50 SAND Model - Mohr-Coulomb
45         ELAS 2 60000.00 30000.00 25.50
46         SAND 3 1290.00 0.50 258.00 0.50 19.50 0.00 25.50 SAND Model - Mohr-Coulomb
47         SAND 4 3065.00 0.50 613.00 0.50 18.80 0.00 35.50 SAND Model - Mohr-Coulomb
48         SAND 5 3370.00 0.50 674.00 0.50 19.50 0.00 35.00 SAND Model - Mohr-Coulomb
49         SAND 6 1290.00 0.50 258.00 0.50 19.50 0.00 25.50 SAND Model - Mohr-Coulomb
50         SAND 7 3370.00 0.50 674.00 0.50 22.00 0.00 35.00 SAND Model - Mohr-Coulomb
51         SAND 8 3100.00 0.50 619.00 0.50 21.70 0.00 37.50 SAND Model - Mohr-Coulomb
52         SAND 9 3065.00 0.50 613.00 0.50 20.70 0.00 35.50 SAND Model - Mohr-Coulomb

```

Report No. WGI-220301
March 1, 2022

```

53 SAND 10 3370.00 0.50 674.00 0.50 22.00 0.00 35.00 SAND Model - Mohr-Coulomb
54 =====
55
56 nl=1, lstep=33; ywt0(>0 to increase RESERVOIR level gradually)=177.700
57 node nodal load: fx, mxy fy
58 1 0.0000 0.0000 0.0000
59
60 nwat=7, lwstep=33
61 point x-coor; y-coor of water table
62 1 -171.00 168.50
63 2 -165.00 168.50
64 3 -114.00 177.70
65 4 9.00 177.70
66 5 53.34 146.30
67 6 88.40 146.30
68 7 145.00 146.30
69 ***** end of data for RUN 1 *****
70 ....
71 ... output for load increments 1 - 32 (omitted in here to save space)
72 ....
73 -----
74 results after load increment ..33
75 -----
76 net degrees of freedom= 18065 bandwidth=254
77 lband*(nnet-1)+1= 4588257 < ak dimension 25600000
78
79 ***runs[i_run - 1].nwatbl0=2
80 Water table pt#1 x= -170.690 y= 144.780
81 Water table pt#2 x= 145.000 y= 144.780
82
83 Reservoir level at ywt0= 177.70 for increment# 33 to 177.70
84 Water table pt#1 x= -170.690 y= 168.500
85 Water table pt#2 x= -165.000 y= 168.500
86 Water table pt#3 x= -114.000 y= 177.700
87 Water table pt#4 x= 9.000 y= 177.700
88 Water table pt#5 x= 53.340 y= 146.300
89 Water table pt#6 x= 88.400 y= 146.300
90 Water table pt#7 x= 145.000 y= 146.300
91
92 *CHECK Node#,fx,fy = 1 0.0, 0.0,
93 Iteration 1 Unbalanced force(UF)= 2393.307, UF ratio=9.4947e-003
94 Iteration 2 Unbalanced force(UF)= 77.428, UF ratio=3.0717e-004
95 Iteration 3 Unbalanced force(UF)= 17.047, UF ratio=6.7630e-005
96 Iteration 4 Unbalanced force(UF)= 8.077, UF ratio=3.2044e-005
97 Iteration 5 Unbalanced force(UF)= 5.001, UF ratio=1.9840e-005
98 Iteration 6 Unbalanced force(UF)= 2.612, UF ratio=1.0361e-005
99 Iteration 7 Unbalanced force(UF)= 1.813, UF ratio=7.1913e-006
100 Iteration 8 Unbalanced force(UF)= 1.576, UF ratio=6.2506e-006
101 Iteration 9 Unbalanced force(UF)= 1.011, UF ratio=4.0092e-006
102 Iteration 10 Unbalanced force(UF)= 0.720, UF ratio=2.8559e-006
103 Iteration 11 Unbalanced force(UF)= 0.574, UF ratio=2.2765e-006
104 Iteration 12 Unbalanced force(UF)= 0.409, UF ratio=1.6217e-006
105 -----
106 node disp-x rot. disp-y elem sig-x(mx0) sig-y(ta) tau-xy(sh.) gamm_xy%(mi) pp su fos sig-m
107 -----

```

```
108      1 0.0000      0.0000 1 -228.84 -561.89 -2.34 0.000 228.23 0.00 0.00 -338.88
109      2 0.0000      0.0000 2 -228.98 -562.25 -7.16 0.000 228.23 0.00 0.00 -339.10
110      ... output continues for node 2 - 9260
111      9261 0.0000      0.0000
112      9262 0.0000      0.0000
```

End of File: LEX-2A_add-w.t.out

Input Files 3 and 4 for Earthquake Loading

Input File 3 Name: LEX-2A(g).PSPA.csv

	A	B	C	D	E	F
1	1	case history performance - Lexington dam in 1989				
2	Prob.Levl	SF_x	SF_y			
3	LomaPrietaEQ	1	1			
4	1	N-points	dt			
5	LX_dam_0	5000	0.01	no Scaling for H0.443g, V0.143g		
6	0	0				
7	0					

The format for the Acceleration Input File Names (Line 5 in Input File 3): LX_dam_0.ACX & LX_dam_0.ACY

```

1 Loma Prieta, 10/18/1989, Los Gatos - Lexington Dam, 0 ACCELERATION in G NPTS= 8192, DT= .0100 SEC
2 3000,0.01,9.81,9
3 1639,5
4 8.08113E-04,8.23073E-04,8.02505E-04,8.18394E-04,8.02370E-04
5 8.20005E-04,8.03703E-04,8.19427E-04,7.92800E-04,8.03090E-04
6 7.85301E-04,8.05999E-04,7.80552E-04,7.93134E-04,7.81818E-04
7 8.21790E-04,8.20319E-04,7.87454E-04,7.41411E-04,7.86812E-04
8 ....

```

Input File 4 Name: LEX-2A(g).dyn

1 Lexington Dam -Section W-W Dyn-2A(g): Rf=Kg*0.75;L-M_Su(no-M6)2% damping
2 0,9.81,9.81,101.3,1
3 9262,9122,4,9122
4 3,0,0.5,1.5
5 999,0.4,999,10
6 7,2
7 1,3,1,6,5428,1,5428,3,5428,4
8 5428,6,7943,1,0,0,0,0,0
9 10
10 1,1
11 11139,0.5,3713,0.5,18.8,2790
12 0,37.5,0,0,3,0
13 0,0,0,0,0,0,0,0,0,0
14 2,3
15 60000,30000,25.5,0,0,0
16 1,2.78,0.0006,0,0,0
17 3,2
18 10330,0.5,1033,0.5,19.5,770
19 20,-0.32,-1,0,2,0
20 4,1
21 9195,0.5,3065,0.5,18.8,2300
22 0,35.5,0,0,3,0
23 0,0,0,0,0,0,0,0,0,0
24 5,1
25 14151,0.5,4717,0.5,19.5,3540
26 0,35,0,0,3,0
27 0,0,0,0,0,0,0,0,0,0
28 6,1
29 3099,0.5,1033,0.5,17.6,770
30 0,25.5,0,0,3,0
31 0,0,0,0,0,0,0,0,0,0
32 7,1
33 14151,0.5,4717,0.5,19.5,3540
34 10,35,0,0,3,0
35 0,0,0,0,0,0,0,0,0,0
36 8,2
37 20500,0,3717,0.5,21.7,2790
38 20,-0.44,-1,0,2,0
39 9,1
40 20500,0,3065,0.5,20.7,2300
41 0,35.5,0,0,3,0
42 0,0,0,0,0,0,0,0,0,0
43 10,1
44 9195,0.5,3065,0.5,18.8,2300
45 0,35.5,0,0,3,0
46 0,0,0,0,0,0,0,0,0,0
47 0, 177.70, 0.00
48 7
49 1,-171,168.5
50 2,-165,168.5
51 3,-114,177.7
52 4,9,177.7
53 5,53.34,146.3

54 6,88.4,146.3
55 7,145,146.3
56 1,2,-170.69,144.78,0,0,0
57 2,2,-170.69,145.69,0,0,1
58 ... node input continues
59 9261,2,145.00,154.84,0,0,1
60 9262,2,145.00,156.20,1,0,1
61 1,5,2,0.00,1,34,35,2
62 2,5,2,0.00,34,68,69,35
63 ... element input continues
64 9121,5,4,0.00,5762,5830,5764,5763
65 9122,5,1,0.00,5093,5159,5160,5160

End of File: LEX-2A(g).dyn

Output File from Input File 4 for Earthquake Loading

File Name: LEX-2A(g)_LomaPrietaEQ.LX_dam_0.oud

```
1          *****
2          |
3          | versat-d2d: dynamic 2-dimensional
4          |       finite element analysis of continua
5          |
6          |       versions 1998 - 2013; 2016
7          |       2018.05 (PSPA)- 2021.06-sv
8          |
9          |       copyright (c) 1998-2021 Dr. G. Wu
10         |       copyright (c) 1998-2021 WGI
11         |       Wutec Geotechnical International
12         |
13         |       input: *.dyn; *.prx; *.ACX; (*.ACY;*.FXY;*.SIN)
14         |       output: *.oud; *.csv; *.oug; *.dis; *.sig
15         |       *.o21; *.o23; *.soil-strength.csv
16         |
17         | *****
18
19         compiled 2021.06.09; 670 MB; max size of [K], variables= 25600000  50400
20
21         Lexington Dam -Section W-W Dyn-2A(g): Rf=Kg*0.75;L-M_Su(no-M6)2% damping
22
23         *****
24         gravity is on (0=yes; 1=no)      0
25         gravity acceleration=           9.81
26         unit weight of water=           9.81
27         atmospheric pressure=            101.30
28         ichang=1: elastic non-linear analysis
29
30         number of nodes                  9262
31         number of elements                9122
32         number of nodes in an element(nnodel)4
33         number of elements having stresses 9122
34
35         INPUT BASE ACCELERATIONS(2=hor;3=hor&vert)=3
36         viscous damping (%) mass & stiffnes  =0.5 1.5
37
38         time interval(s) for node/element response =999
39         time interval(s) for updating viscous damping=0.4
40         PWP not generated afte this time (sec) =999
41         static iterations at end of dynamic loads =10
42
43         total no. of time history output  7
44         List of node & element number for time history output
45         1  3
46         1  6
47         5428  1
48         5428  3
49         5428  4
50         5428  6
51         7943  1
```

Report No. WGI-220301
March 1, 2022

52
53
54
55
56
57
58
59
60
61
62
63
64
65
66
67
68
69
70
71
72
73
74
75
76
77
78
79
80
81
82
83
84
85
86
87
88
89
90
91
92
93
94
95
96
97
98
99
100
101
102
103
104
105
106

total number of materials 10

```

=====
      ky      area  i  unit. w  rr  [C]_a  [C]_b (beam)
      kb      k-sh  unit. w  [C]_a  [C]_b (elas)
SOIL  kb  n  kg  m  unit. w  c  phi/-k  Rf  Soil Shear Strength (ss): Mohr-Coulomb
-----
SAND 1 11139.00 0.50 3713.00 0.50 18.80 0.00 37.50 2790.00 SAND Model: ss=f(current stresses, c, phi)
ELAS 2 60000.00 30000.00 25.50 2.780 0.000600
CLAY 3 10330.00 0.50 1033.00 0.50 19.50 20.00 -0.32 770.00 CLAY Model: ss=f(pre-existing stresses, c, phi/k)
SAND 4 9195.00 0.50 3065.00 0.50 18.80 0.00 35.50 2300.00 SAND Model: ss=f(current stresses, c, phi)
SAND 5 14151.00 0.50 4717.00 0.50 19.50 0.00 35.00 3540.00 SAND Model: ss=f(current stresses, c, phi)
SAND 6 3099.00 0.50 1033.00 0.50 17.60 0.00 25.50 770.00 SAND Model: ss=f(current stresses, c, phi)
SAND 7 14151.00 0.50 4717.00 0.50 19.50 10.00 35.00 3540.00 SAND Model: ss=f(current stresses, c, phi)
CLAY 8 20500.00 0.00 3717.00 0.50 21.70 20.00 -0.44 2790.00 CLAY Model: ss=f(pre-existing stresses, c, phi/k)
SAND 9 20500.00 0.00 3065.00 0.50 20.70 0.00 35.50 2300.00 SAND Model: ss=f(current stresses, c, phi)
SAND 10 9195.00 0.50 3065.00 0.50 18.80 0.00 35.50 2300.00 SAND Model: ss=f(current stresses, c, phi)

```

***** PWP parameters *****

```

(SAND) No. , 1
PWP Model Type: Wu model ,M=0
No PWP: Soil Dry, 0
Vol. strn constant C1 =, 0
Vol. strn constant C2 =, 3

(SAND) No. , 4
PWP Model Type: Wu model ,M=0
No PWP: Soil Dry, 0
Vol. strn constant C1 =, 0
Vol. strn constant C2 =, 3

(SAND) No. , 5
PWP Model Type: Wu model ,M=0
No PWP: Soil Dry, 0
Vol. strn constant C1 =, 0
Vol. strn constant C2 =, 3

(SAND) No. , 6
PWP Model Type: Wu model ,M=0
No PWP: Soil Dry, 0
Vol. strn constant C1 =, 0
Vol. strn constant C2 =, 3

(SAND) No. , 7
PWP Model Type: Wu model ,M=0
No PWP: Soil Dry, 0
Vol. strn constant C1 =, 0
Vol. strn constant C2 =, 3

(SAND) No. , 9
PWP Model Type: Wu model ,M=0
No PWP: Soil Dry, 0
Vol. strn constant C1 =, 0
Vol. strn constant C2 =, 3

```

```

107 (SAND) No. , 10
108 PWP Model Type: Wu model ,M=0
109 No PWP: Soil Dry, 0
110 Vol. strn constant C1 =, 0
111 Vol. strn constant C2 =, 3
112
113 *****
114
115 Loma Prieta, 10/18/1989, Los Gatos - Lexington Dam, 0 ACCELERATION in G NPTS= 8192, DT= .0100 SEC
116 number of time increments used in analysis=3000
117 maximum allowed time increment (nmaxeq) =100000
118 time increment (sec) =0.01
119 number of sub time step(0,1,2,3,4) nrsub =9
120 input data are multiplied; & sf_EQ =9.81 1
121 number of lines in the input data(*.ACX) =1639
122 numbers per line =5
123
124 Loma Prieta, 10/18/1989 Los Gatos - Lexington Dam UP ACCELERATION in G NPTS= 8192 DT= .0100 SEC
125 input data for vertical scaled by & sf_EQ =9.81 1
126 note: time increment of vert. motion is treated as the same as for hori. motion
127 number of lines in the input data (vert.) =1639
128 numbers per line =5
129 peak scaled acceleration in record (hori. & vert.) =4.343 1.405
130 peak accelerations used in analysis (hori.&vert.) = 0.443g 0.143g
131
132 number of nodes having loads (nl)=0 & ywt0(>0 to update water loads)=177.7
133
134 number of points defining a water table (nwat)= 7
135 point x-coor; y-coor of water table
136 1 -171.00 168.50
137 2 -165.00 168.50
138 3 -114.00 177.70
139 4 9.00 177.70
140 5 53.34 146.30
141 6 88.40 146.30
142 7 145.00 146.30
143
144 net degrees of freedom= 18065 bandwidth=254
145 lband*(nnet-1)+1= 4588257 < ak dimension 25600000
146 **ichang=1: pwp computed but not used in the analysis
147
148 number of nodes with free field stress boundary=0
149
150 =====
151 state at the end of earthquake, except PEAKgamm_max, including static @ time=29.9910 sec
152 =====
153 -----
154 node disp-x disp-y acc-x(g) acc-y(g) elem sig-x(mx0) sig-y(ta) tauxy(sh.) gamm_xy%(mj) PEAKgamm_max(%) vol(%) ppr(FSliq)
155 -----
156 1 0.0000 0.0000 0.0023 0.0004 1 -240.69 -590.70 -2.52 0.000 0.000 0.00 0.00 ppr
157 2 0.0000 0.0000 0.0023 0.0004 2 -240.71 -590.67 -7.56 0.000 0.000 0.00 0.00 ppr
158 ... continue to end
159 9262 0.000 0.000

```

End of File: LEX-2A(g)_LomaPrietaEQ.LX_dam_0.oud

Report No. WGI-220301
March 1, 2022

Not to be reproduced without the permission of WGI

APPENDIX E FULL SIZE GRAPHS FOR MODEL & RESULT

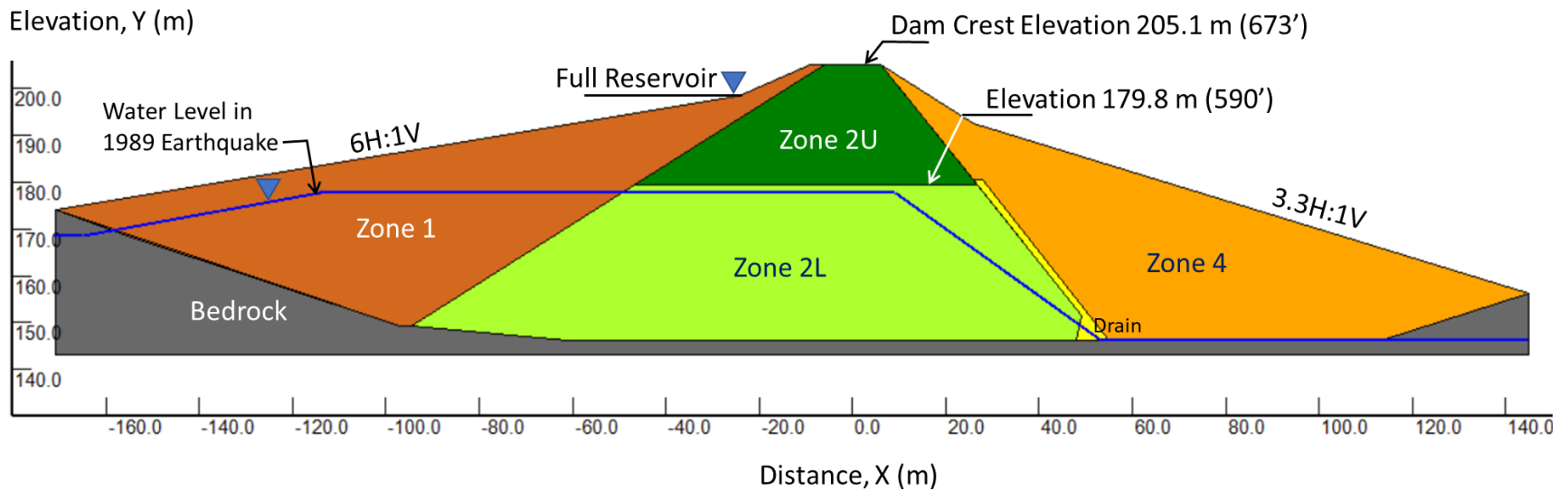


Fig. 3 **Lenihan Dam** - cross-section W-W' showing

- Soil and rock zones, and
- Phreatic surface from Dawson and Mejia (2021)

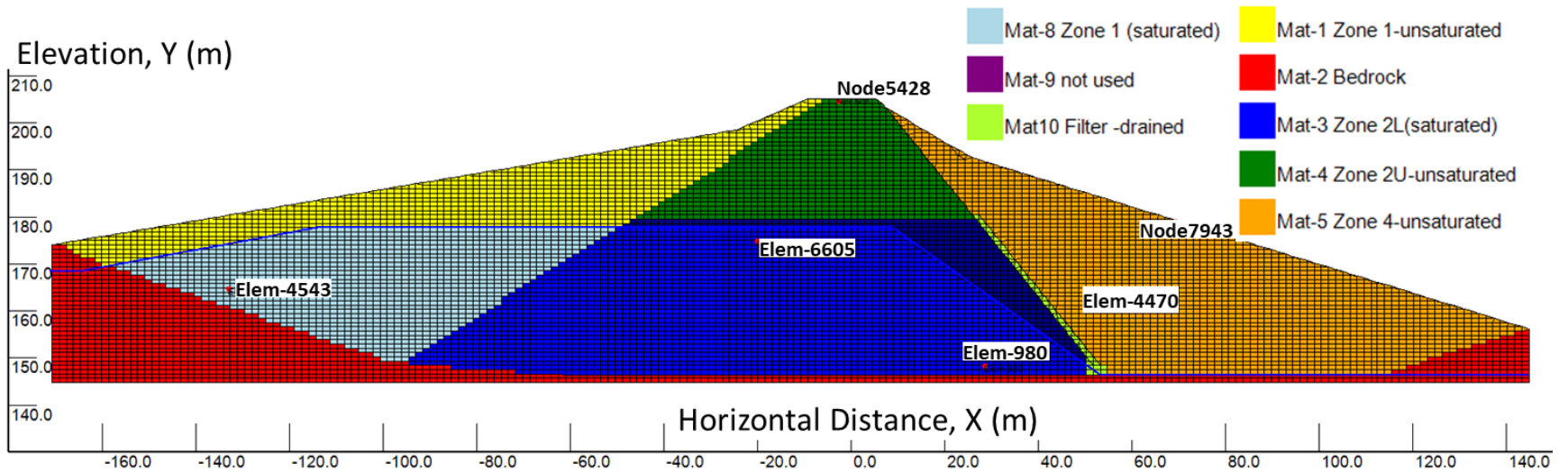


Fig. 6 VERSAT-2D MODEL (9122 elements) FOR SECTION W-W'

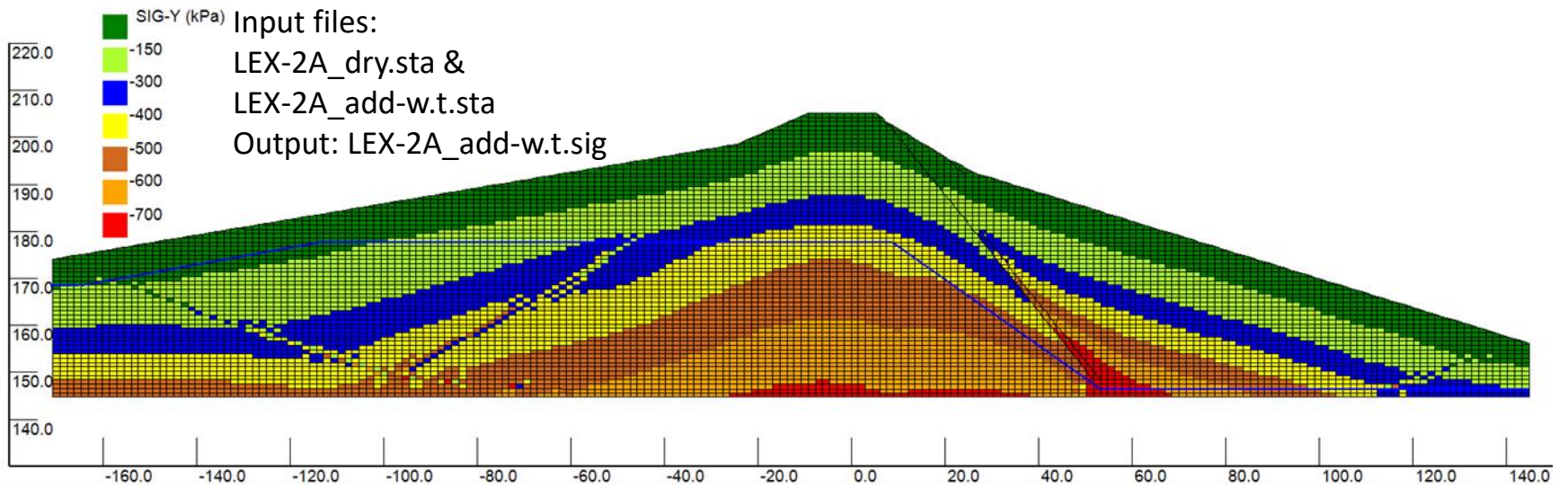


Fig. 7(a)

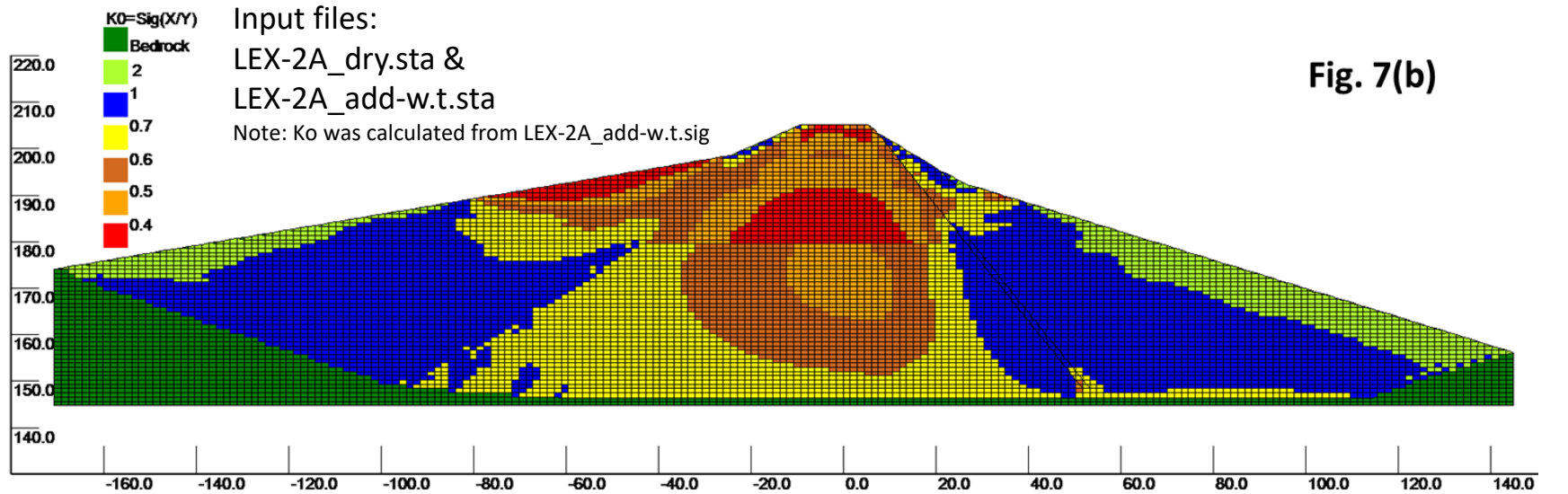


Fig. 7(b)

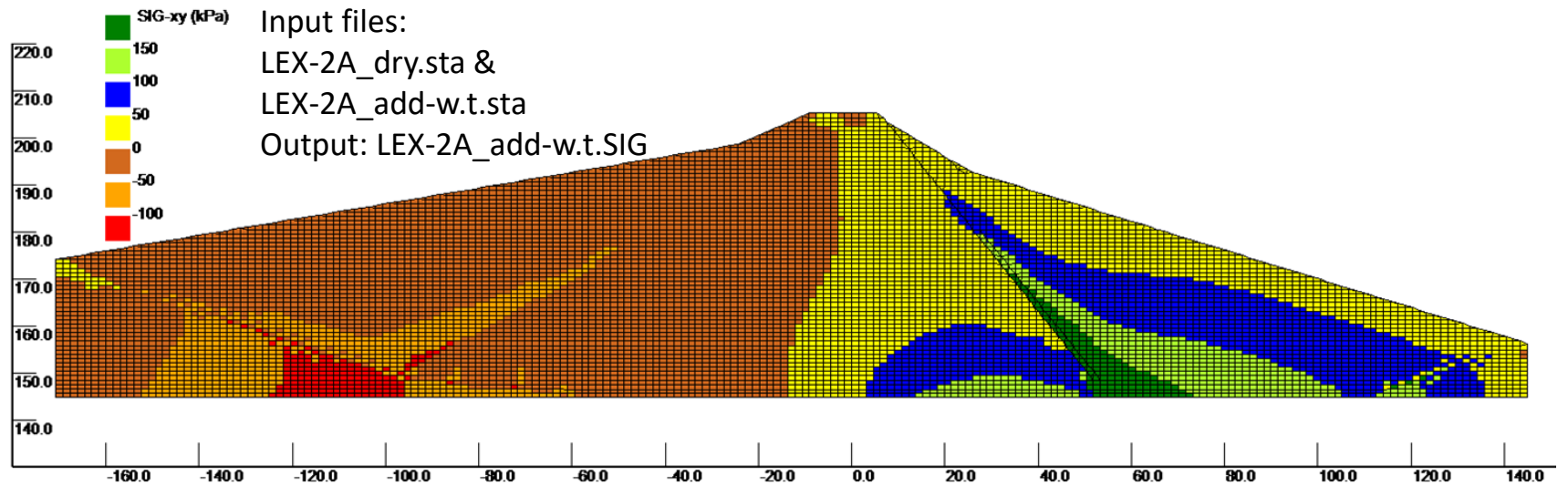


Fig. 7(c)

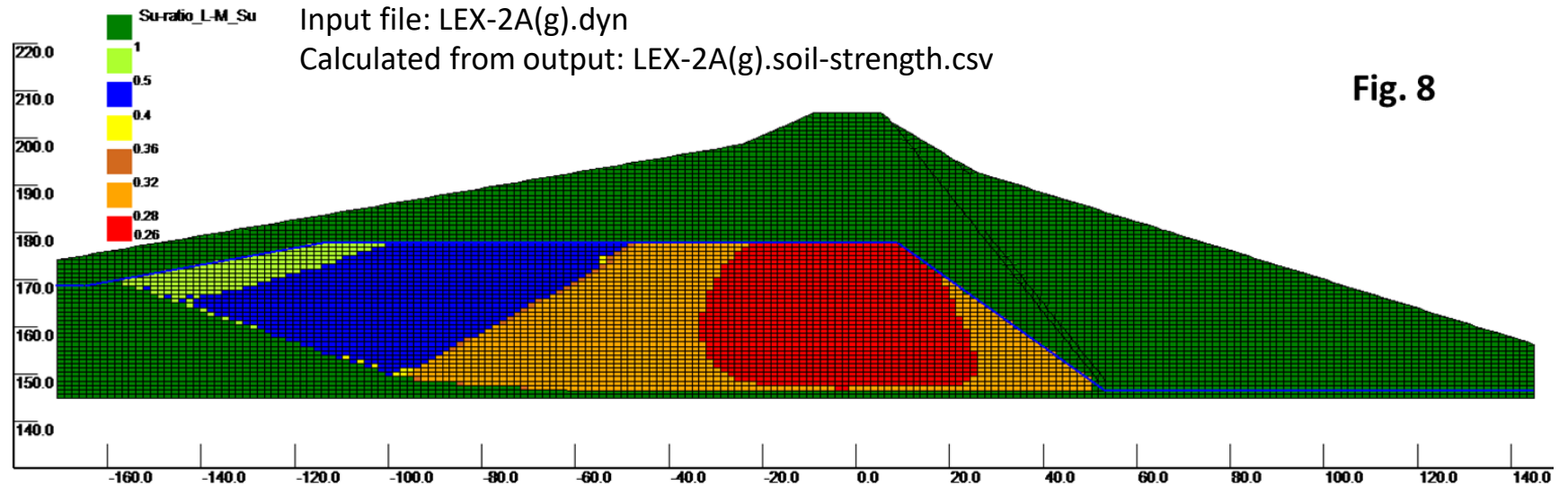
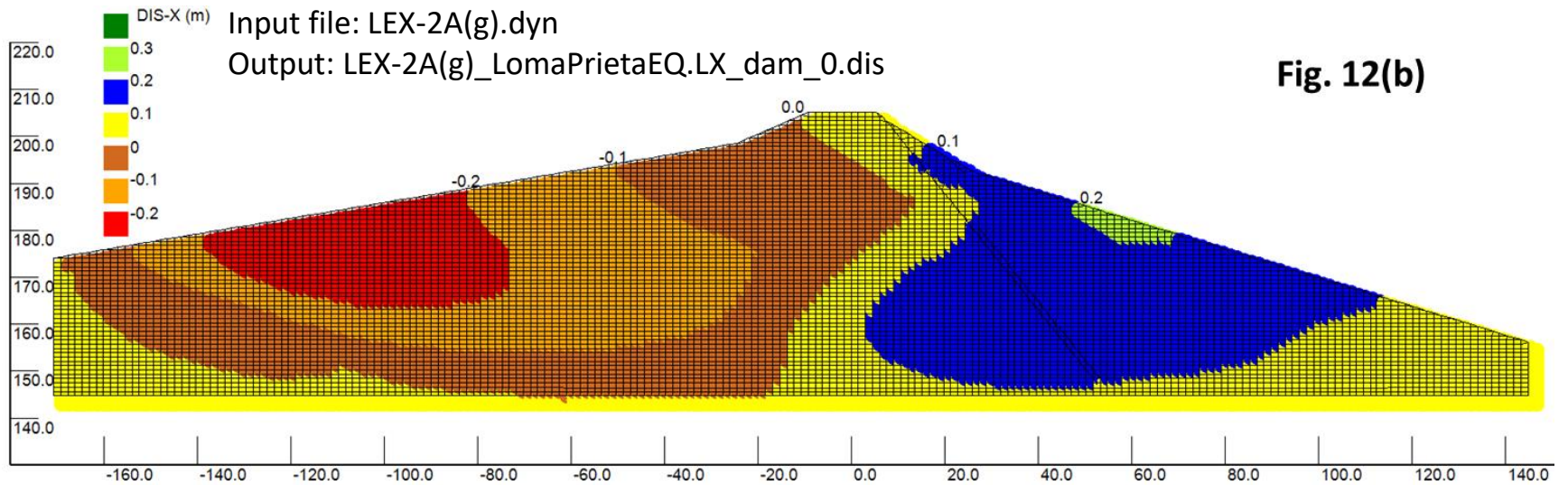
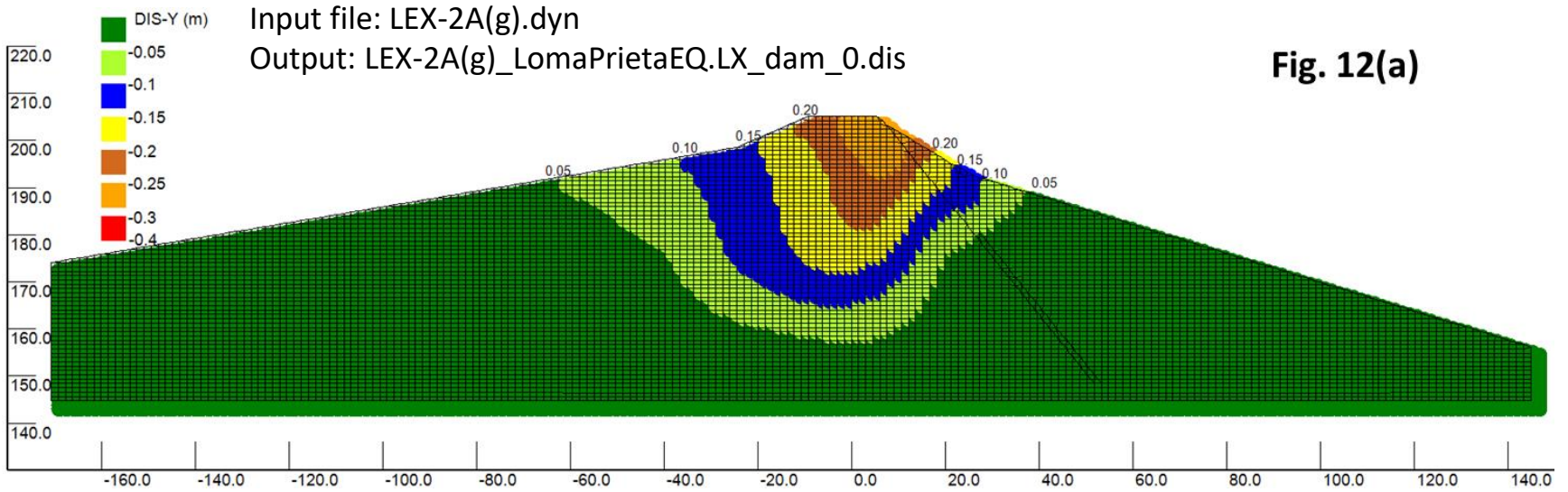


Fig. 8



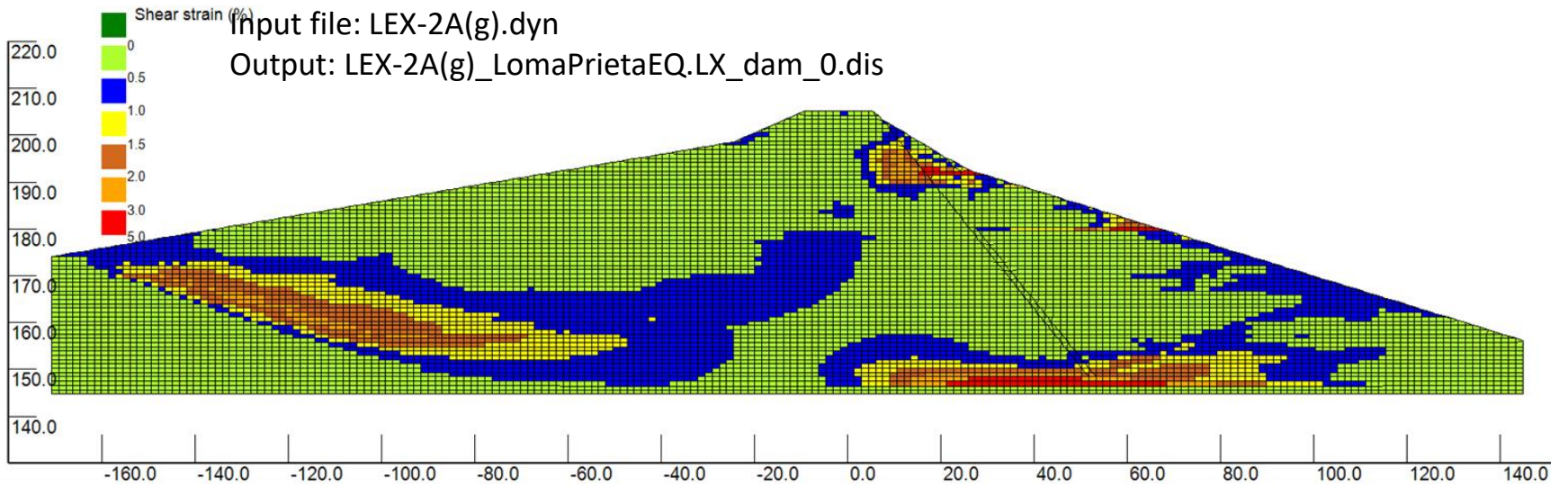


Fig. 13

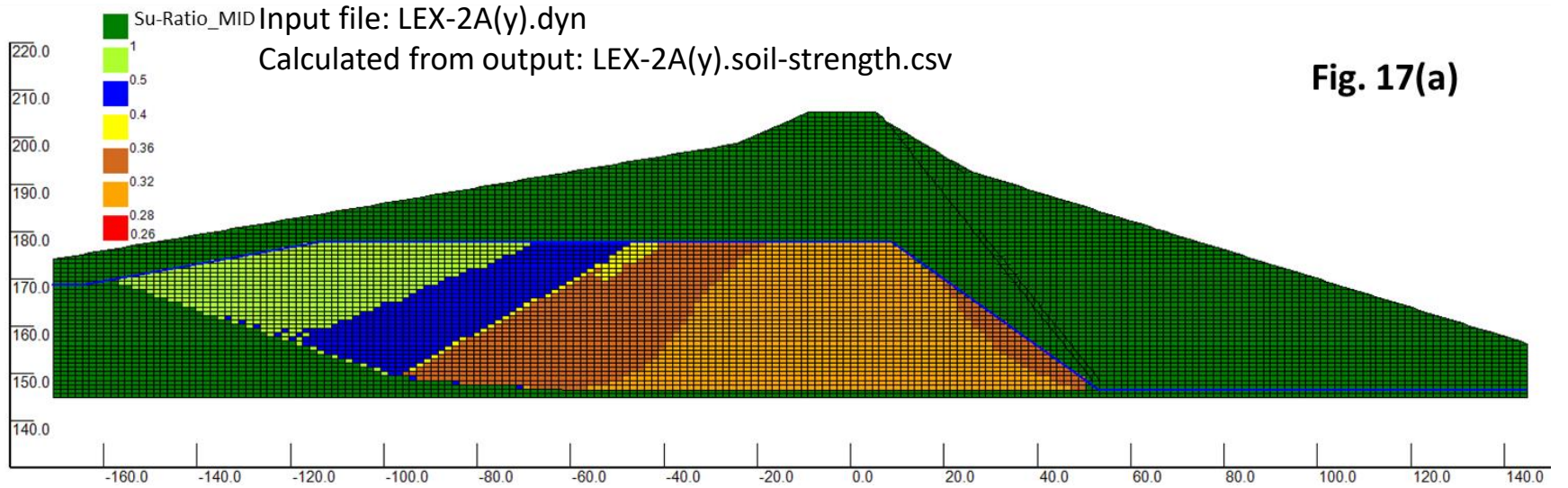


Fig. 17(a)

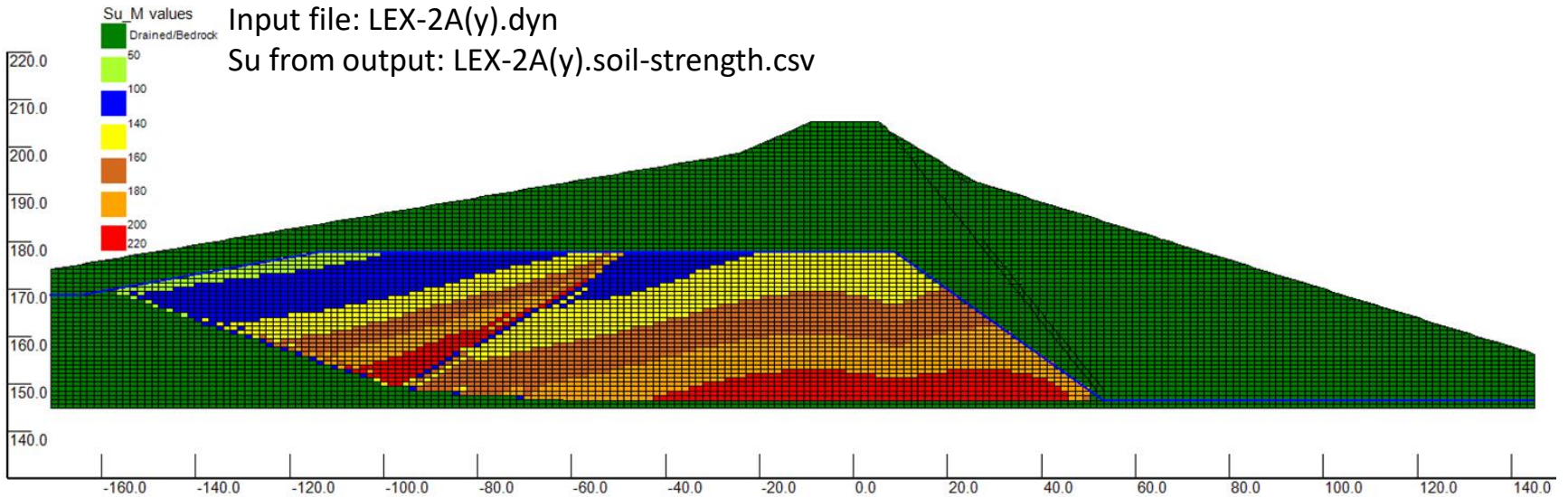
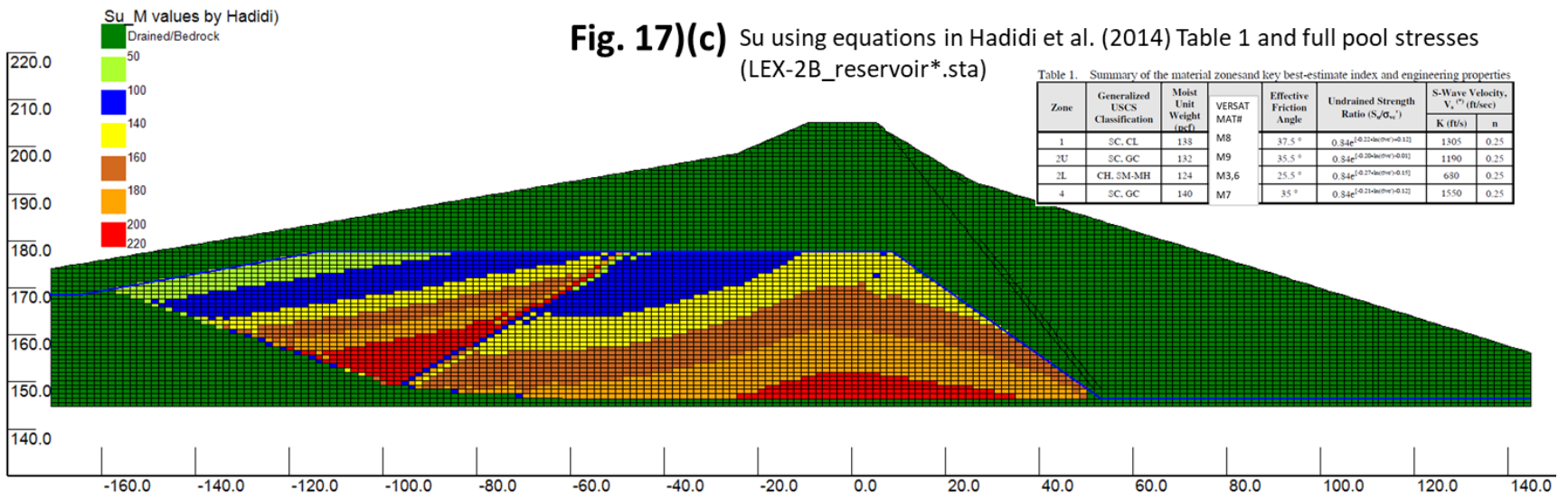
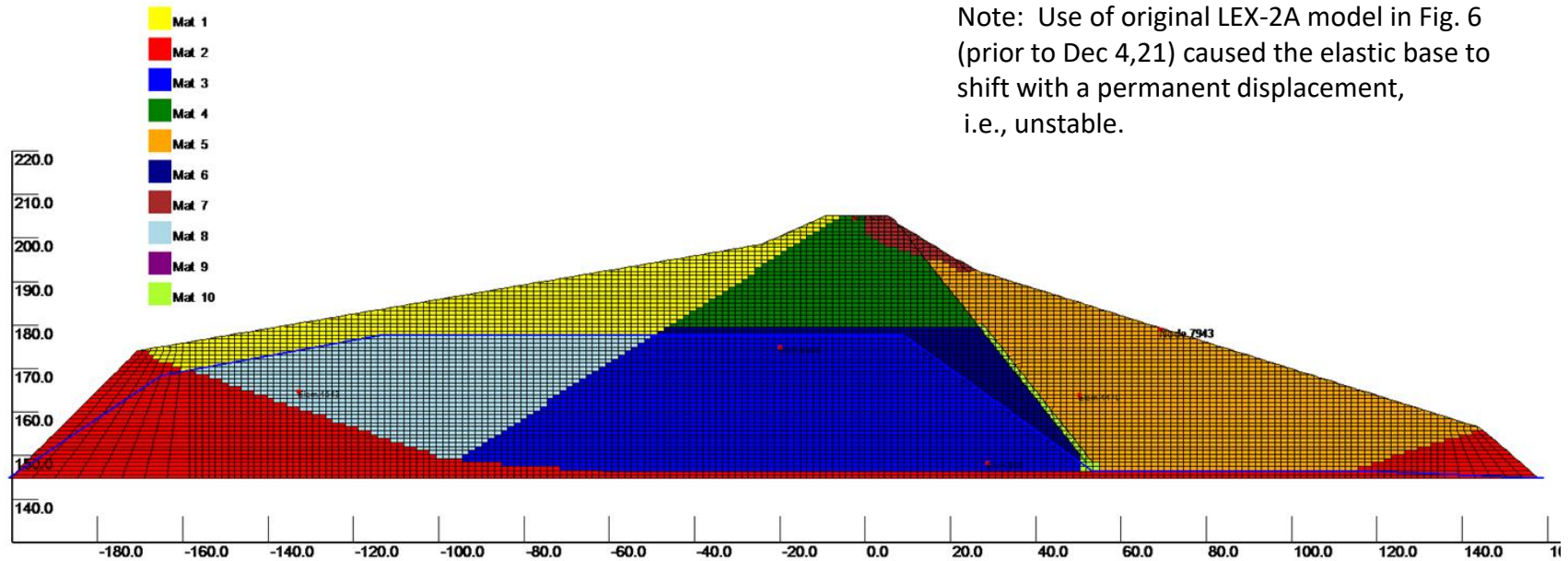


Fig. 17(b)



For: LEX-2A_el(y).dyn

Note: Use of original LEX-2A model in Fig. 6 (prior to Dec 4,21) caused the elastic base to shift with a permanent displacement, i.e., unstable.



VERSAT-2D model (9122 elements) used for Case-2A_el(y), i.e., the elastic-base model.

Note: Repeating Case 2A(g) in Table 3 using this model gave identical results as when the model in Fig. 6 was used, indicating robust calculations by VERSAT-2D.

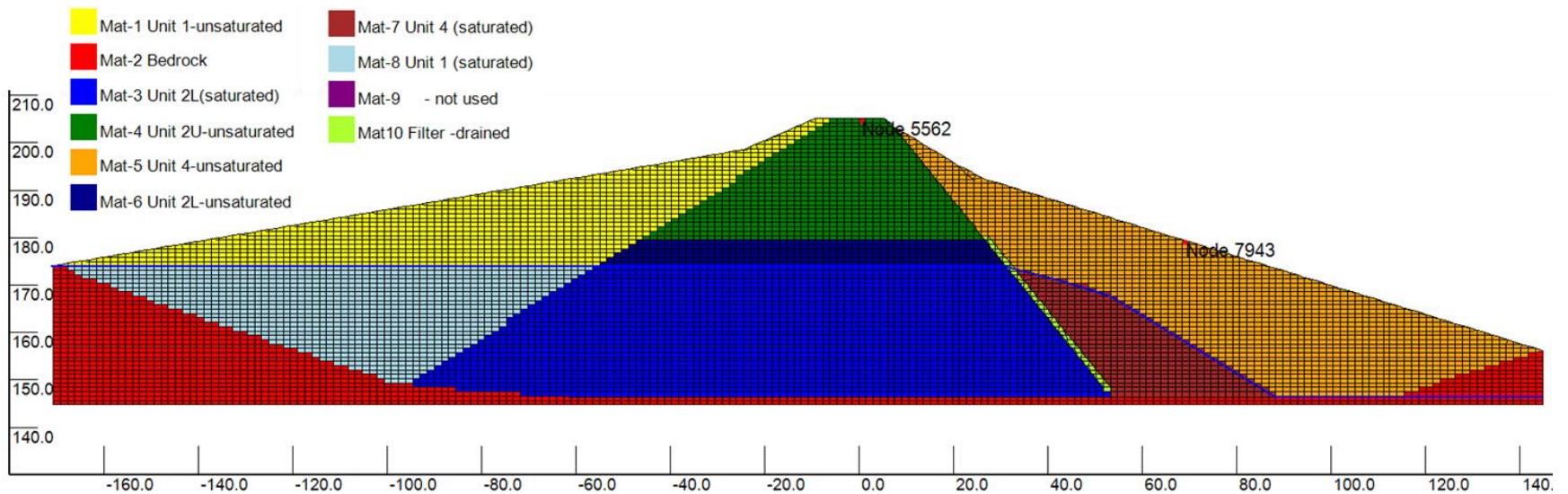


Fig. 19 VERSAT-2D model (9122 elements) for Section W-W' Case 2: assuming reservoir at El. 174.0 m and phreatic surface modified from Fig. 2-3 in SCVWD (2012)

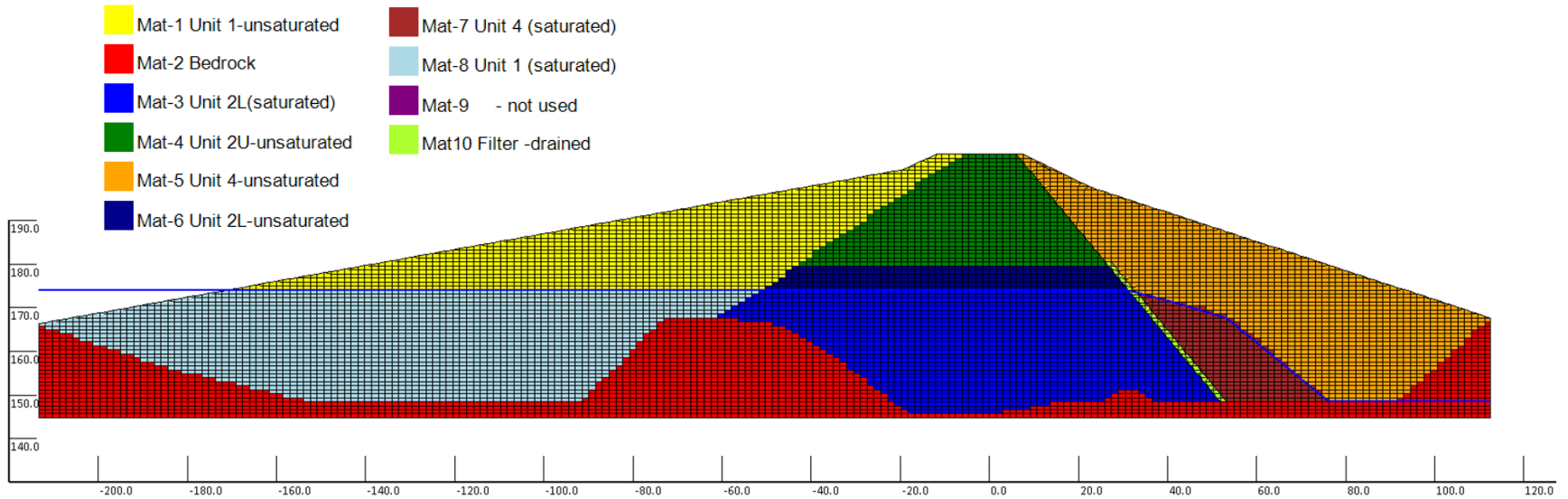
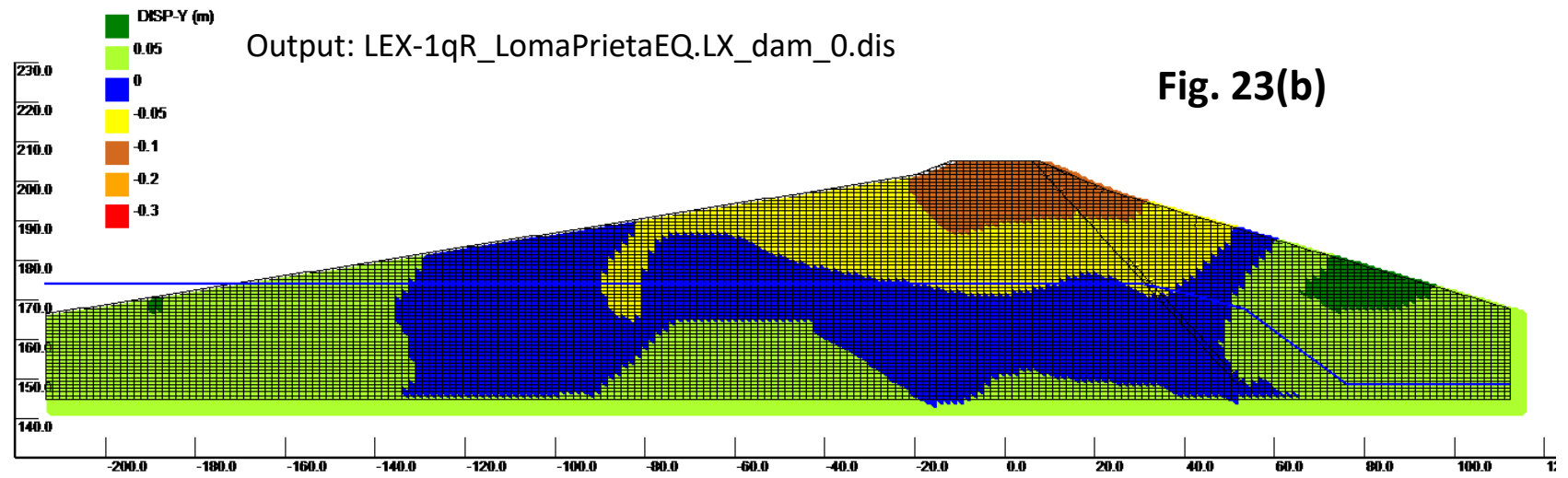
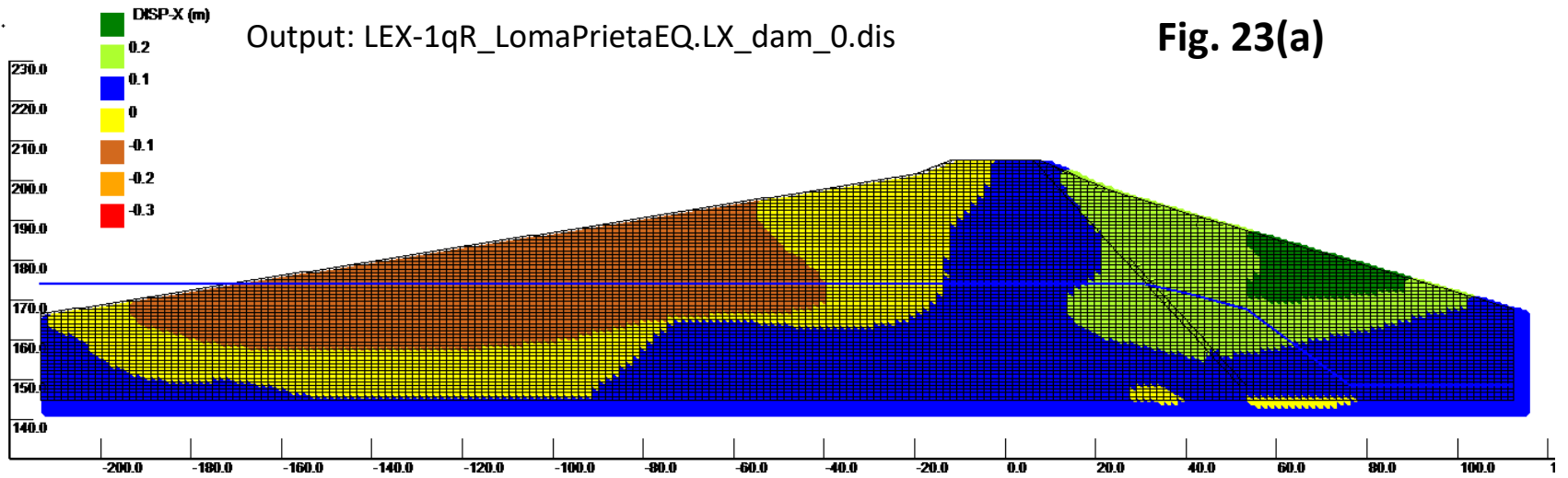


Fig. 22 VERSAT-2D model (9843 elements) for Section B-B' Case 1: assuming reservoir at El. 174.0 m and phreatic surface modified from Fig. 2-3 in SCVWD (2012)



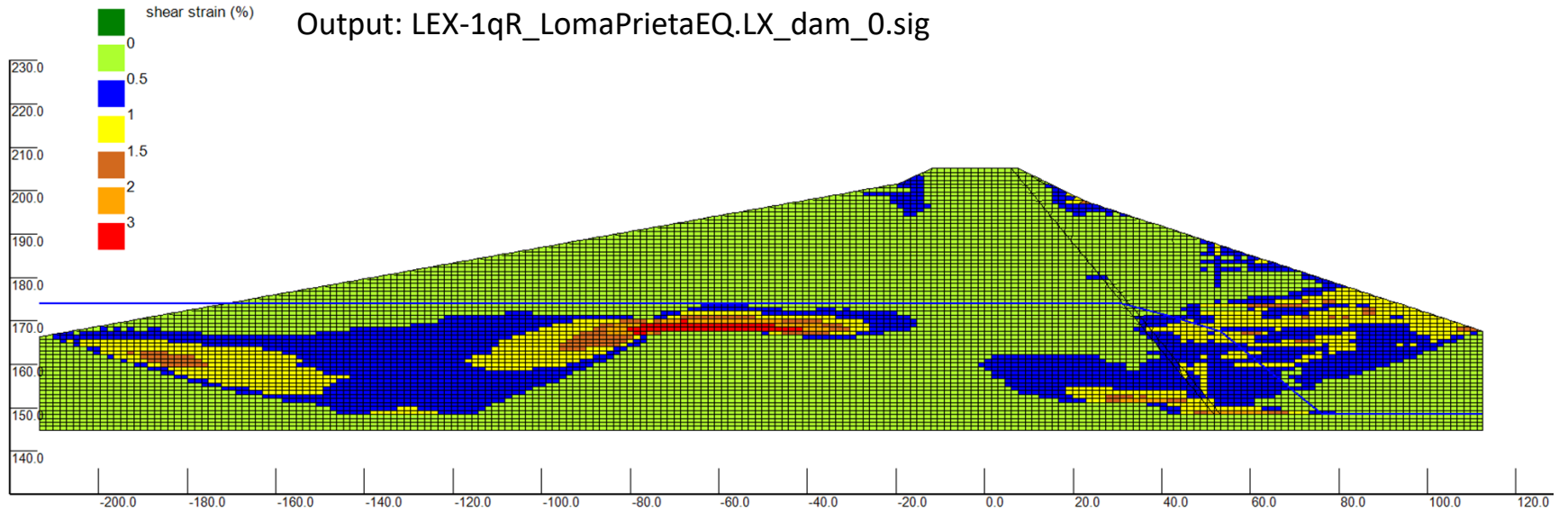


Fig. 23(c) Absolute values of residual shear strains (%) at end of EQ for Case 1(q)

